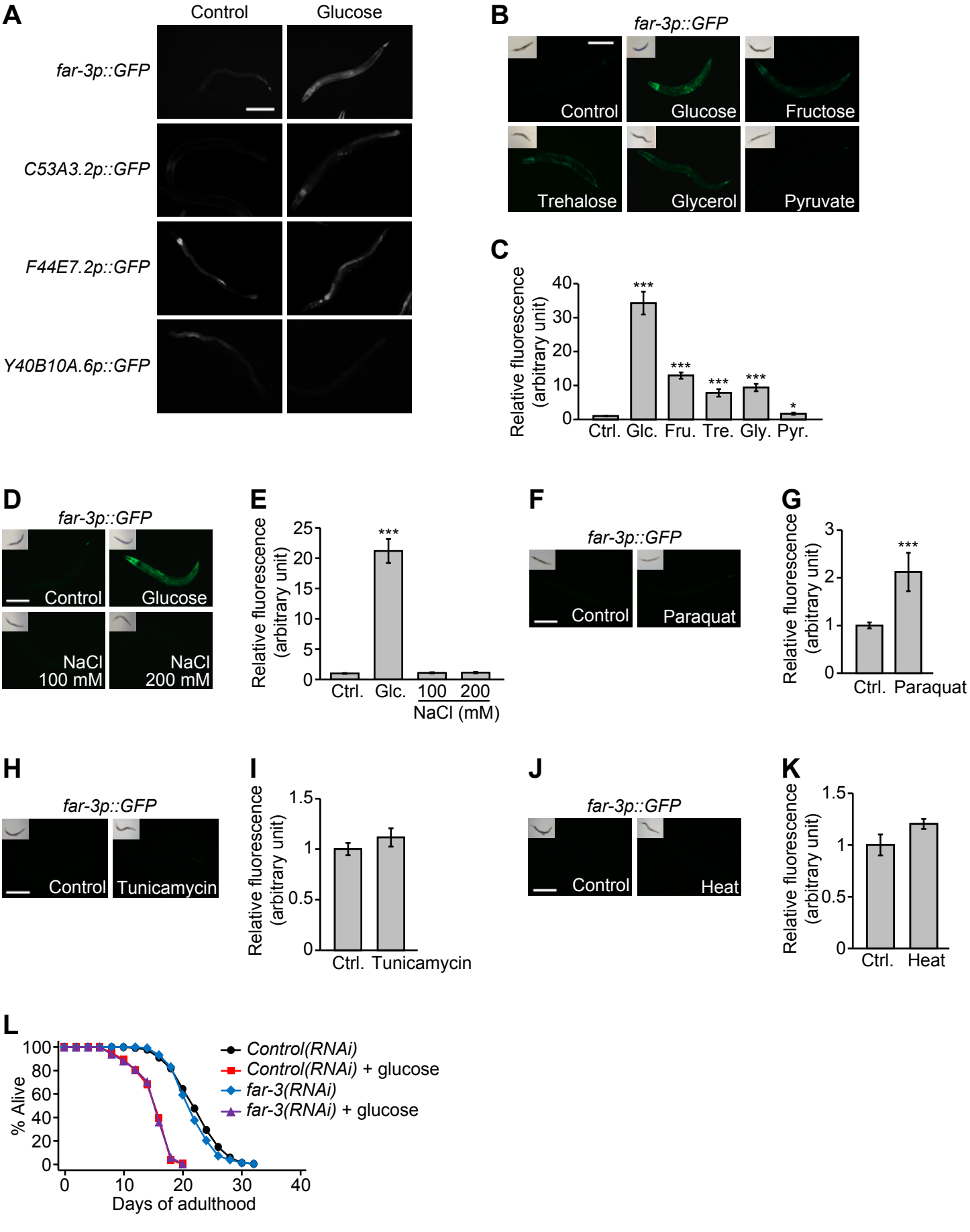
A
Control
Glucose
far-3p::GFP
C53A3.2p::GFP
F44E7.2p::GFP
Y40B10A.6p::GFP
B
far-3p::GFP
Control
Glucose
Fructose
Trehalose
Glycerol
Pyruvate
C
Relative fluorescence (arbitrary unit)
40
30
20
10
0
***
***
***
***
*
Ctrl. Glc. Fru. Tre. Gly. Pyr.
D
far-3p::GFP
Control
Glucose
NaCl 100 mM
NaCl 200 mM
E
Relative fluorescence (arbitrary unit)
25
20
15
10
5
0
***
Ctrl. Glc. 100 200
NaCl (mM)
F
far-3p::GFP
Control
Paraquat
G
Relative fluorescence (arbitrary unit)
3
2
1
0
***
Ctrl. Paraquat
H
far-3p::GFP
Control
Tunicamycin
I
Relative fluorescence (arbitrary unit)
1.5
1
0.5
0
Ctrl. Tunicamycin
J
far-3p::GFP
Control
Heat
K
Relative fluorescence (arbitrary unit)
1.5
1
0.5
0
Ctrl. Heat
L
% Alive
100
80
60
40
20
0
0 10 20 30 40
Days of adulthood
Control(RNAi)
Control(RNAi) + glucose
far-3(RNAi)
far-3(RNAi) + glucose

Figure S1. A genome-wide RNAi screen using glucose-responsive *far-3p::GFP C. elegans*.

(**A**) Fluorescence in transgenic animals that expressed GFP under the promoters of glucose-induced genes (*far-3p::GFP*, *C53A3.2p::GFP*, *F44E7.2p::GFP*, and *Y40B10A.6p::GFP*), which were identified in our previous paper (Lee et al., 2009), was examined with or without additional 2% glucose treatment. Among them *far-3p::GFP* was highly induced by glucose-rich diet feeding. *C53A3.2p::GFP* was also induced by glucose feeding, but the GFP intensity was dimmer than that of *far-3p::GFP*. Scale bars indicate 200 μm in this figure. (**B**) *far-3p::GFP* was induced by sugars or sugar metabolites that can be converted to glucose. These include fructose (Fru., 2%), trehalose (Tre., 4%), glycerol (Gly., 1%) and pyruvate (Pyr., 1%). Although the molar concentrations were very similar, the induction of *far-3p::GFP* by these metabolites was smaller than that by glucose (Glc., 2%). A normal food (OP50) condition was used as a control (Ctrl.). (**C**) Quantification of the data shown in panel **B** ($n \geq 22$ from one or two independent experiments). For panels **C**, **E**, **G**, **I**, and **K**, error bars represent standard error of the mean (SEM) (two-tailed Student's *t*-test, $*p<0.05$, $***p<0.001$). (**D**) *far-3p::GFP* was greatly induced by 2% glucose (111 mM) but not by similar (100 mM) or higher concentrations (200 mM) of NaCl treatment. (**E**) Quantification of data shown in panel **D** ($n \geq 30$ from four independent experiments). (**F**) The effects of paraquat (25 mM) treatment on *far-3p::GFP* expression. (**G**) Quantification of the induction of *far-3p::GFP* by paraquat treatment in panel **F** (n=30 from four independent experiments). Note that the fold change of *far-3p::GFP* by paraquat (approximately two fold) was much smaller than that by dietary glucose (10-30 fold) (Fig. **1B**; Supplemental Fig. **S1C**,**E**). (**H**) *far-3p::GFP* was not induced by tunicamycin (5 μg/ml) treatment. (**I**) Quantification of the data shown in panel **H** (n=34 from three independent experiments). (**J**)

Heat shock (35°C for 1 hour) did not affect the expression of *far-3p::GFP*. (**K**) Quantification of the data in panel **J** (n=34 from three independent experiments). (**L**) RNAi knockdown of *far-3* had little or no effect on the lifespan of control diet-fed worms or glucose-rich diet-fed worms. See Supplemental Table S3 for additional repeats and statistical analysis for lifespan data shown in this figure.

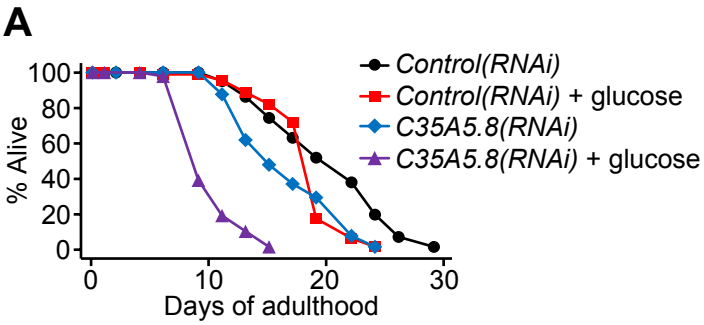
A
Control(RNAi)
Control(RNAi) + glucose
C35A5.8(RNAi)
C35A5.8(RNAi) + glucose
% Alive
Days of adulthood

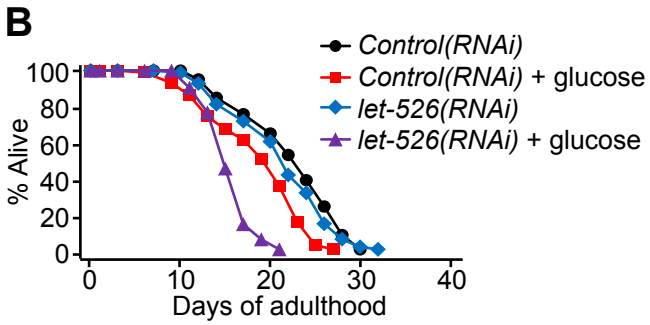
B
Control(RNAi)
Control(RNAi) + glucose
let-526(RNAi)
let-526(RNAi) + glucose
% Alive
Days of adulthood

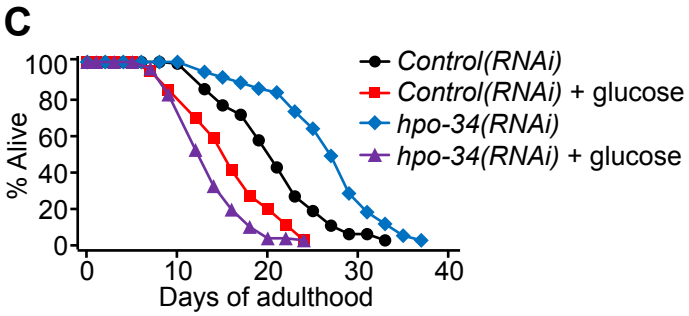
C
Control(RNAi)
Control(RNAi) + glucose
hpo-34(RNAi)
hpo-34(RNAi) + glucose
% Alive
Days of adulthood

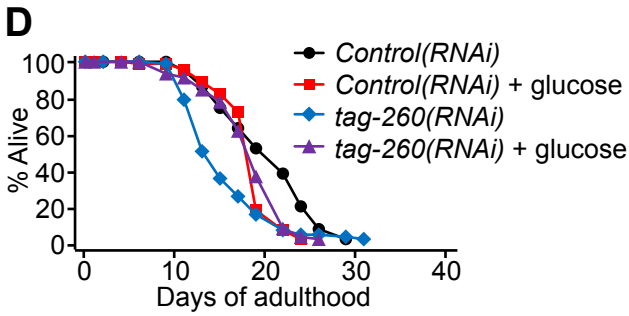
D
Control(RNAi)
Control(RNAi) + glucose
tag-260(RNAi)
tag-260(RNAi) + glucose
% Alive
Days of adulthood

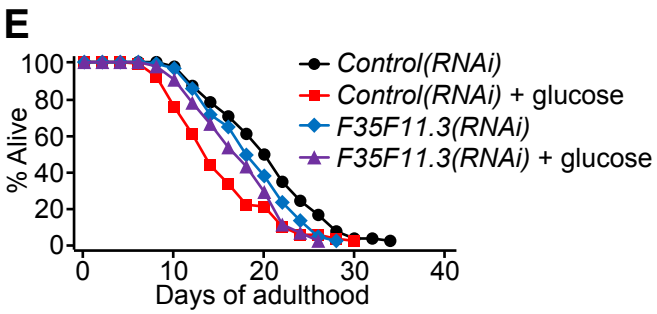
E
Control(RNAi)
Control(RNAi) + glucose
F35F11.3(RNAi)
F35F11.3(RNAi) + glucose
% Alive
Days of adulthood

Figure S2. RNAi clones that have differential effects on lifespan with or without glucose feeding. (**A**,**B**) Knockdown of *C35A5.8* (exportin 7 homolog) (**A**) or *let-526* (a component of SWI/SNF complex required for chromatin remodeling) (**B**) further shortened the lifespan of glucose-fed worms. (**C**) Knockdown of *hpo-34* (Hypersensitive to POre- forming toxin 34) increased lifespan in control conditions, while decreasing lifespan in glucose-rich diet-fed conditions. (**D**) RNAi targeting *tag-260* (homology to interferon regulatory factor 2-binding protein 2) shortened lifespan on a control diet, but did not on a glucose-rich diet. (**E**) *F35F11.3* (homology to F-box C proteins) RNAi decreased the lifespan of animals fed with control food, while increasing the lifespan of glucose-rich diet-fed animals. See Supplemental Table S3 for additional repeats and statistical analysis for lifespan data shown in this figure.

Lee_Fig S3

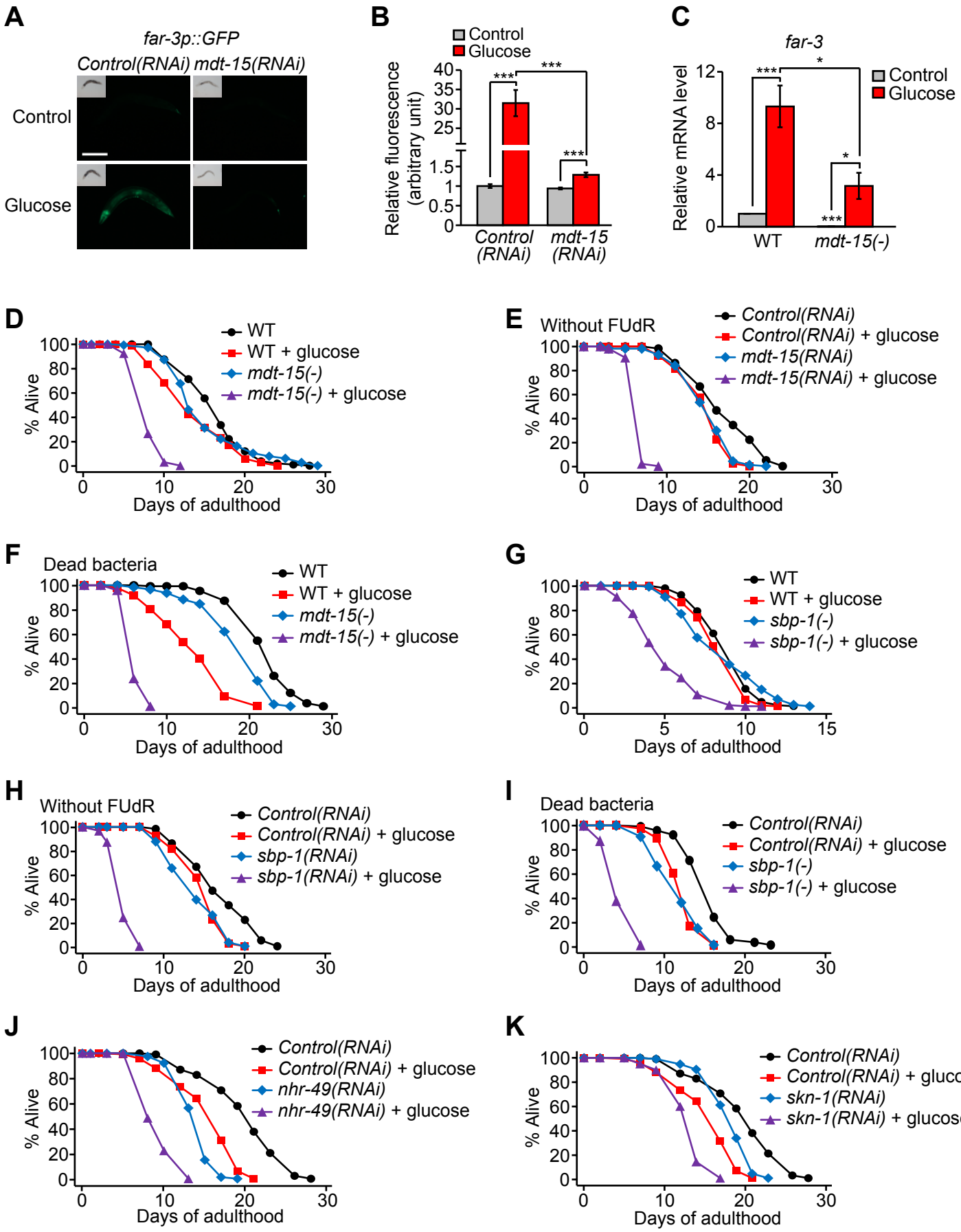
A
far-3p::GFP
Control(RNAi) mdt-15(RNAi)
Control
Glucose
B
Control
Glucose
Relative fluorescence (arbitrary unit)
Control (RNAi)
mdt-15 (RNAi)
C
far-3
Relative mRNA level
Control
Glucose
WT
mdt-15(-)
D
WT
WT + glucose
mdt-15(-)
mdt-15(-) + glucose
% Alive
Days of adulthood
E
Without FUdR
Control(RNAi)
Control(RNAi) + glucose
mdt-15(RNAi)
mdt-15(RNAi) + glucose
F
Dead bacteria
G
sbp-1(-)
sbp-1(-) + glucose
H
Without FUdR
sbp-1(RNAi)
sbp-1(RNAi) + glucose
I
Dead bacteria
J
nhr-49(RNAi)
nhr-49(RNAi) + glucose
K
skn-1(RNAi)
skn-1(RNAi) + glucose

Figure S3. Inhibition of *mdt-15* or *sbp-1* further decreased lifespan on a glucose-enriched diet. (**A**) Glucose-induced *far-3p::GFP* was significantly decreased by *mdt-15* RNAi (scale bar: 200 μm). (**B**) Quantification of the data in panel **A** (n≥31 from three independent experiments). (**C**) mRNA levels of *far-3* were measured by using qRT-PCR. Highly increased expression of *far-3* mRNA upon glucose treatment was significantly decreased by *mdt-15(tm2182)* mutation [*mdt-15(-)*] (n≥3). WT: wild-type (N2). For panels **B** and **C**, error bars represent SEM (two-tailed Student's *t*-test, **p*<0.05, ****p*<0.001). (**D**) *mdt-15(-)* mutation further reduced lifespan upon glucose-rich diet feeding. (**E**) *mdt-15* RNAi treatment greatly shortened the lifespan of glucose-fed worms without FUdR treatment. (**F**) Glucose-treated *mdt-15(-)* mutants had very short lifespan on dead bacteria as well. (**G**) *sbp-1(ep79)* [*sbp-1(-)*] mutation greatly decreased lifespan on a glucose-rich diet. Lifespan assays for panels **G** and **I** were performed at 25°C from L4 stage throughout adulthood. Please note that the effects of glucose on the lifespan of wild-type were variable at 25°C, as previously reported (Brokate-Llanos et al., 2014). (**H**) *sbp-1* RNAi further decreased the short lifespan of glucose-treated worms without FUdR treatment. (**I**) *sbp-1(-)* mutants displayed very short lifespan upon glucose feeding on dead bacteria. These results confirmed our findings that glucose-rich diet feeding and inhibition of SBP-1/MDT-15 synergistically decreased lifespan. In addition, dead bacteria feeding experiments confirmed that dietary glucose but not bacterial metabolites generated by glucose shortened lifespan in animals with reduced *mdt-15* or *sbp-1*. WT and *mdt-15(-)* mutant animals were treated with glucose feeding only during adulthood in panels **D** and **F**. Worms were treated with *mdt-15* RNAi from adulthood and *sbp-1* RNAi for whole life in panels **E** and **H**. See Supplemental Materials and Methods for details. (**J**,**K**) Knockdown of *nhr-49* (**J**) or *skn-1* (**K**) shortened the lifespan of both

control diet- and glucose-rich diet-fed worms to similar degrees. See Supplemental Table S4 for additional repeats and statistical analysis for lifespan data shown in this figure.

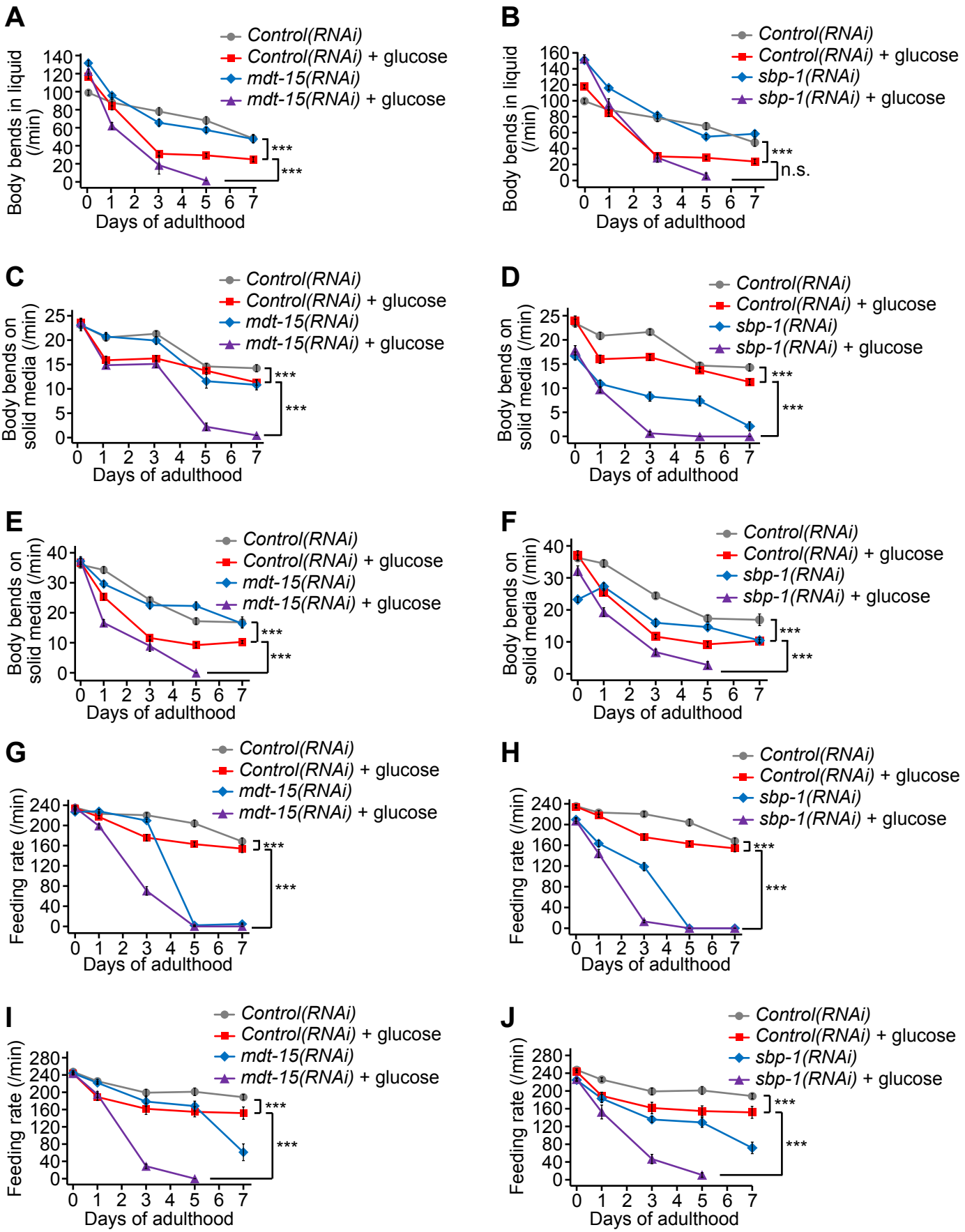
A
Body bends in liquid (/min)
Days of adulthood
Control(RNAi)
Control(RNAi) + glucose
mdt-15(RNAi)
mdt-15(RNAi) + glucose
***
***
B
Body bends in liquid (/min)
Days of adulthood
Control(RNAi)
Control(RNAi) + glucose
sbp-1(RNAi)
sbp-1(RNAi) + glucose
***
n.s.
C
Body bends on solid media (/min)
Days of adulthood
Control(RNAi)
Control(RNAi) + glucose
mdt-15(RNAi)
mdt-15(RNAi) + glucose
***
***
D
Body bends on solid media (/min)
Days of adulthood
Control(RNAi)
Control(RNAi) + glucose
sbp-1(RNAi)
sbp-1(RNAi) + glucose
***
***
E
Body bends on solid media (/min)
Days of adulthood
Control(RNAi)
Control(RNAi) + glucose
mdt-15(RNAi)
mdt-15(RNAi) + glucose
***
***
F
Body bends on solid media (/min)
Days of adulthood
Control(RNAi)
Control(RNAi) + glucose
sbp-1(RNAi)
sbp-1(RNAi) + glucose
***
***
G
Feeding rate (/min)
Days of adulthood
Control(RNAi)
Control(RNAi) + glucose
mdt-15(RNAi)
mdt-15(RNAi) + glucose
***
***
H
Feeding rate (/min)
Days of adulthood
Control(RNAi)
Control(RNAi) + glucose
sbp-1(RNAi)
sbp-1(RNAi) + glucose
***
***
I
Feeding rate (/min)
Days of adulthood
Control(RNAi)
Control(RNAi) + glucose
mdt-15(RNAi)
mdt-15(RNAi) + glucose
***
***
J
Feeding rate (/min)
Days of adulthood
Control(RNAi)
Control(RNAi) + glucose
sbp-1(RNAi)
sbp-1(RNAi) + glucose
***
***

Figure S4. Knockdown of MDT-15 or SBP-1 further enhances age-dependent declines in locomotion and feeding rates. (**A**,**B**) Knockdown of *mdt-15* (**A**) or *sbp-1* (**B**) enhanced the age-dependent declines in body bending rates in liquid media. *sbp-1(*RNAi) worms displayed rapid decline in body bending rates upon glucose feeding, although the difference between glucose-fed *control(RNAi)* and *sbp-1(RNAi)* worms was not significant. *p* values were calculated by using two-way ANOVA test in this figure (***$p<0.001$, n.s.: not significant). These results are additional repeats of the experiments shown in Fig. **2E**,**F**. Please note that the feeding rates of *mdt-15(RNAi)* and *sbp-1(RNAi)* worms at day 7 were not determined, because all the animals were already dead under glucose-feeding conditions in panels **A**, **B**, **E**, **F**, **I**, and **J**. (**C**-**F**) Body bending rates on solid media were rapidly decreased during aging by *mdt-15* RNAi (**C**,**E**) or *sbp-1* RNAi (**D**,**F**) on a glucose-enriched diet. Panels **C**,**E** and **D**,**F** are replicates of the body bending measurements. (**G**,**H**,**I**,**J**) Glucose treatments exacerbated the age-dependent decline in pumping rates of *mdt-15(RNAi)* (**G**,**I**) and *sbp-1(RNAi)* (**H**,**J**) worms. Panels **G**,**I** and **H**,**J** are replicates. Fifteen worms were examined in each condition at a specific age and error bars represent SEM in all panels in this figure. See Supplemental Table S5 for statistics of all the data in this figure and the data in Fig. **2E**,**F** at specific time points.

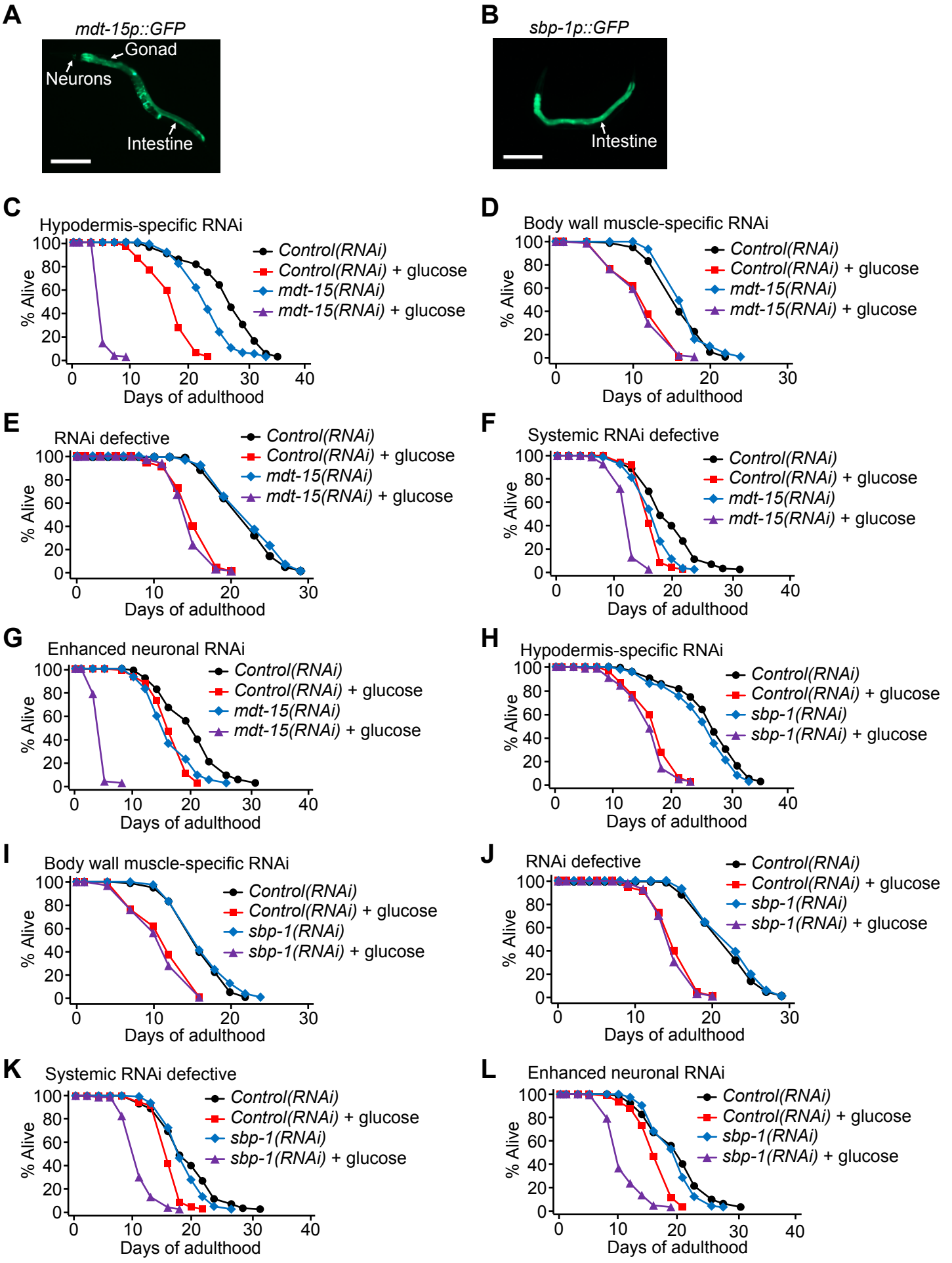
A
mdt-15p::GFP
Gonad
Neurons
Intestine
B
sbp-1p::GFP
Intestine
C
Hypodermis-specific RNAi
D
Body wall muscle-specific RNAi
E
RNAi defective
F
Systemic RNAi defective
G
Enhanced neuronal RNAi
H
Hypodermis-specific RNAi
I
Body wall muscle-specific RNAi
J
RNAi defective
K
Systemic RNAi defective
L
Enhanced neuronal RNAi
% Alive
Days of adulthood
Control(RNAi)
Control(RNAi) + glucose
mdt-15(RNAi)
mdt-15(RNAi) + glucose
sbp-1(RNAi)
sbp-1(RNAi) + glucose

Figure S5. Hypodermis- or neuron-specific knockdown of *mdt-15* further decreases the lifespan of glucose-fed worms. (**A**,**B**) *mdt-15p::GFP* was expressed in the intestine, several neurons in the head, and gonads (**A**), whereas *sbp-1p::GFP* was strongly expressed in the intestine (**B**). These data are consistent with previous reports (Taubert et al., 2006; Mckay et al., 2003). Worms are at day 1 adulthood and scale bars indicate 200 μm. (**C**) *mdt-15* RNAi specifically in the hypodermis by using a *wrt-2* promoter-driven *rde-1* in an RNAi-defective *rde-1(ne219)* mutant background further decreased the short lifespan of glucose-fed worms. This is not consistent with the result showing that the *mdt-15* promoter-driven GFP was undetectable in hypodermis shown in panel **A**. We speculate that our *mdt-15* promoter-driven GFP was expressed in the hypodermis but perhaps the expression was below a detection threshold. (**D**) RNAi targeting *mdt-15* in the body wall muscle (*rde-1* rescue by an *hlh-1* promoter-driven *rde-1* in an *rde-1* mutant background) did not influence lifespan. (**E**) *mdt-15* RNAi had little effect on the lifespan of the *rde-1* mutants. (**F**) *mdt-15* RNAi decreased the lifespan of systemic RNAi-defective *sid-1(pk3321)* mutants similarly on control and glucose-rich diets. Please note that *sid-1(pk3321)* mutants were not RNAi defective, at least for these lifespan assays. (**G**) *mdt-15* RNAi further decreased the lifespan of animals that are sensitive to neuronal RNAi (*sid-1(pk3321); unc-119p::sid-1*) upon glucose-rich diet feeding. These data suggest that hypodermal and neuronal MDT-15 contributes to preventing life-shortening effects of glucose together with the intestine (Fig. **2G**). (**H**) Hypodermis-specific *sbp-1* RNAi did not affect lifespan. (**I**) Knockdown of *sbp-1* by RNAi in the body wall muscle did not affect lifespan. (**J**) *sbp-1* RNAi did not influence the lifespan of the RNAi-defective *rde-1* mutant. (**K**,**L**) The life-shortening effects of *sbp-1* RNAi were similar on the lifespan of *sid-1(pk3321)* mutants (**K**) and *sid-1(pk3321); unc-119p::sid-1* worms (**L**) upon glucose feeding. Therefore, the results regarding the effects of

neuronal *sbp-1* RNAi on lifespan are negative. Our data indicate that SBP-1 functions in the intestine for reducing the lifespan-shortening effects of glucose, whereas MDT-15 acts in diverse tissues, including intestine, hypodermis and neurons. However, we cannot exclude the possibility that *sbp-1* RNAi efficiency was low in non-intestinal tissues. Thus, it will be important to rescue *mdt-15* and *sbp-1* in different tissues to further determine the tissue-specific roles of MDT-15 and SBP-1 in the lifespan-decreasing effects of dietary glucose. As MDT-15 is a mediator that interacts with many transcription factors, MDT-15 may function in the hypodermis or neurons with transcription factors other than SBP-1 (Taubert et al., 2006; Goh et al., 2014). Various nuclear receptors that regulate the expression of metabolic genes are potential interacting partners of MDT-15 (Arda et al., 2010). Future studies aiming the identification of other glucose-responsive MDT-15-interacting factors will provide insights into the tissue-specific roles of MDT-15 in the detoxification of glucose. See Supplemental Table S6 for additional repeats and statistical analysis for lifespan data shown in this figure.

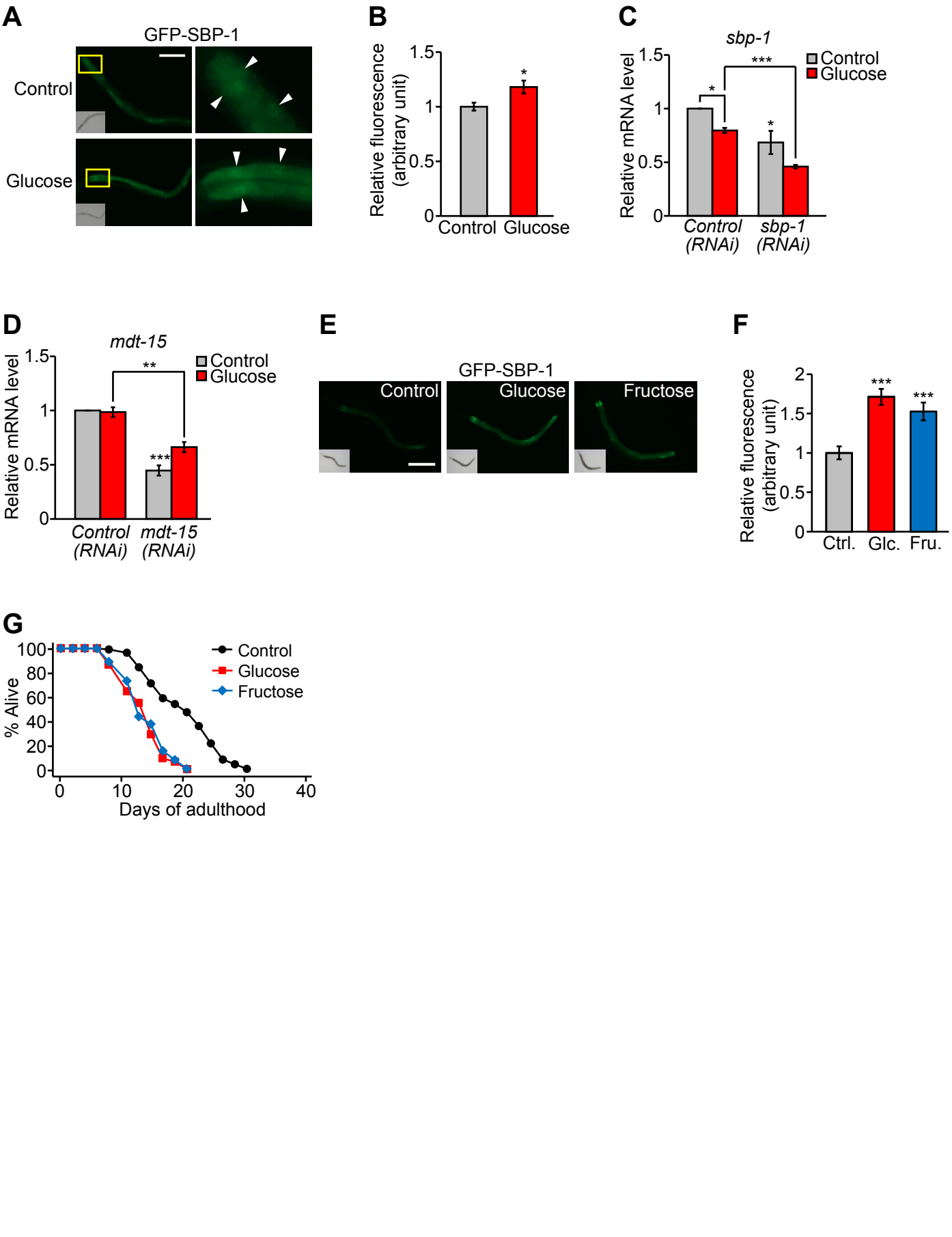
A
GFP-SBP-1
Control
Glucose
B
Relative fluorescence (arbitrary unit)
1.5
1
0.5
0
*
Control
Glucose
C
sbp-1
Relative mRNA level
1.5
1
0.5
0
*
***
*
Control
Glucose
Control (RNAi)
sbp-1 (RNAi)
D
mdt-15
Relative mRNA level
1.5
1
0.5
0
**
***
Control
Glucose
Control (RNAi)
mdt-15 (RNAi)
E
GFP-SBP-1
Control
Glucose
Fructose
F
Relative fluorescence (arbitrary unit)
2
1.5
1
0.5
0
***
***
Ctrl.
Glc.
Fru.
G
% Alive
100
80
60
40
20
0
0
10
20
30
40
Days of adulthood
Control
Glucose
Fructose

Figure S6. Glucose or fructose feeding up-regulates SBP-1. (**A**) Glucose-rich diet feeding increased the fluorescence intensity of GFP-SBP-1 proteins in intestinal cells of IJ582 *sbp-1p::GFP::sbp-1* animals (L4 larvae). Arrowheads indicate the intestinal nuclei (scale bar: 100 μm). Yellow boxes indicate the enlarged regions. (**B**) Quantification of the GFP levels in panel **A** (n=21 from three independent experiments). (**C**) *sbp-1* mRNA levels were not increased but rather decreased by glucose treatment. In addition, *sbp-1* RNAi significantly reduced the mRNA levels of *sbp-1* on both control and glucose-rich diets (n=3). Previously, glucose treatment was shown to increase the mRNA levels of mammalian *SREBP* (Hasty et al., 2000) and *C. elegans sbp-1* (Nomura et al., 2010). Moreover, high glucose treatments increase mature form of SREBP in nucleus (Guillet-Deniau et al., 2004). It is possible that glucose treatment increases mammalian SREBP levels at the transcription level and *C. elegans* SBP-1 at the post-transcriptional level. In the case of the difference between our data and those of Nomura et al., it is worth noting that the experimental conditions were different. We prepared plates containing 2% glucose (111 mM) and fed worms with glucose from hatching to day 1 adulthood. Nomura et al. cultured worms without glucose treatment until adulthood and then treated with 100 μl of glucose solution in various concentrations (0, 10, 100, and 500 mM) for 12 or 24 hours (Nomura et al., 2010). It will be important to extensively determine the possible mechanisms by which glucose up-regulates SREBP and SBP-1 in the future. (**D**) *mdt-15* mRNA levels were significantly reduced by *mdt-15* RNAi. Glucose feeding did not affect the expression of *mdt-15* mRNA (n=4). (**E**) Glucose or fructose feeding increased GFP levels in IJ1208 *sbp-1p::GFP::sbp-1* worms (day 1 adults). Scale bar indicates 200 μm. (**F**) Quantified GFP levels in panel **E** (n=21 from three independent experiments). A previous study showed that glucose increases the expression of SREBP, but fructose does not (Hasty et al., 2000). Our data suggest

that the effects of fructose on *C. elegans* SBP-1 and on mammalian SREBP are different. Error bars represent standard error of the mean (SEM) (two-tailed Student's *t*-test, **p*<0.05, ***p*<0.01, ****p*<0.001). (**G**) Additional glucose or fructose feeding decreased lifespan. See Supplemental Table S7 for additional repeats and statistical analysis for lifespan data shown in this figure.

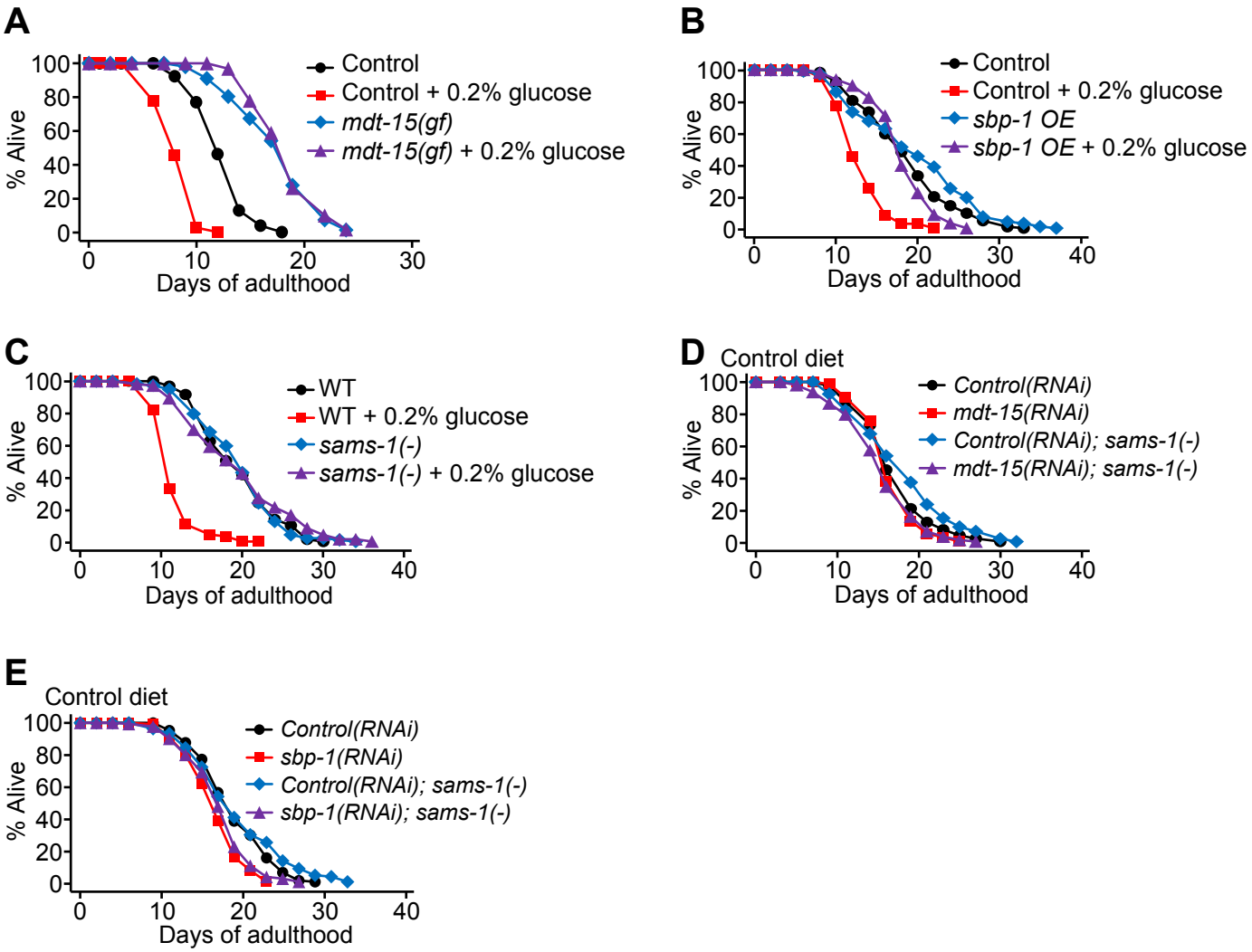
A
% Alive
Days of adulthood
Control
Control + 0.2% glucose
mdt-15(gf)
mdt-15(gf) + 0.2% glucose
B
% Alive
Days of adulthood
Control
Control + 0.2% glucose
sbp-1 OE
sbp-1 OE + 0.2% glucose
C
% Alive
Days of adulthood
WT
WT + 0.2% glucose
sams-1(-)
sams-1(-) + 0.2% glucose
D
Control diet
% Alive
Days of adulthood
Control(RNAi)
mdt-15(RNAi)
Control(RNAi); sams-1(-)
mdt-15(RNAi); sams-1(-)
E
Control diet
% Alive
Days of adulthood
Control(RNAi)
sbp-1(RNAi)
Control(RNAi); sams-1(-)
sbp-1(RNAi); sams-1(-)

Figure S7. Up-regulation of MDT-15 or SBP-1 suppresses the short lifespan of 0.2% glucose-fed worms. (**A**) *mdt-15(et14)* gain-of-function (*gf*) mutation fully suppressed the lifespan-shortening effect of 0.2% glucose. Please note that *paqr-2(tm3410)* mutant background was used for all four conditions, because *mdt-15(et14)* mutation is tightly linked (0.33 cM) with *paqr-2(tm3410)* (Svensk et al., 2013). (**B**) *sbp-1* overexpression (*OE*) restored lifespan of 0.2% glucose-fed worms. Transgenic worms carrying roller injection marker (CF1290) were used as a control. (**C**) *sams-1(ok3033)* [*sams-1(-)*] mutation suppressed the short lifespan of 0.2% glucose-fed animals. (**D**,**E**) Lifespan changes of *sams-1* mutants by *mdt-15* RNAi (**D**) or *sbp-1* RNAi (**E**) on control diets. See Supplemental Table S7 for additional repeats and statistical analysis for lifespan data shown in this figure.

Lee_Fig S8

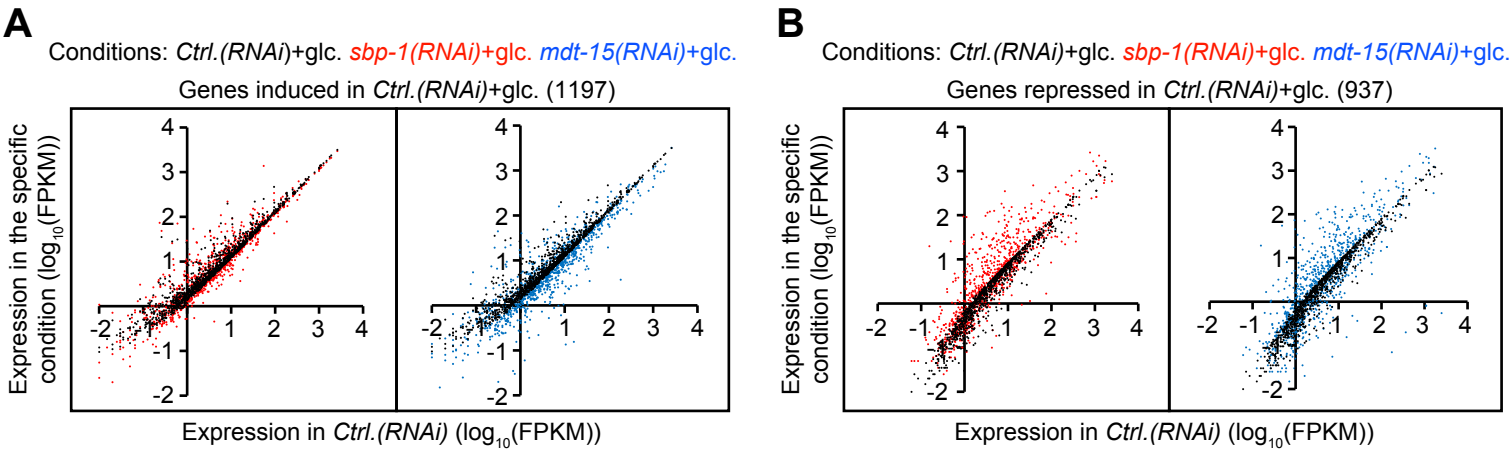
A
Conditions: Ctrl.(RNAi)+glc. sbp-1(RNAi)+glc. mdt-15(RNAi)+glc.
Genes induced in Ctrl.(RNAi)+glc. (1197)
Expression in the specific condition (log10(FPKM))
Expression in Ctrl.(RNAi) (log10(FPKM))
B
Conditions: Ctrl.(RNAi)+glc. sbp-1(RNAi)+glc. mdt-15(RNAi)+glc.
Genes repressed in Ctrl.(RNAi)+glc. (937)
Expression in the specific condition (log10(FPKM))
Expression in Ctrl.(RNAi) (log10(FPKM))

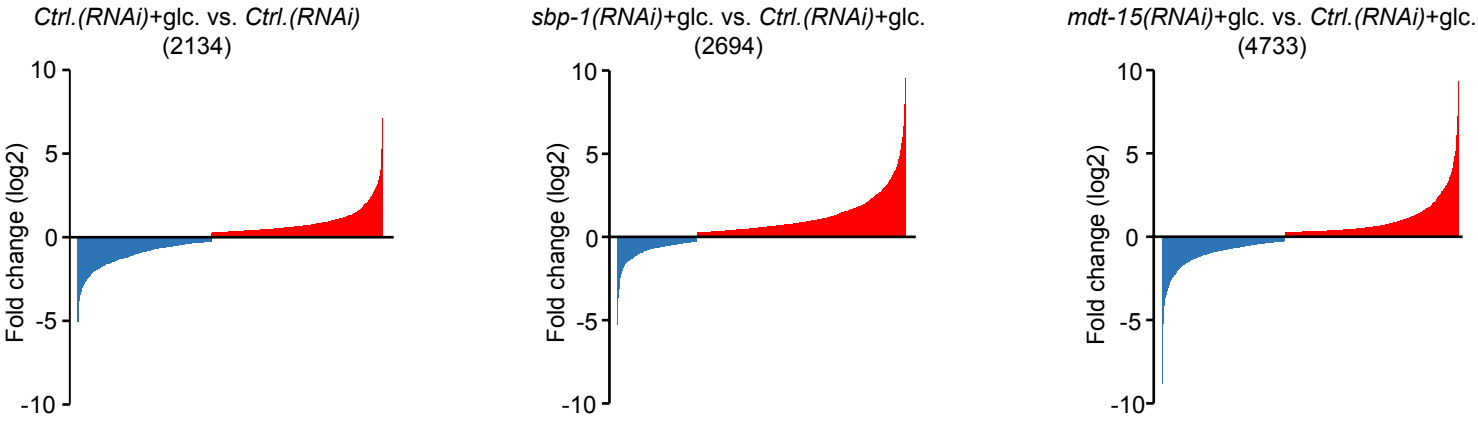
C
Ctrl.(RNAi)+glc. vs. Ctrl.(RNAi)
(2134)
Fold change (log2)
D
sbp-1(RNAi)+glc. vs. Ctrl.(RNAi)+glc.
(2694)
Fold change (log2)
E
mdt-15(RNAi)+glc. vs. Ctrl.(RNAi)+glc.
(4733)
Fold change (log2)


F
Repressed by sbp-1(RNAi) (1842)
Repressed by mdt-15(RNAi) (1530)
1017
825
705
G
Induced by sbp-1(RNAi) (2907)
Induced by mdt-15(RNAi) (5220)
860
2047
3173

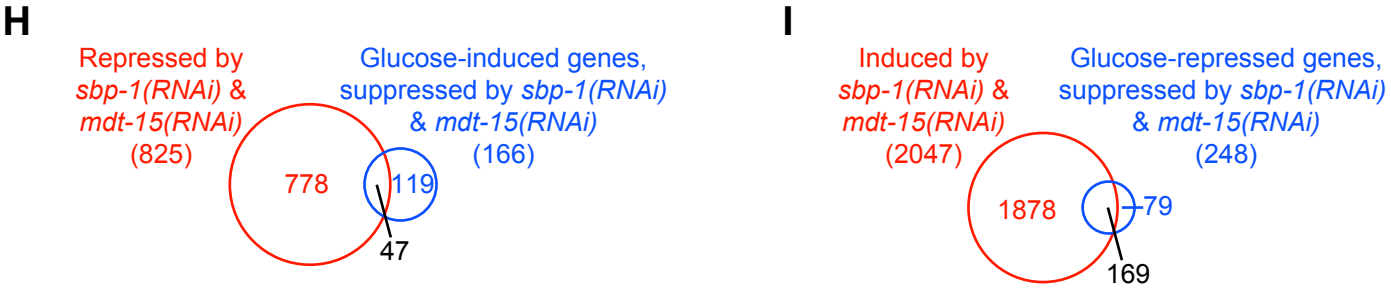
H
Repressed by sbp-1(RNAi) & mdt-15(RNAi) (825)
Glucose-induced genes, suppressed by sbp-1(RNAi) & mdt-15(RNAi) (166)
778
119
47
I
Induced by sbp-1(RNAi) & mdt-15(RNAi) (2047)
Glucose-repressed genes, suppressed by sbp-1(RNAi) & mdt-15(RNAi) (248)
1878
79
169

Figure S8. mRNA sequencing analysis for genes whose expression is influenced by glucose feeding, *mdt-15* RNAi, and/or *sbp-1* RNAi. (**A**) Glucose-rich diet (glc.)-induced genes that were differentially expressed by *sbp-1* RNAi or *mdt-15* RNAi. *Ctrl.(RNAi)* indicates control RNAi-treated wild-type (N2) animals. (**B**) Glucose-rich diet-repressed genes regulated by *sbp-1* RNAi or *mdt-15* RNAi. Numbers on axes indicate $\log_{10}$ scale of FPKM (fragments per kilobase of transcript per million fragments). (**C**-**E**) Fold changes of genes whose expression was significantly (p<0.05 and fold change>1.2; Yao et al., 2015) affected by glucose-rich diet feeding (**C**), *sbp-1* RNAi (**D**), and *mdt-15* RNAi (**E**). (**F**,**G**) Venn diagrams show overlaps between genes down-regulated (**F**) or up-regulated (**G**) in *sbp-1(RNAi)* and *mdt-15(RNAi)* in control diet-fed conditions. The overlaps of genes in both panel **F** and panel **G** were significant (p=0, hypergeometric probability test). (**H**) A Venn diagram shows an overlap between glucose-induced genes that were repressed by both *sbp-1* RNAi and *mdt-15* RNAi (Fig. **4C**), and genes that were repressed by both *sbp-1* RNAi and *mdt-15* RNAi on a control diet (**F**). (**I**) A Venn diagram indicates an overlap between glucose-repressed genes that were induced by both *sbp-1* RNAi and *mdt-15* RNAi (Fig. **4D**), and genes that were induced by both *sbp-1* RNAi and *mdt-15* RNAi on a control diet (**G**). The overlaps were significant ($p<10^{-23}$ in panel **H** and $p<10^{-94}$ in panel **I**, hypergeometric probability test), and the overlapping genes are shown in Supplemental Table S8. Please see the Materials and Methods for statistics used for calculating the significance of the overlaps.

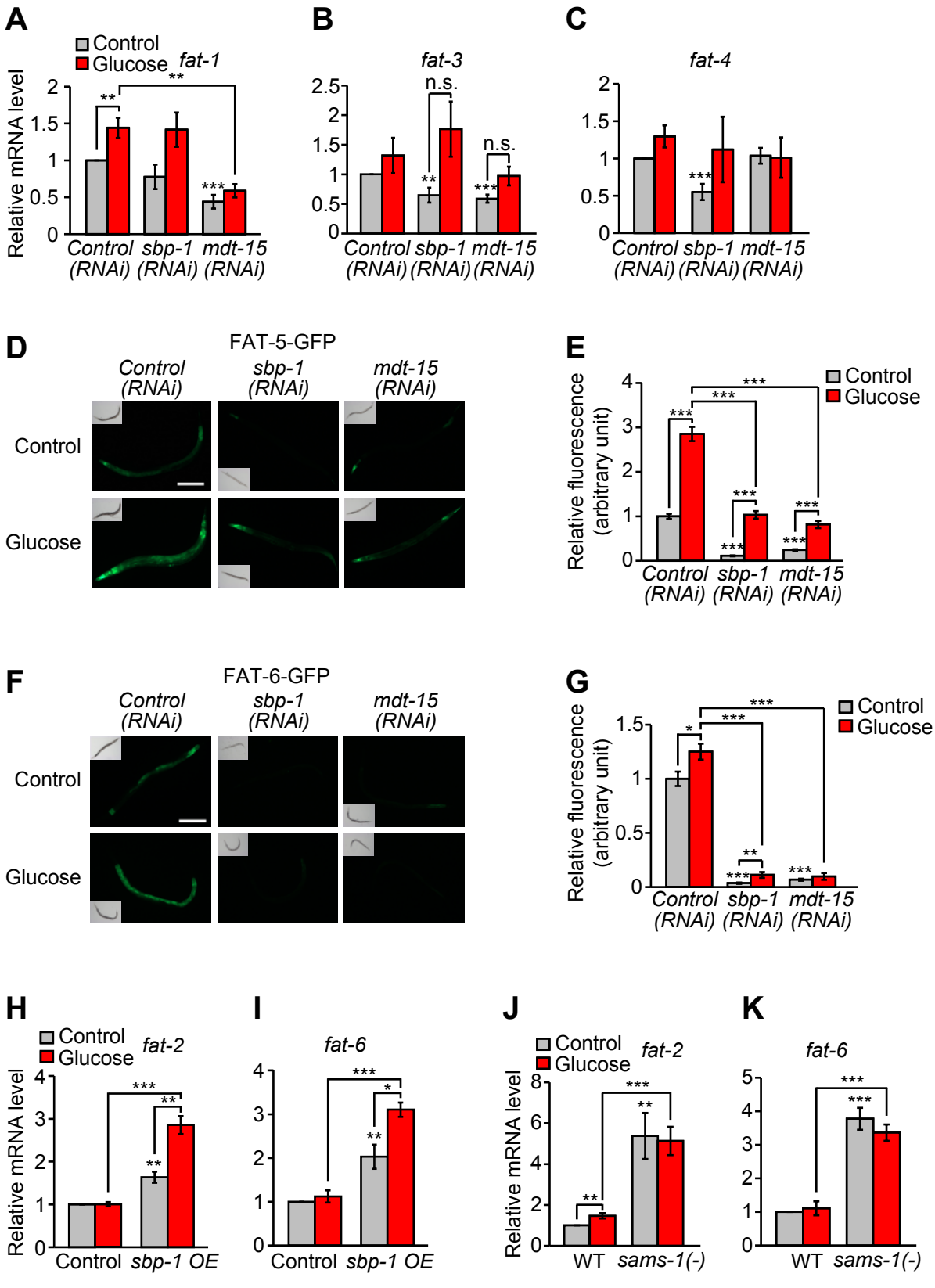
A
Control
Glucose
fat-1
Relative mRNA level
Control (RNAi)
sbp-1 (RNAi)
mdt-15 (RNAi)
B
fat-3
n.s.
C
fat-4
D
FAT-5-GFP
Control (RNAi)
sbp-1 (RNAi)
mdt-15 (RNAi)
Control
Glucose
E
Relative fluorescence (arbitrary unit)
F
FAT-6-GFP
G
H
fat-2
Control
sbp-1 OE
I
fat-6
J
WT
sams-1(-)
K

Figure S9. Fatty acid desaturases are repressed by inhibition of MDT-15 or SBP-1. (**A**-**C**) qRT-PCR data for measuring mRNA levels of *fat-1* (**A**), *fat-3* (**B**), and *fat-4* (**C**) in *control(RNAi)*, *mdt-15(RNAi)* and *sbp-1(RNAi)* worms on control or glucose-rich diets (n≥4). (**D**) Glucose-induced *fat-5p::fat-5::GFP* (FAT-5-GFP) was significantly suppressed by RNAi knockdown of *sbp-1* or *mdt-15* (scale bar: 200 μm). (**E**) Quantification of the data in **D** (n≥21 from three independent experiments). (**F**) RNAi targeting *sbp-1* or *mdt-15* decreased the level of *fat-6p::fat-6::GFP* (FAT-6-GFP), which was induced upon glucose feeding (scale bar: 200 μm). (**G**) Quantification of the data in **F** (n≥21 from three independent experiments). (**H**,**I**) Changes in mRNA levels of *fat-2* (**H**) and *fat-6* (**I**) by *sbp-1* overexpression (*OE*) were measured by using qRT-PCR (n=4). Injection marker (roller)-transgenic worms (CL2070) were used as a control. (**J**,**K**) *sams-1(ok3033)* mutation [*sams-1(-)*] increased the mRNA levels of *fat-2* (**J**) and *fat-6* (**K**) (n=5). Note that the induction of *fat-2* and *fat-6* by glucose-rich diet feeding was marginal at best in panels **H-K**, different from the data shown in Fig. **5D**,**F**. The *E. coli* strain HT115 was used for RNAi experiments in Fig. **5D**,**F**, whereas OP50 was used in the panels **H-K**. We therefore speculate that the glucose-responsive induction of *fat-2* and *fat-6* was sensitive to bacterial strains, as OP50 and HT115 have different metabolite compositions (Brooks et al., 2009). Error bars indicate SEM (two-tailed Student's *t*-test, **p*<0.05, ***p*<0.01, ****p*<0.001, n.s.: not significant (p≥0.05). See Supplemental Table S7 for additional repeats and statistical analysis for lifespan data shown in this figure.

Lee_Fig S10

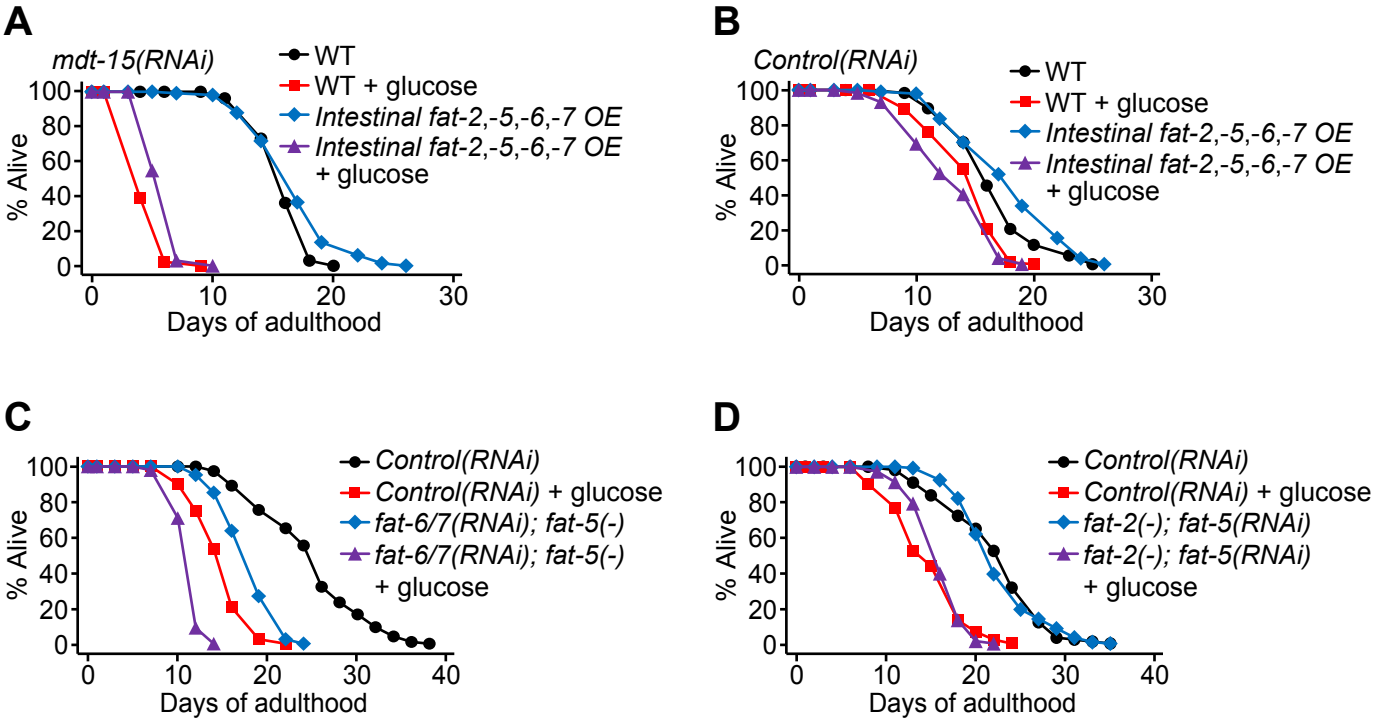
A
mdt-15(RNAi)
WT
WT + glucose
Intestinal fat-2,-5,-6,-7 OE
Intestinal fat-2,-5,-6,-7 OE + glucose
% Alive
Days of adulthood
B
Control(RNAi)
WT
WT + glucose
Intestinal fat-2,-5,-6,-7 OE
Intestinal fat-2,-5,-6,-7 OE + glucose
% Alive
Days of adulthood
C
Control(RNAi)
Control(RNAi) + glucose
fat-6/7(RNAi); fat-5(-)
fat-6/7(RNAi); fat-5(-) + glucose
% Alive
Days of adulthood
D
Control(RNAi)
Control(RNAi) + glucose
fat-2(-); fat-5(RNAi)
fat-2(-); fat-5(RNAi) + glucose
% Alive
Days of adulthood

Figure S10. Intestinal overexpression of fatty acid desaturases partly suppressed very short lifespan of *mdt-15(RNAi)* worms on a glucose-rich diet. (**A**) Overexpression of *fat-2*, *fat-5*, *fat-6*, and *fat-7* in the intestine (*intestinal fat-2,-5,-6,-7 OE*: *ges-1p::fat-2,-5,-6,-7*) partly suppressed the short lifespan of *mdt-15* RNAi-treated worms in a glucose-rich condition. We found that the expression of *ges-1* was decreased by *mdt-15* RNAi in our RNA sequencing data (data not shown). In addition, *mdt-15* expression in non-intestinal tissues, including neurons and hypodermis, contributed to the protection against the glucose toxicity (Supplemental Fig. **S5C**,**G**). Thus, we speculate that the effects of intestinal *fat-2*, *-5*, *-6* and *-7* transgenes in *mdt-15(RNAi)* animals are not strong as those in *sbp-1(RNAi)* animals (Fig. **5M**). (**B**) Intestinal overexpression of *fat-2*, *fat-5*, *fat-6*, and *fat-7* by using a *ges-1* promoter marginally increased the lifespan of control diet-fed worms, while slightly decreasing that of glucose-rich diet-fed worms. (**C**,**D**) The lifespan of *fat-6*/*7* RNAi-treated *fat-5(tm420)* mutants (**C**) and *fat-5* RNAi-treated *fat-2(wa17)* mutants (**D)**. Both RNAi treatments decreased lifespan similarly with or without additional dietary glucose. See Supplemental Table S7 for additional repeats and statistical analysis for lifespan data shown in this figure.

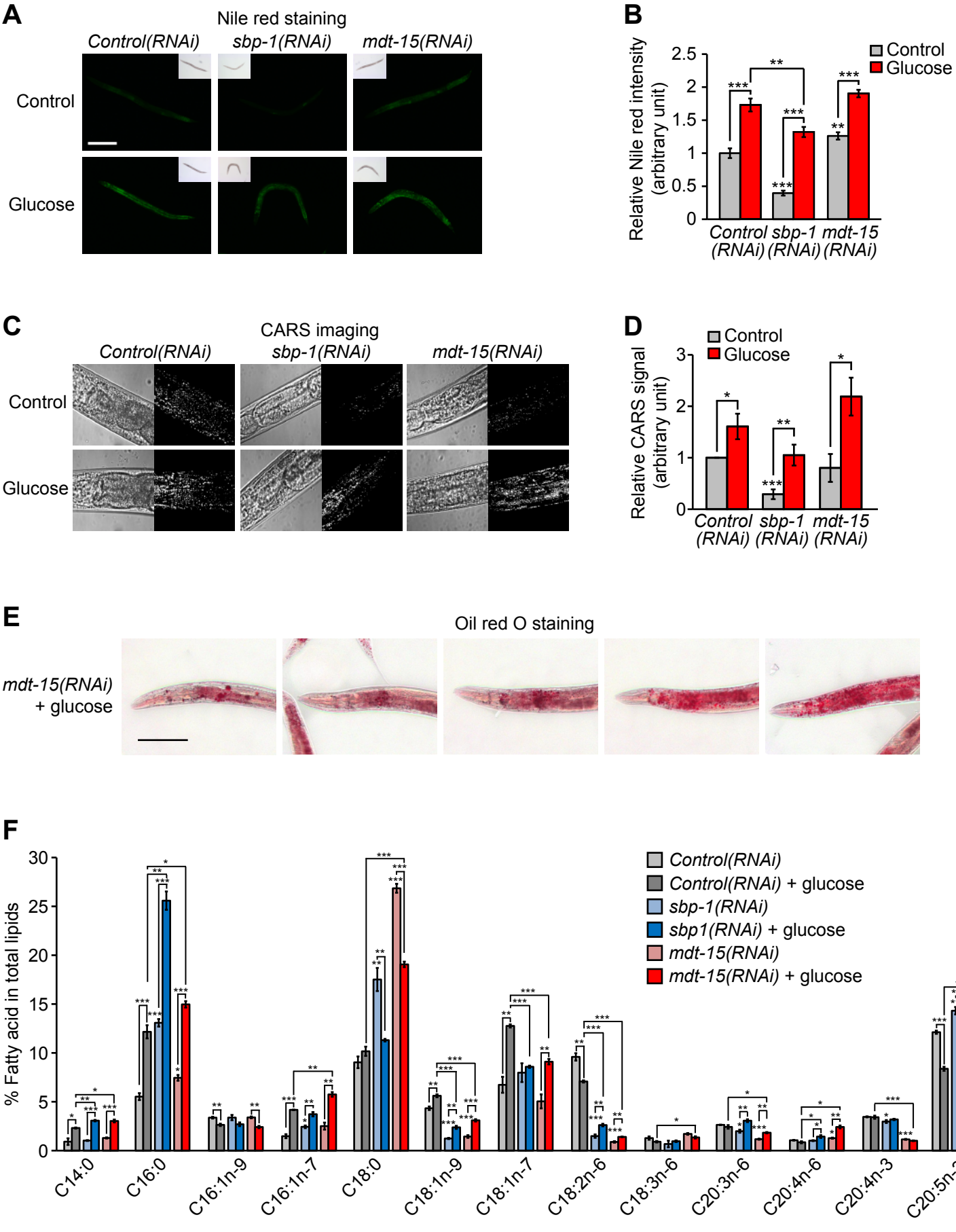
A
Nile red staining
Control(RNAi)
sbp-1(RNAi)
mdt-15(RNAi)
Control
Glucose
B
Relative Nile red intensity (arbitrary unit)
Control
Glucose
Control (RNAi)
sbp-1 (RNAi)
mdt-15 (RNAi)
C
CARS imaging
Control(RNAi)
sbp-1(RNAi)
mdt-15(RNAi)
Control
Glucose
D
Relative CARS signal (arbitrary unit)
Control
Glucose
Control (RNAi)
sbp-1 (RNAi)
mdt-15 (RNAi)
E
Oil red O staining
mdt-15(RNAi) + glucose
F
% Fatty acid in total lipids
Control(RNAi)
Control(RNAi) + glucose
sbp-1(RNAi)
sbp1(RNAi) + glucose
mdt-15(RNAi)
mdt-15(RNAi) + glucose
C14:0
C16:0
C16:1n-9
C16:1n-7
C18:0
C18:1n-9
C18:1n-7
C18:2n-6
C18:3n-6
C20:3n-6
C20:4n-6
C20:4n-3
C20:5n-3

Figure S11. Knockdown of *mdt-15* or *sbp-1* increased the level of saturated fatty acids in glucose-fed worms. (**A**) *sbp-1(RNAi)* or *mdt-15(RNAi)* worms treated with or without additional glucose were fixed and stained with Nile red (scale bar: 200 μm). (**B**) Quantification of the data in panel **A** (n≥20 from three independent experiments). (**C**) Representative images taken by using coherent anti-Stokes Raman scattering (CARS) of *mdt-15(RNAi)* or *sbp-1(RNAi)* worms with or without glucose-rich diet treatment. Images were represented as flattened 60 to 80 frames by Z-projection using ImageJ. Backgrounds were extracted by changing brightness and contrast. (**D**) Quantification of the CARS images in panel **C** (n=5). (**E**) Representative Oil red O images of glucose-fed *mdt-15(RNAi)* worms that displayed variable staining patterns (scale bar: 100 μm). (**F**) Gas chromatography/mass spectrometry (GC/MS) data showing changes in the individual fatty acid levels in *sbp-1(RNAi)* or *mdt-15(RNAi)* worms in control diet- or glucose-rich diet-fed conditions (n=3). Percent of individual fatty acids in total fatty acids (mole/mole) was calculated. Saturated fatty acids (C14:0 and C16:0) were further increased by inhibition of *sbp-1* or *mdt-15* upon glucose feeding. Knockdown of *sbp-1* or *mdt-15* significantly reduced the levels of monounsaturated fatty acids (C18:1n-9 and C18:1n-7) and a polyunsaturated fatty acid (C18:2n-6) on a glucose-rich diet. Error bars represent SEM (two-tailed Student's *t*-test, **p*<0.05, ***p*<0.01, ****p*<0.001).

Lee_Fig S12

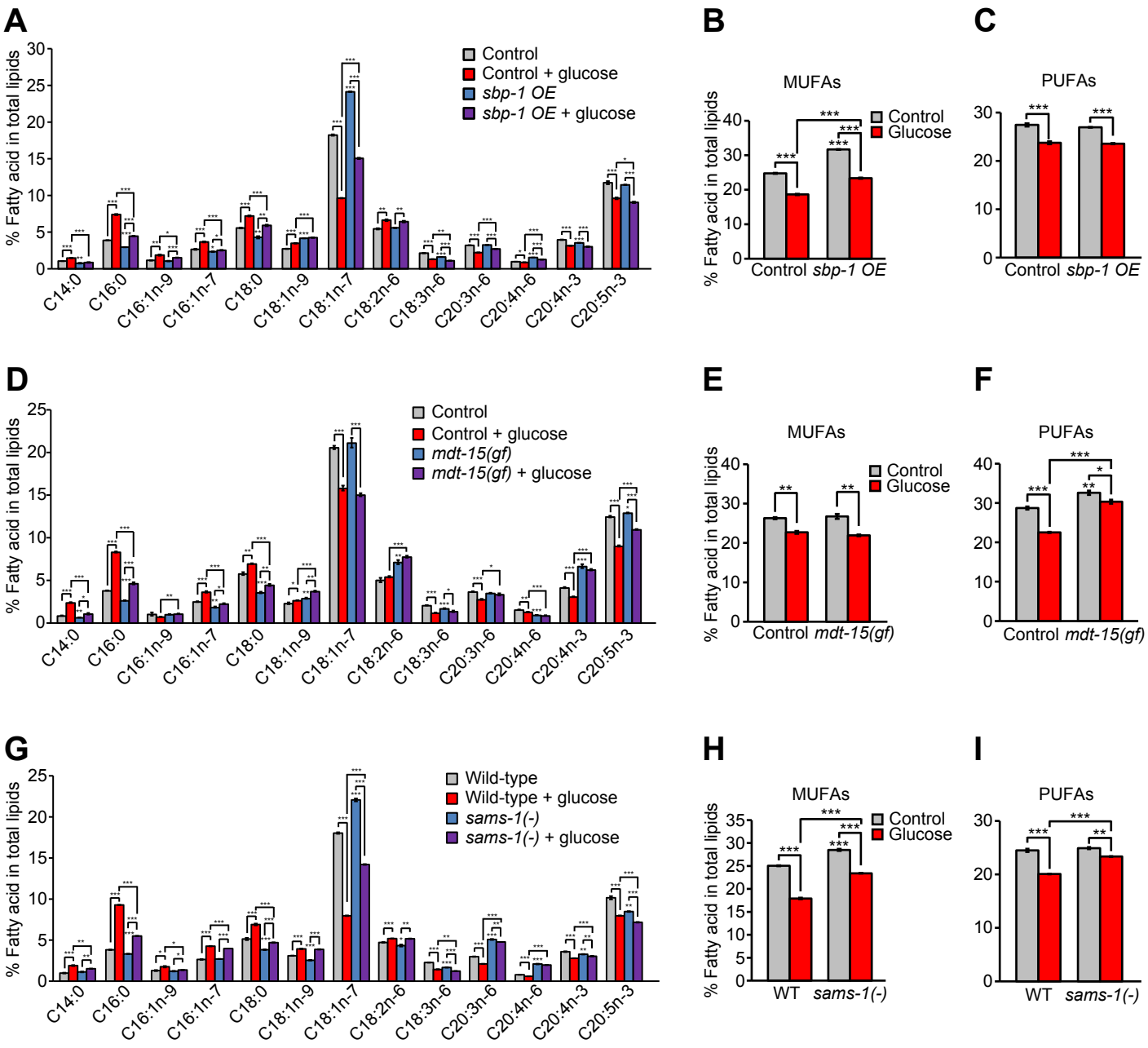
A
% Fatty acid in total lipids
Control
Control + glucose
sbp-1 OE
sbp-1 OE + glucose
C14:0
C16:0
C16:1n-9
C16:1n-7
C18:0
C18:1n-9
C18:1n-7
C18:2n-6
C18:3n-6
C20:3n-6
C20:4n-6
C20:4n-3
C20:5n-3
B
MUFAs
% Fatty acid in total lipids
Control
Glucose
Control
sbp-1 OE
C
PUFAs
Control
sbp-1 OE
D
% Fatty acid in total lipids
Control
Control + glucose
mdt-15(gf)
mdt-15(gf) + glucose
E
MUFAs
% Fatty acid in total lipids
Control
Glucose
Control
mdt-15(gf)
F
PUFAs
Control
mdt-15(gf)
G
% Fatty acid in total lipids
Wild-type
Wild-type + glucose
sams-1(-)
sams-1(-) + glucose
H
MUFAs
% Fatty acid in total lipids
Control
Glucose
WT
sams-1(-)
I
PUFAs
WT
sams-1(-)

Figure S12. *sbp-1* overexpression, *mdt-15* gain-of-function, or *sams-1* mutation reduces the accumulation of saturated fatty acids on glucose-rich diets. (**A**) Gas chromatography/mass spectrometry (GC/MS) data displaying changes in the levels of individual fatty acids by *sbp-1* overexpression (*OE*) with or without additional glucose feeding (n=3). Percents of individual fatty acids in total fatty acids (mole/mole) were calculated. All measured SFAs (C14:0, C16:0, and C18:0) were significantly decreased in *sbp-1* overexpression (*OE*) worms. *sbp-1 OE* reduced the levels of MUFAs containing 16 carbons (C16:1n-9 and C16:1n-7) on a glucose-rich diet, while increasing MUFAs containing 18 carbons (C18:1n-9 and C18:1n-7). *sbp-1 OE* had small or no effects on PUFA levels. IJ893 *sbp-1p::GFP::sbp-1* and control (IJ1243) worms were treated with glucose from hatching to day 1 adult stage. (**B**,**C**) The levels of overall monounsaturated fatty acids (MUFAs) (**B**) and polyunsaturated fatty acids (PUFAs) (**C**). Total MUFAs are the sum of C16:1n-9, C16:1n-7, C18:1n-9, and C18:1n-7; total PUFAs are the sum of C18:2n-6, C18:3n-6, C20:3n-6, C20:4n-6, C20:4n-3, and C20:5n-3, which are shown in panel **A**. *sbp-1 OE* animals displayed elevation in MUFA (**B**), but no changes in PUFA levels (**C**). (**D**) Percent fatty acid composition in *mdt-15(et14)* gain-of-function (*gf*) mutation (n=3). *paqr-2(tm3410)* background was used for both control and *mdt-15(gf)* mutant animals (Svensk et al., 2013). *paqr-2(tm3410)* and *mdt-15(et14) paqr-2(tm3410)* worms were treated with glucose from L4 stage for 24 hours. The *mdt-15(gf)* worms displayed lower levels of SFAs (C14:0, C16:0, and C18:0) than control worms. Among MUFAs, C16:1n-7 was decreased, C18:1n-9 was increased, and others (C16:1n-9 or C18:1n-7) displayed small or no changes in *mdt-15(gf)* animals. *mdt-15(gf)* worms contained higher levels of several PUFAs such as C18:2n-6, C20:4n-3, and C20:5n-3, while having lower levels of C20:4n-6 than control. (**E**,**F**) Shown are overall levels of MUFAs (**E**) and PUFAs (**F**) in *mdt-15(gf)* animals calculated form panel **D**. *mdt-15(gf)* did not

affect overall MUFA levels (**E**), but elevated overall PUFA levels (**F**). (**G**) Individual fatty acids in wild-type (N2) and *sams-1(ok3033)* mutants [*sams-1(-)*] treated with control or glucose-rich diets from hatching to day 1 adult stage (n=3). Consistent with data from *sbp-1 OE* or *mdt-15(gf)*, the levels of SFAs (C14:0, C16:0, and C18:0) were significantly decreased in *sams-1(-)* on a glucose-rich diet. *sams-1* mutation increased C18:1n-7 level, but had small or no effects on other MUFAs (C16:1n-9, C16:1n-7, or C18:1n-9). The levels of several PUFAs such as C20:3n-6 and C20:4n-6 were increased, whereas C18:3n-6, C20:4n-3, and C20:5n-3 levels were reduced by *sams-1* mutation. (**G**) *sams-1* mutation significantly incrased MUFA levels on control and glucose-enriched diets (**H**), and elevated PUFA levels only upon glucose feeding (**I**). These data imply that *sbp-1 OE*, *mdt-15(gf)*, or *sams-1(-)* consistently reduced SFA levels on control and glucose-rich diets. Please note that worms had lower levels of overall MUFAs on a glucose-rich diet than on a control diet. This is seemingly in contrast to the data showing that glucose feeding increased the levels of MUFAs shown in Fig. **6F**. One noticeable difference is that standard OP50 strain was used for mutant and transgenic animals in this figure, whereas HT115 strain was used for standard RNAi feeding experiments for Fig. **6F**. Therefore, we speculate that different bacterial food sources may have caused these variable results. Consistent with this idea, we found that the expression levels of several fatty acid desaturases upon glucose feeding were variable depending on bacterial food sources, as mentioned in Supplemental Fig **S9** legends. Error bars represent standard error of the mean (SEM) (two-tailed Student's *t*-test, *$p<0.05$, **$p<0.01$, ***$p<0.001$)

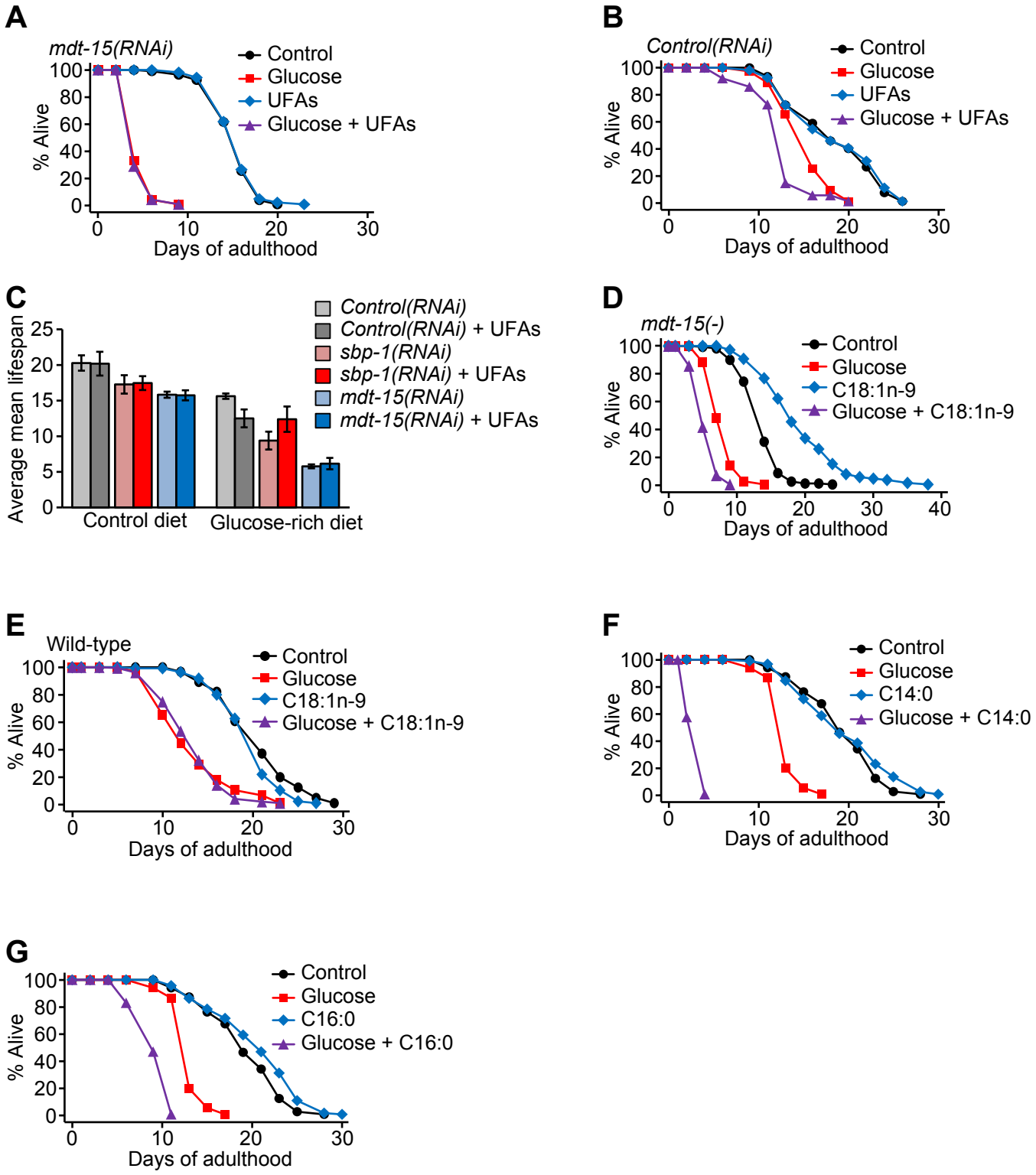
A
mdt-15(RNAi)
Control
Glucose
UFAs
Glucose + UFAs
% Alive
Days of adulthood
B
Control(RNAi)
Control
Glucose
UFAs
Glucose + UFAs
% Alive
Days of adulthood
C
Control(RNAi)
Control(RNAi) + UFAs
sbp-1(RNAi)
sbp-1(RNAi) + UFAs
mdt-15(RNAi)
mdt-15(RNAi) + UFAs
Average mean lifespan
Control diet
Glucose-rich diet
D
mdt-15(-)
Control
Glucose
C18:1n-9
Glucose + C18:1n-9
% Alive
Days of adulthood
E
Wild-type
Control
Glucose
C18:1n-9
Glucose + C18:1n-9
% Alive
Days of adulthood
F
Control
Glucose
C14:0
Glucose + C14:0
% Alive
Days of adulthood
G
Control
Glucose
C16:0
Glucose + C16:0
% Alive
Days of adulthood

Figure S13. The effects of fatty acid feeding on dietary glucose-induced short lifespan. (**A**) Dietary UFA mixture (UFAs: 600 μM of C18:1n-9, C18:1n-7, and C18:2n-6 with 0.1% NP-40) did not rescue the short lifespan of *mdt-15(RNAi)* worms upon glucose-rich diet feeding (three out of five trials). NP-40 (0.1%) was added for all experimental conditions in panels **A**-**C**, **F**, and **G**. Please note that the curves look very similar, but they are not identical. (**B**) Feeding UFAs decreased the lifespan of glucose-rich diet-fed worms, while not changing the lifespan of control diet-fed worms. We speculate that additional UFAs may have down-regulated fatty acid desaturases via a feedback mechanism, and this may in turn increase the level of SFAs and may decrease lifespan on a high-glucose diet. Consistent with this idea, fat metabolism is tightly regulated by feedback mechanisms (Ye and DeBose-Boyd, 2011). (**C**) Average mean lifespan data from the UFA feeding experiments that were repeated five times. UFA treatments partly suppressed the short lifespan of glucose-fed *sbp-1(RNAi)* worms (Fig. **7A**), but the effects were variable (Supplemental Table S9). Error bars represent standard error of the mean (SEM). (**D**) Oleic acid (C18:1n-9) supplementation (600 μM) increased the lifespan of *mdt-15(tm2182)* mutants [*mdt-15(-)*] on a control diet, while further decreasing lifespan on a glucose-rich diet. (**E**) Oleic acid (C18:1n-9) feeding did not alter the lifespan of wild-type with or without additional dietary glucose. UFA treatment has been shown to suppress the short lifespan of *mdt-15(RNAi)* worms (Taubert et al., 2006) and to increase the lifespan of wild-type (O'Rourke et al., 2013). We observed that UFA mixture feeding slightly increased the lifespan of *mdt-15(RNAi)* worms only one out of five experiments. Probably, different composition or amount of UFAs (100 μM C20:5 and 100 μM C20:3n-6 in Taubert et al., 2006; 10 μM C20:3n-6 or 10 μM C20:4n-6 in O'Rourke et al., 2013) exert different effects on lifespan. (**F**) Addition of myristic acid (C14:0, 600 μM) greatly shortened the lifespan of glucose-treated worms. (**G**) Palmitic acid

(C16:0, 600 μM) treatment further reduced the short lifespan of worms fed with a glucose-enriched diet. See Supplemental Table S9 for additional repeats and statistical analysis for lifespan data shown in this figure.

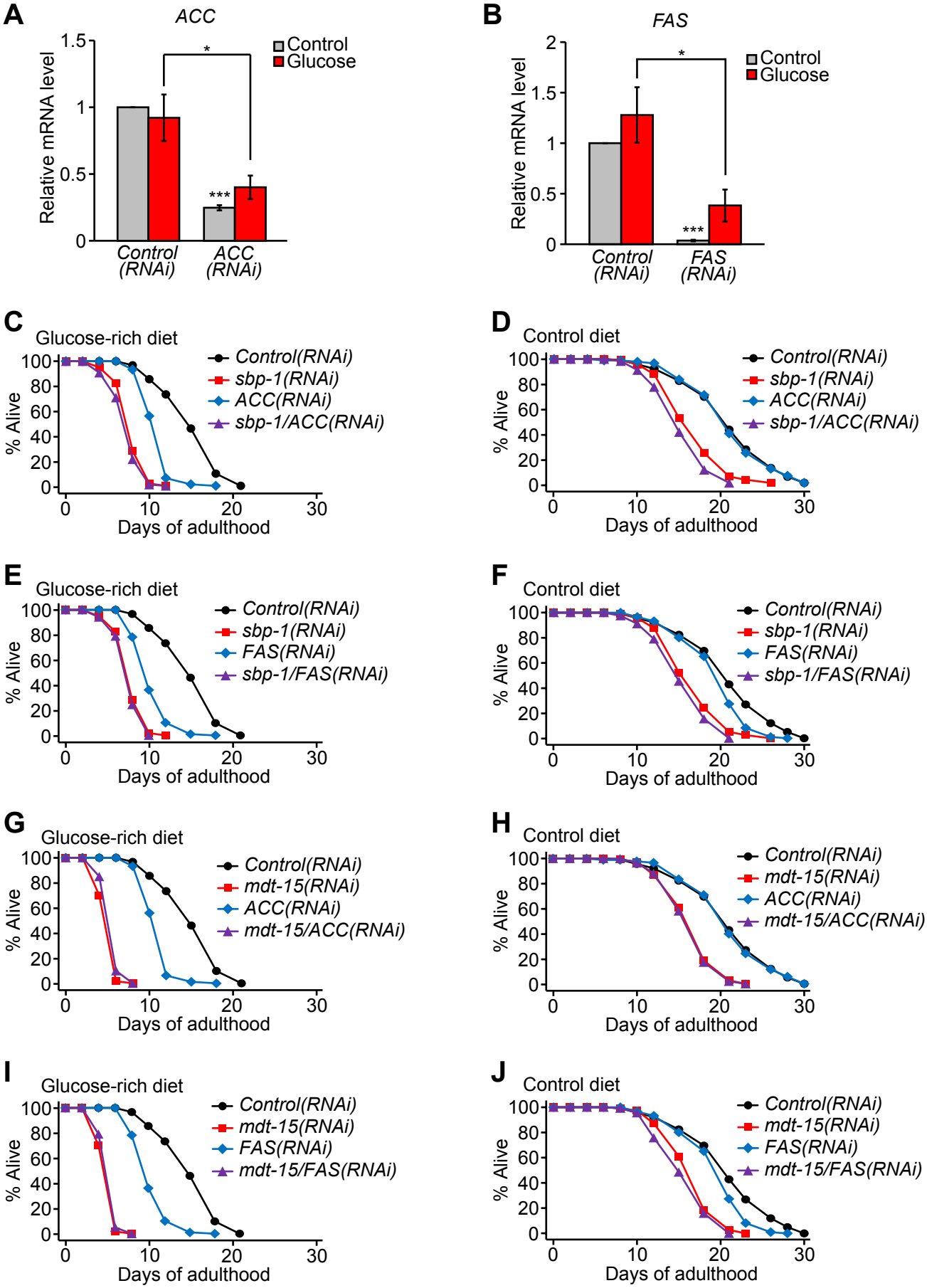
A
ACC
Relative mRNA level
Control
Glucose
Control (RNAi)
ACC (RNAi)
B
FAS
Relative mRNA level
Control
Glucose
Control (RNAi)
FAS (RNAi)
C
Glucose-rich diet
% Alive
Days of adulthood
Control(RNAi)
sbp-1(RNAi)
ACC(RNAi)
sbp-1/ACC(RNAi)
D
Control diet
% Alive
Days of adulthood
Control(RNAi)
sbp-1(RNAi)
ACC(RNAi)
sbp-1/ACC(RNAi)
E
Glucose-rich diet
% Alive
Days of adulthood
Control(RNAi)
sbp-1(RNAi)
FAS(RNAi)
sbp-1/FAS(RNAi)
F
Control diet
% Alive
Days of adulthood
Control(RNAi)
sbp-1(RNAi)
FAS(RNAi)
sbp-1/FAS(RNAi)
G
Glucose-rich diet
% Alive
Days of adulthood
Control(RNAi)
mdt-15(RNAi)
ACC(RNAi)
mdt-15/ACC(RNAi)
H
Control diet
% Alive
Days of adulthood
Control(RNAi)
mdt-15(RNAi)
ACC(RNAi)
mdt-15/ACC(RNAi)
I
Glucose-rich diet
% Alive
Days of adulthood
Control(RNAi)
mdt-15(RNAi)
FAS(RNAi)
mdt-15/FAS(RNAi)
J
Control diet
% Alive
Days of adulthood
Control(RNAi)
mdt-15(RNAi)
FAS(RNAi)
mdt-15/FAS(RNAi)

Figure S14. Acetyl-CoA carboxylase (ACC) and fatty acid synthase (FAS) appear to act in the same pathway with SBP-1/MDT-15 to regulate lifespan on a glucose-rich diet. (**A**,**B**) mRNA levels of *ACC*/*pod-2* (n=5) (**A**) and *FAS*/*fasn-1* (n=4) (**B**) were significantly reduced by respective RNAi treatments. (**C**-**F**) Shown are the lifespan of animals treated with *sbp-1*/*ACC* double RNAi on a glucose-rich diet (**C**) and on a control diet (**D**), and with *sbp-1*/*FAS* double RNAi on a glucose-rich diet (**E**) and on a control diet (**F**). *ACC* RNAi or *FAS* RNAi did not further decrease the short lifespan of glucose-treated *sbp-1(RNAi)* worms upon high-glucose feeding. Worms were grown on *sbp-1* RNAi bacteria and then moved to *sbp-1*/*ACC* RNAi or *sbp-1*/*FAS* RNAi plates at day 1 adulthood. *sbp-1* RNAi, *mdt-15* RNAi, *ACC* RNAi, or *FAS* RNAi bacteria were mixed with control RNAi bacteria (dilution to 50%) for single RNAi treatments for lifespan assays in this figure. (**G-J**) Effects of *mdt-15*/*ACC* double RNAi on lifespan in a glucose-rich condition (**G**) and in a control diet condtion (**H**). The effects of *mdt-15*/*FAS* double RNAi on lifespan upon feeding a glucose-rich diet (**I**) or a control diet (**J**). *mdt-15*/*ACC* double RNAi or *mdt-15*//*FAS* double RNAi showed lifespan-shortening effects comparable to *mdt-15* RNAi upon glucose feeding. Worms cultured on control RNAi bacteria were transferred to *mdt-15* RNAi, *mdt-15*/*ACC* RNAi, or *mdt-15*/*FAS* RNAi bacteria at day 1 adulthood. These data suggest that SBP-1/MDT-15, and ACC and FAS act in the same pathway for lifespan regulation upon glucose feeding. One caveat is that *mdt-15(RNAi)* animals and *sbp-1(RNAi)* animals may have lived too short to display further decrease in lifespan upon high-glucose feeding. See Supplemental Table S9 for additional repeats and statistical analysis for lifespan data shown in this figure.

Lee_Fig S15

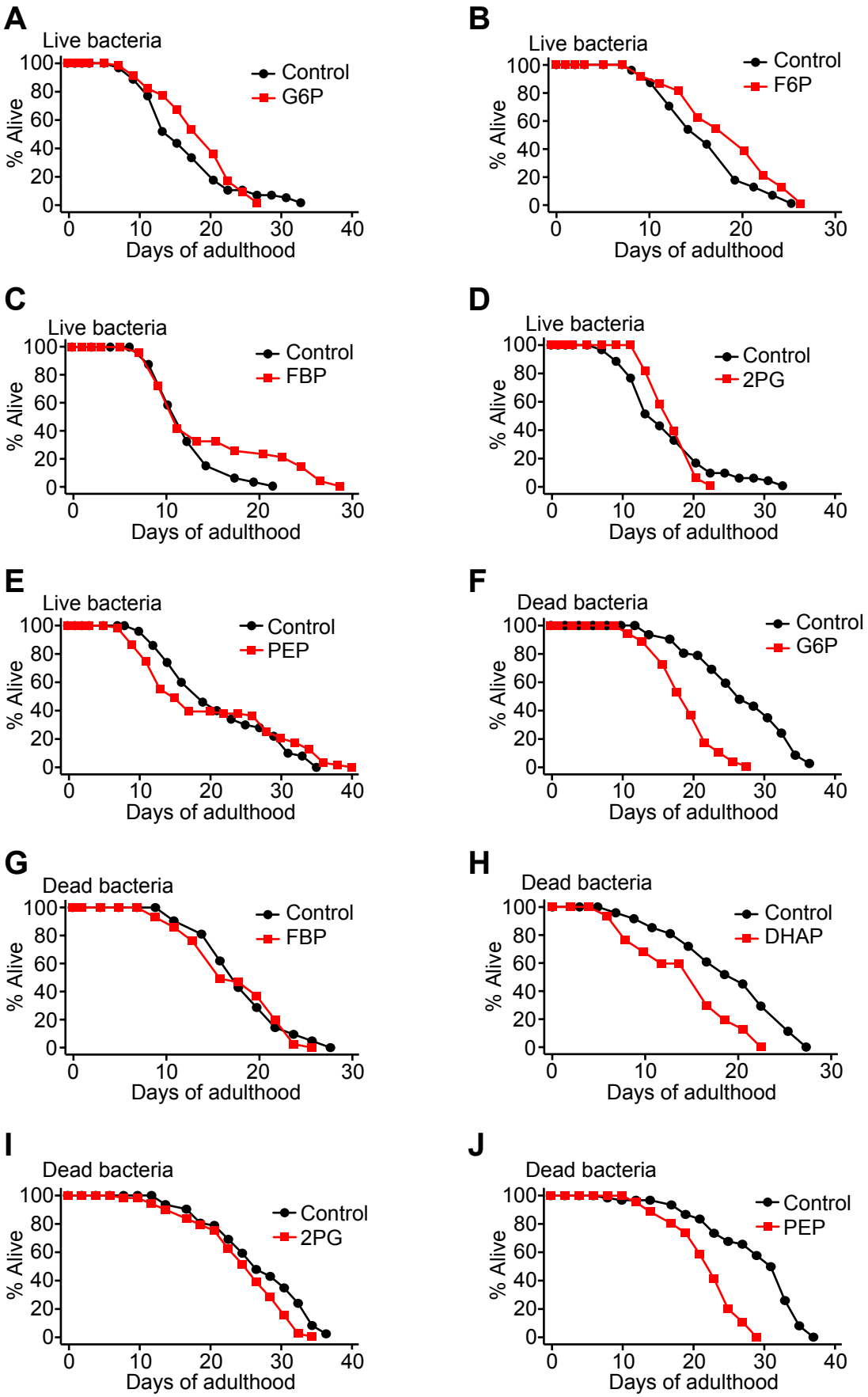
A
Live bacteria
Control
G6P
% Alive
Days of adulthood
B
Live bacteria
Control
F6P
% Alive
Days of adulthood
C
Live bacteria
Control
FBP
% Alive
Days of adulthood
D
Live bacteria
Control
2PG
% Alive
Days of adulthood
E
Live bacteria
Control
PEP
% Alive
Days of adulthood
F
Dead bacteria
Control
G6P
% Alive
Days of adulthood
G
Dead bacteria
Control
FBP
% Alive
Days of adulthood
H
Dead bacteria
Control
DHAP
% Alive
Days of adulthood
I
Dead bacteria
Control
2PG
% Alive
Days of adulthood
J
Dead bacteria
Control
PEP
% Alive
Days of adulthood

Figure S15. Effects of glycolytic intermediate metabolites on lifespan. Live bacteria were used for food sources in panels in **A**-**E**, and dead bacteria were used in panels in **F**-**J**. (**A**) Glucose-6-phosphate sodium salt (G6P, 111 mM) did not significantly influence lifespan. NaCl (111 mM) was used as a salt control in panels **A**, **D**, **F**, and **I**. (**B**) Fructose-6-phosphate disodium salt (111 mM) feeding increased lifespan. NaCl (222 mM) was used as a salt control. (**C**) Addition of fructose-1,6-bisphosphate trisodium salt (FBP, 111 mM) resulted in a slight lifespan extension, but the change was not significant (p=0.0824). NaCl (333 mM) was used as a salt control. (**D**) Mean lifespan was not influenced by 2-phosphoglycerate sodium salt (2PG, 111 mM) treatment. (**E**) Phosphoenolpyruvate potassium salt (PEP, 111 mM) did not influence lifespan. KCl (111 mM) was used as a control in panels **E** and **J**. (**F**) Glucose-6-phosphate sodium salt (G6P, 111 mM) reduced lifespan. NaCl (111 mM) was used as a salt control. (**G**) Fructose-1,6-bisphosphate trisodium salt (FBP, 111 mM) treatment did not affect lifespan. NaCl (333 mM) was used as a salt control. (**H**) Dihydroxyacetone phosphate lithium salt (DHAP, 111 mM)-treated worms displayed short lifespan compared to control (111 mM LiCl)-treated worms. (**I**) The lifespan of animals was not significantly affected by treatment with 2-phosphoglycerate sodium salt (2PG, 111 mM). (**J**) The lifespan of phosphoenolpyruvate potassium salt (PEP, 111 mM)-treated animals. Some glycolysis intermediates were not tested due to following reasons. Glyceraldehyde-3-phosphate (G3P) was supplied as a solution and the concentration (276 mM) is lower than the stock concentration (1.11 M) required for our experiments; 1,3-bisphosphoglycerate or 3-phosphoglycericerate was not commercially available; bacterial lawn became very crispy by treating with pyruvate and therefore worms did not seem to feed on the bacteria properly. Please note that we needed at least 250-500 mg of reagents to prepare plates that contained chemicals at concentrations comparable to 2% glucose (111 mM). See

Supplemental Table S9 for additional repeats and statistical analysis for lifespan data shown in this figure.

Supplemental Tables

Table S1. Summary of data reagarding *far-3p::GFP* suppressor RNAi clones

Gene ID	Gene name	Description	Lifespan change (%)		
			Control diet condition	Glucose-rich diet condition	Glucose specificity
R12B2.5	*mdt-15*	Mediator subunit orthologous to human MED15	-10	-61	-51
F29G6.3[#]	*hpo-34*	Hypersensitive to pore-forming toxin	+29	-14	-43
C35A5.8[#]	*C35A5.8*	Exportin-7	-18	-44	-26
C01G8.9	*let-526*	A homolog of a component of the SWI/SNF complex	+1	-20	-21
F09G2.4	*cpsf-2*	Cleavage and polyadenylation specificity factor subunit 2	+18	-1	-19
K10C3.6	*nhr-49*	HNF4 (hepatocyte nuclear factor 4) family of NHRs	-32	-46	-14
H19N07.1[#]	*erfa-3*	An ortholog of human G1 to S phase transition 1	+1	-9	-10
C26D10.2	*hel-1*	ATP-dependent RNA helicase DDX39	+4	-5	-9
F23H11.5	*F23H11.5*	Unknown	+3	-5	-8
T27E9.7	*abcf-2*	ATP-binding cassette sub-family F member 2	+4	-4	-8
T26A8.4	*T26A8.4*	Zinc finger CCCH domain-containing protein 4	-39	-46	-7
F40F4.6[#]	*F40F4.6*	Wnt inhibitory factor 1	+1	-6	-7
F13B10.1	*tir-1*	Sterile alpha and TIR motif-containing protein 1	-9	-16	-7
Y65B4BR.5	*icd-2*	Nascent polypeptide-associated complex subunit alpha	-23	-29	-6
ZC410.1	*nhr-11*	HNF4 (hepatocyte nuclear factor 4) family of NHRs	-5	-10	-5
Y113G7B.23	*swsn-1*	SWI/SNF complex subunit SMARCC1	-6	-10	-4
B0286.4	*ntl-2*	CCR4-NOT transcription complex subunit 2	-18	-22	-4
Y48G1A.5	*xpo-2*	Exportin-2	-8	-11	-3
C56C10.8	*icd-1*	Nascent polypeptide-associated complex subunit beta	+9	+6	-3

C46G7.1	*C46G7.1*	Ribonuclease kappa	+3	+2	-1
C11D9.1[#]	*tiam-1*	T-lymphoma invasion and metastasis-inducing protein 2	-6	-7	-1
F11C1.6	*nhr-25*	Orphan nuclear receptor NR5A2	-4	-4	0
F22D6.2	*F22D6.2*	AN1-type zinc finger protein 6	+17	+17	0
T08G11.5[#]	*unc-29*	Neuronal acetylcholine receptor subunit alpha-4	+10	+10	0
K04G7.3	*ogt-1*	O-linked N-acetylglucosamine (O-GlcNAc) transferase	-12	-12	0
F21A3.1	*srh-276*	Serpentine receptor, class H	0	0	0
T20H4.4	*adr-2*	Double-stranded RNA-specific adenosine deaminase	+8	+11	+3
Y22D7AR.5	*glb-30*	Neuroglobin	+1	+4	+3
F32D1.2	*hpo-18*	Hypersensitive to pore-forming toxin	-2	+2	+4
F46C8.1[#]	*F46C8.1*	Unknown	+3	+7	+4
ZK354.5	*msp-51*	Vesicle-associated membrane protein-associated protein A	-4	+1	+5
T05A10.1	*sma-9*	Zinc finger protein 853	+2	+7	+5
Y55F3C.3	*kvs-5*	Potassium voltage-gated channel subfamily B member 2	-2	+4	+6
F25G6.9	*F25G6.9*	Unknown	-4	+3	+7
R08C7.1	*R08C7.1*	Unknown	-4	+3	+7
C49A1.2[#]	*best-10*	Bestrophin-3	-4	+3	+7
C29F9.1	*C29F9.1*	Unknown	-20	-12	+8
C45E1.4[#]	*C45E1.4*	Unknown	-9	+1	+10
F59E11.2	*F59E11.2*	Dehydrogenase/reductase SDR family member 1	-8	+3	+11
Y50E8A.12	*Y50E8A.12*	THAP or THAP-like domain-containing protein	-9	+3	+12
ZK829.7	*ZK829.7*	Sorbitol dehydrogenase	-4	+9	+13
C07H6.5	*cgh-1*	ATP-dependent RNA helicase DDX6	-53	-35	+18
F35F11.3	*F35F11.3*	F-box C proteins homolog	-8	+15	+23
M04G12.1[#]	*tag-260*	Interferon regulatory factor 2-binding protein 2	-24	0	+24

Lifespan change (%) indicates percent change of mean lifespan by specific RNAi compared to that of control RNAi, in a control

diet condition or a glucose-rich diet condition as shown.

The lifespan change (%) is an average of two independent lifespan assay data except some RNAi clones that were tested once ([#]).

Glucose-specificity was calculated by subtracting the lifespan change (%) in a control diet condition from the lifespan change (%) in a glucose-rich diet condition.

Genes were sorted by the ascending order of glucose specificity.

See Supplemental Table S3 for repeats and statistical analysis for lifespan data shown in this table.

Table S2. The list of *far-3p::GFP* enhancer RNAi clones

Gene ID	Gene name	Description
B0334.10	*B0334.10*	Unknown
B0336.3	*B0336.3*	RNA-binding protein 26
B0393.1	*rps-0*	40S ribosomal protein SA
B0395.2	*mboa-1*	Acyl-CoA:cholesterol ('sterol') O-acyltransferase
B0511.6	*B0511.6*	ATP-dependent RNA helicase DDX18
C01C10.1	*clc-2*	Claudin-like in Caenorhabditis
C01G10.1	*C01G10.1*	Unknown
C01H6.5	*nhr-23*	Nuclear receptor ROR-beta

C04B4.3	*lips-2*	Lipase-related protein
C04F12.4	*rpl-14*	Ribosomal protein L14 variant
C05C8.7	*phi-49*	Mannose-6-phosphate isomerase
C05D11.8	*C05D11.8*	Protein FAM160A1
C06A1.1	*cdc-48.1*	Transitional endoplasmic reticulum ATPase
C08F1.3	*fbxb-13*	F-box B protein
C08F1.9	*C08F1.9*	Unknown
C10G11.5	*pnk-1*	Pantothenate kinase 4
C12C8.3	*lin-41*	Tripartite motif-containing protein 71
C13B9.3	*copd-1*	Coatomer subunit delta
C14B9.4	*plk-1*	Serine/threonine-protein kinase PLK2
C16A3.3	*let-716*	Protein RRP5 homolog
C17E4.5	*pabp-2*	Polyadenylate-binding protein 2
C18D11.3	*C18D11.3*	Unknown
C18F10.2	*C18F10.2*	Unknown
C26E6.2	*flh-2*	FLYWCH zinc finger transcription factor
C27H6.2	*ruvb-1*	RuvB-like 1
C29A12.1	*C29A12.1*	Unknown
C29E4.2	*kle-2*	Condensin-2 complex subunit H2
C29F3.5	*clec-230*	C-type lectin
C29H12.3	*rgs-3*	Regulator of G-protein signaling 8
C34E10.6	*atp-2*	ATP synthase subunit beta
C34G6.6	*noah-1*	PAN and ZP domain-containing protein
C36B1.4	*pas-4*	Proteasome subunit alpha type-7
C41D11.9	*C41D11.9*	TM2 domain-containing protein 3
C42D8.5	*acn-1*	ACE (angiotensin converting enzyme)-like protein

C45B2.7	*ptr-4*	Niemann-Pick C1 protein
C47B2.4	*pbs-2*	Proteasome subunit beta type-7
C47D12.6	*tars-1*	Threonyl amino-acyl tRNA synthetase
C47E12.4	*pyp-1*	Inorganic pyrophosphatase
C50B6.3	*C50B6.3*	Unknown
C50C3.6	*prp-8*	Pre-mRNA-processing-splicing factor 8
C52E4.3	*snr-4*	Small nuclear ribonucleoprotein Sm D2
C52E4.4	*rpt-1*	26S protease regulatory subunit 7
C54G10.3	*pmp-3*	ABC transporter
C55B7.2	*gly-2*	Alpha-1,6-mannosylglycoprotein 6-beta-N-acetylglucosaminyltransferase A
C56G2.6	*let-767*	Steroid dehydrogenase
CD4.6	*pas-6*	Proteasome subunit alpha type-1
D1081.8	*phi-7*	Cell division cycle 5-like protein
E02A10.1	*mrps-5*	28S ribosomal protein S5
E04A4.5	*E04A4.5*	Mitochondrial import inner membrane translocase subunit Tim17-B
EGAP2.3	*pho-1*	Prostatic acid phosphatase
F01F1.12	*aldo-2*	Fructose-bisphosphate aldolase
F07A11.6	*din-1*	Msx2-interacting protein
F12F6.6	*sec-24.1*	Protein transport protein Sec24C
F14B4.3	*rpoa-2*	DNA-directed RNA polymerase I subunit RPA2
F22E5.8	*F22E5.8*	BTB/POZ domain-containing adapter for CUL3-mediated RhoA degradation protein 3
F23B12.4	*F23B12.4*	Ferric-chelate reductase 1
F26A10.2	*F26A10.2*	MDS1 and EVI1 complex locus protein EVI1
F26F4.11	*rpb-8*	DNA-directed RNA polymerases I, II, and III subunit RPABC3
F26H9.6	*rab-5*	Ras-related protein Rab-5B
F29G9.4	*fos-1*	Proto-oncogene c-Fos

F30H5.1	*unc-45*	Protein that contains an N-terminal TRP (tetratricopeptide repeat)
F31E3.1	*ceh-20*	Pre-B-cell leukemia transcription factor 2
F32D1.10	*mcm-7*	DNA replication licensing factor MCM7
F32H2.5	*fasn-1*	Fatty acid synthase
F33C8.1	*tag-53*	Attractin
F36A2.6	*rps-15*	40S ribosomal protein S15
F37C12.11	*rps-21*	40S ribosomal protein S21
F37C12.9	*rps-14*	40S ribosomal protein S14
F37E3.1	*ncbp-1*	Nuclear cap-binding protein subunit 1
F37H8.4	*sfxn-1.2*	Sideroflexin (mitochondrial iron transporter)
F39H11.5	*pbs-7*	Proteasome subunit beta type-4
F40F8.10	*rps-9*	40S ribosomal protein S9
F43E2.2	*rpb-4*	DNA-directed RNA polymerase II subunit RPB4
F44B9.3	*cit-1.2*	Cyclin-K
F48C1.1	*aman-3*	Alpha-mannosidase 2
F49E8.2	*F49E8.2*	Unknown
F53B7.3	*F53B7.3*	Pre-mRNA-splicing factor ISY1 homolog
F53B7.4	*F53B7.4*	Unknown
F53F4.11	*F53F4.11*	Ribosomal L1 domain-containing protein 1
F54B8.3	*fbxa-69*	F-box A protein
F55C10.4	*F55C10.4*	Unknown
F55C5.8	*srpa-68*	Signal recognition particle 68 kDa protein
F56B3.2	*F56B3.2*	Unknown
H02I12.5	*H02I12.5*	Unknown
H13N06.3	*gob-1*	Trehalose-6-phosphatase
H37A05.1	*lpin-1*	Phosphatidate phosphatase LPIN1, LPIN2, and LPIN3

K04G7.10	*rnp-7*	U1 small nuclear ribonucleoprotein 70 kDa
K06B4.4	*K06B4.4*	Unknown
K07C5.4	*K07C5.4*	Nucleolar protein 56
K08A8.2	*sox-2*	Transcription factor SOX-2
K08D12.1	*pbs-1*	Proteasome subunit beta type-6
K08E3.6	*cyk-4*	Rac GTPase-activating protein 1
K11E8.1	*unc-43*	Calcium/calmodulin-dependent protein kinase type II subunit delta
K12D12.1	*top-2*	DNA topoisomerase 2
M01E11.4	*pqn-52*	Prion-like-(Q/N-rich)- domain-bearing protein
M01G12.14	*M01G12.14*	Unknown
M03F4.6	*phi-61*	Unknown
M03F8.3	*phi-12*	Crooked neck-like protein 1
M110.5	*dab-1*	Disabled homolog 2
R05H10.1	*R05H10.1*	Unknown
R10D12.7	*R10D12.7*	Unknown
R11A8.6	*iars-1*	Isoleucyl-tRNA synthetase
R11A8.7	*R11A8.7*	Ankyrin repeat and KH domain-containing protein 1
R74.3	*xbp-1*	X-box-binding protein 1
T01C3.8	*mut-15*	Mutator
T01E8.3	*plc-3*	Phospholipase C gamma
T01G9.6	*kin-10*	Casein kinase II subunit beta
T01G9.6	*kin-10*	Casein kinase II subunit beta
T04A8.6	*T04A8.6*	MKI67 FHA domain-interacting nucleolar phosphoprotein
T05E11.1	*rps-5*	40S ribosomal protein S5
T05G11.6	*srw-55*	Serpentine receptor, class W
T05G5.3	*cdk-1*	Cyclin-dependent kinase

T05H4.6	*etf-1*	Eukaryotic peptide chain release factor subunit 1
T06G6.8	*T06G6.8*	Unknown
T08A11.2	*phi-11*	Splicing factor 3B subunit 1
T08B2.10	*rps-17*	40S ribosomal protein S17
T08B2.9	*fars-1*	Phenylalanyl-t-RNA synthetase
T09E8.2	*him-17*	High incidence of males
T10F2.4	*prp-19*	Pre-mRNA-processing factor 19
T12F5.4	*lin-59*	Probable histone-lysine N-methyltransferase ASH1L
T13H5.4	*phi-8*	Splicing factor 3A subunit 3
T14B4.7	*dpy-10*	Cuticle collagen protein
T14F9.1	*vha-15*	V-type proton ATPase subunit H
T14G10.5	*T14G10.5*	Coatomer subunit gamma-2
T16H12.4	*T16H12.4*	General transcription factor IIH subunit 2
T19B10.2	*phi-59*	Unknown
T19D12.8	*sra-26*	Serpentine receptor, class A (alpha)
T20B12.3	*T20B12.3*	Nucleolar complex protein 4 homolog
T20B12.8	*hmg-4*	FACT (facilitates chromatin transcription) complex subunit SSRP1
T20G5.1	*chc-1*	Clathrin heavy chain 1
T22D1.10	*ruvb-2*	RuvB-like 2
T22D1.9	*rpn-1*	26S proteasome non-ATPase regulatory subunit 2
T23B5.1	*prmt-3*	Protein arginine N-methyltransferase 10
T26E3.3	*par-6*	PDZ-domain-containing protein
T27A10.6	*T27A10.6*	Proteoglycan 4
T27B1.2	*pat-9*	Zinc finger protein 544
W02A2.1	*fat-2*	Delta-12 fatty acyl desaturase
W04G3.1	*lpr-6*	Lipocalin-related protein

W04G3.8	*lpr-3*	Lipocalin-related protein
W08E3.1	*snr-2*	SM-B of small nuclear ribonucleoprotein-associated proteins B and B'
W08F4.6	*mlt-8*	Molting defective
W09B6.1	*pod-2*	Acetyl-CoA carboxylase 2
Y110A7A.11	*use-1*	Vesicle transport protein USE1
Y111B2A.11	*epc-1*	Enhancer of polycomb homolog 2
Y116A8C.35	*uaf-2*	Splicing factor U2AF 35 kDa subunit isoform b
Y116A8C.42	*snr-1*	Small nuclear ribonucleoprotein Sm D3
Y11D7A.9	*Y11D7A.9*	Post-GPI attachment to proteins factor 2
Y38C1BA.2	*snn-1*	Synapsin-2 isoform IIa
Y41C4A.9	*Y41C4A.9*	DIEXF (digestive organ expansion factor) homolog
Y41D4B.19	*npp-8*	Nuclear pore complex protein Nup155
Y46G5A.4	*snrp-200*	Small nuclear ribonucleoprotein
Y46G5A.6	*phi-3*	Unknown
Y47D9A.1	*Y47D9A.1*	Mannose-1-phosphate guanyltransferase alpha
Y47G6A.20	*rnp-6*	Poly(U)-binding-splicing factor PUF60
Y48G8AL.7	*Y48G8AL.7*	Unknown
Y49E10.1	*rpt-6*	26S protease regulatory subunit 8
Y53F4B.14	*Y53F4B.14*	Unknown
Y55F3AR.3	*cct-8*	T-complex protein 1 subunit theta
Y73B6A.7	*mir-1834*	MicroRNA
Y75B12B.5	*cyn-3*	Cyclophilin A
Y76A2B.3	*acs-5*	Fatty acid CoA synthetase
Y80D3A.6	*Y80D3A.6*	Unknown
Y82E9BR.16	*Y82E9BR.16*	Unknown
Y92C3B.2	*uaf-1*	Splicing factor U2AF 65 kDa subunit

ZC328.6	*ZC328.6*	Unknown
ZC64.3	*ceh-18*	POU-class homeodomain transcription factor
ZK112.2	*ncl-1*	Alpha of tripartite motif-containing protein 3
ZK328.2	*eftu-2*	U5 small nuclear ribonucleoprotein component isoform b
ZK652.1	*snr-5*	Small nuclear ribonucleoprotein F
ZK858.4	*mel-26*	Speckle-type POZ protein

Genes were sorted by the alphabetical order of Gene ID.

Table S3. Lifespan data of suppressor RNAi clones related to Figure 1 (and Supplemental Figure S1 and S2)

Strain/treatment	Mean lifespan ±s.e.m. (days)	75th percentile	% change	Number of animals that died/total	*p* value vs. control	Figure in text
WT/control RNAi	22.6±0.4	26		117/150		Fig. S1L
	22.6±0.4	26		123/150		
WT/control RNAi + glc.	15.5±0.3	18	-32%	75/150	<0.0001	Fig. S1L
	14.3±0.3	18	-34%	94/150	<0.0001	
WT/*far-3* RNAi	22.1±0.3	24	-3%	116/150	0.1289	Fig. S1L
	22.5±0.4	26	+4%	117/150	0.0469	
WT/*far-3* RNAi + glc.	15.5±0.3	18	-32%	62/150	<0.0001	Fig. S1L
	14.3±0.4	18	-34%	91/150	<0.0001	
WT/control RNAi	18.0±0.5	22		88/120		
	22.5±0.6	26		61/90		Fig. S2B
	20.8±0.6	23		76/90		
WT/control RNAi + glc.	17.2±0.4	20	-5%	74/120	0.0461	
	18.7±0.6	23	-17%	85/90	<0.0001	Fig. S2B
	16.7±0.6	17	-25%	80/90	<0.0001	
WT/*mdt-15* RNAi*$^{\gamma}$	17.6±0.3	19	-2%	90/120	0.1170	
*	18.4±0.4	22	-18%	76/90	<0.0001	
WT/*mdt-15* RNAi + glc.*$^{\gamma}$	5.7±0.1	9	-67% (-67%$^{ctrl+glc.}$)	76/90	<0.0001 (<0.0001$^{ctrl+glc.}$)	
*	8.5±0.2	13	-54% (-55%$^{ctrl+glc.}$)	83/90	<0.0001 (<0.0001$^{ctrl+glc.}$)	
WT/*let-526* RNAi*	19.2±0.5	22	+7%	87/120	0.1196	
*	21.5±0.6	26	-4%	72/90	0.2740	Fig. S2B
WT/*let-526* RNAi + glc.*	13.2±0.2	15	-31% (-23%	90/120	<0.0001 (<0.0001^{ctrl+}	

			ctrl+glc.)		glc.)	
*	15.6±0.3	19	-27% (-16% ctrl+glc.)	76/90	<0.0001 (<0.0001 ctrl+glc.)	Fig. S2B
WT/*nhr-25* RNAi*	19.0±0.6	22	+6%	78/120	0.1938	
*	19.6±0.5	22	-13%	72/90	0.0001	
WT/*nhr-25* RNAi + glc.*	16.8±0.3	20	-12% (-2% ctrl+glc.)	76/120	0.0001 (0.3278 ctrl+glc.)	
*	17.6±0.5	21	-11% (-6% ctrl+glc.)	79/90	0.0032 (0.0328 ctrl+glc.)	
WT/*hel-1* RNAi*	21.9±0.5	26	+22%	101/120	<0.0001	
*	19.6±0.5	22	-13%	48/90	0.0002	
WT/*hel-1* RNAi + glc.*	16.8±0.3	20	-24% (-2% ctrl+glc.)	93/120	<0.0001 (0.3268 ctrl+glc.)	
*	17.2±0.5	21	-12% (-8% ctrl+glc.)	74/90	0.0064 (0.0082 ctrl+glc.)	
WT/*swsn-1* RNAi*	18.6±0.5	22	+4%	99/120	0.4502	
*	19.1±0.5	22	-15%	68/90	<0.0001	
WT/*swsn-1* RNAi + glc.*	16.5±0.4	20	-12% (-4% ctrl+glc.)	61/120	0.0001 (0.2721 ctrl+glc.)	
*	15.6±0.5	19	-19% (-17% ctrl+glc.)	75/90	<0.0001 (<0.0001 ctrl+glc.)	
WT/*xpo-2* RNAi*	18.5±0.3	22	+3%	91/120	0.7283	
*	18.2±0.4	22	-19%	52/90	<0.0001	
WT/*xpo-2* RNAi + glc.*	14.0±0.3	17	-24% (-18% ctrl+glc.)	95/120	<0.0001 (<0.0001 ctrl+glc.)	
*	17.8±0.4	21	-2% (-5% ctrl+glc.)	76/90	0.3066 (<0.0001 ctrl+glc.)	
WT/*ntl-2* RNAi*	15.6±0.4	19	-13%	86/120	0.0001	
*	17.5±0.4	20	-22%	78/90	<0.0001	

WT/*ntl-2* RNAi + glc.*	13.4±0.3	15	-14% (-22% $^{ctrl+glc.}$)	46/120	0.0015 (<0.0001 $^{ctrl+glc.}$)	
*	14.4±0.3	17	-18% (-23% $^{ctrl+glc.}$)	74/90	<0.0001 (0.0009 $^{ctrl+glc.}$)	
WT/*icd-1* RNAi*	21.7±0.5	26	+21%	94/120	<0.0001	
*	20.1±0.6	23	-3%	73/90	0.4213	
WT/*icd-1* RNAi + glc.*	18.2±0.4	22	-16% (+6% $^{ctrl+glc.}$)	80/120	<0.0001 (0.0251 $^{ctrl+glc.}$)	
*	17.7±0.6	21	-12% (+6% $^{ctrl+glc.}$)	77/92	0.0142 (0.1508 $^{ctrl+glc.}$)	
WT/*F23H11.5* RNAi*	18.7±0.5	22	+4%	85/120	0.4046	
*	21.5±0.5	26	+3%	62/90	0.5175	
WT/*F23H11.5* RNAi + glc.*	15.7±0.4	20	-16% (-9% $^{ctrl+glc.}$)	78/120	<0.0001 (0.0094 $^{ctrl+glc.}$)	
*	16.4±0.6	21	-24% (-2% $^{ctrl+glc.}$)	76/90	<0.0001 (0.9859 $^{ctrl+glc.}$)	
WT/*C46G7.1* RNAi*	18.9±0.6	24	+5%	81/120	0.1754	
*	21.0±0.6	26	+1%	74/90	0.6934	
WT/*C46G7.1* RNAi + glc.*	18.0±0.4	22	-5% (+5% $^{ctrl+glc.}$)	83/120	0.0788 (0.0217 $^{ctrl+glc.}$)	
*	16.4±0.7	21	-22% (-2% $^{ctrl+glc.}$)	82/90	<0.0001 (0.8384 $^{ctrl+glc.}$)	
WT/*hpo-18* RNAi*	18.9±0.5	22	+5%	71/120	0.2760	
*	19.0±0.6	23	-9%	74/90	0.0596	
WT/*hpo-18* RNAi + glc.*	17.4±0.5	22	-8% (+1% $^{ctrl+glc.}$)	84/120	0.0376 (0.2246 $^{ctrl+glc.}$)	
*	17.0±0.6	21	-11% (+2% $^{ctrl+glc.}$)	81/92	0.059 (0.4344 $^{ctrl+glc.}$)	

WT/*cpsf-2* RNAi*	23.7±0.5	28	+32%	100/120	<0.0001	
*	21.7±0.6	26	+4%	72/91	0.2907	
WT/*cpsf-2* RNAi + glc.*	17.3±0.4	20	-27% (+1%$^{ctrl+glc.}$)	78/120	<0.0001 (0.7708$^{ctrl+glc.}$)	
*	16.3±0.6	21	-25% (-2%$^{ctrl+glc.}$)	83/90	<0.0001 (0.9806$^{ctrl+glc.}$)	
WT/*erfa-3* RNAi*	20.0±0.3	22	+11%	102/120	0.0422	
*	19.0±0.4	21	-9%	72/90	0.0070	
WT/*erfa-3* RNAi + glc.*	14.7±0.3	17	-27% (-15%$^{ctrl+glc.}$)	85/110	<0.0001 (<0.0001$^{ctrl+glc.}$)	
*	16.1±0.5	19	-15% (-3%$^{ctrl+glc.}$)	74/90	0.0001 (0.1865$^{ctrl+glc.}$)	
WT/control RNAi	20.2±0.6	24		72/90		Fig. S2A and S2D
WT/control RNAi + glc.	18.3±0.3	22	-9%	83/90	<0.0006	Fig. S2A and S2D
WT/*C35A5.8* RNAi	16.6±0.5	22	-18%	66/90	<0.0001	Fig. S2A
WT/*C35A5.8* RNAi + glc.	10.2±0.2	13	-38% (-44%$^{ctrl+glc.}$)	80/90	0.0065 (<0.0001$^{ctrl+glc.}$)	Fig. S2A
WT/*tag-260* RNAi	15.4±0.5	17	-24%	80/90	<0.0001	Fig. S2D
WT/*tag-260* RNAi + glc.	18.4±0.4	22	+19% (0%$^{ctrl+glc.}$)	84/90	<0.0001 (0.3972$^{ctrl+glc.}$)	Fig. S2D
WT/*C45E1.4* RNAi	18.3±0.6	24	-9%	83/90	0.1529	
WT/*C45E1.4* RNAi + glc.	18.4±0.4	22	0% (+1%$^{ctrl+glc.}$)	84/90	0.2872 (0.396$^{ctrl+glc.}$)	
WT/*tiam-1* RNAi	19.3±0.7	24	-6%	69/89	0.4022	
WT/*tiam-1* RNAi + glc.	17.1±0.4	19	-10% (-7%$^{ctrl+glc.}$)	86/90	0.0012 (0.0067$^{ctrl+glc.}$)	
WT/*unc-29* RNAi	22.2±0.7	26	+10%	52/90	0.0187	

WT/*unc-29* RNAi + glc.	20.0±0.5	24	-10% (+10%$^{ctrl+glc.}$)	82/90	0.0005 (0.0001$^{ctrl+glc.}$)	
WT/*best-10* RNAi	19.3±0.6	22	-4%	80/90	0.3397	
WT/*best-10* RNAi + glc.	18.8±0.4	22	-2% (+3% $^{ctrl+glc.}$)	81/90	0.1175 (0.1325$^{ctrl+glc.}$)	
WT/control RNAi	20.7±0.5	23		91/120		Fig. S2C
WT/control RNAi + glc.	15.8±0.5	20	-24%	85/120	<0.0001	Fig. S2C
WT/*hpo-34* RNAi	26.6±0.6	31	+29%	82/120	<0.0001	Fig. S2C
WT/*hpo-34* RNAi + glc.	13.5±0.3	16	-49% (-14% $^{ctrl+glc.}$)	100/120	<0.0001 (<0.0001$^{ctrl+glc.}$)	Fig. S2C
WT/*F40F4.6* RNAi	20.8±0.4	23	+1%	87/120	0.8027	
WT/*F40F4.6* RNAi + glc.	14.8±0.5	18	-29% (-6% $^{ctrl+glc.}$)	88/120	<0.0001 (0.1474$^{ctrl+glc.}$)	
WT/*F46C8.1* RNAi	21.3±0.6	27	+3%	86/120	0.3769	
WT/*F46C8.1* RNAi + glc.	16.8±0.5	18	-21% (+7%$^{ctrl+glc.}$)	85/120	<0.0001 (0.1311$^{ctrl+glc.}$)	
WT/control RNAi	21.3±0.5	24		72/90		
	20.4±0.6	24		91/120		Fig S2E
WT/control RNAi + glc.	15.0±0.3	17	-30%	81/90	<0.0001	
	15.1±0.5	18	-26%	97/120	<0.0001	Fig S2E
WT/*F35F11.3* RNAi	19.6±0.6	24	-8%	74/90	0.0603	
	18.7±0.5	22	-8%	97/120	0.0093	Fig S2E
WT/*F35F11.3* RNAi + glc.	17.2±0.4	19	-12% (+15%$^{ctrl+glc.}$)	83/90	0.0001 (<0.0001$^{ctrl+glc.}$)	
	17.3±0.5	22	-7% (+15%$^{ctrl+glc.}$)	71/90	0.0441 (0.0267$^{ctrl+glc.}$)	Fig S2E
WT/*C29F9.1* RNAi	16.3±0.3	20	-24%	49/60	<0.0001	

	16.8±0.3	20	-17%	93/120	<0.0001	
WT/*C29F9.1* RNAi + glc.	13.1±0.3	17	-20% (-13% $^{ctrl+glc.}$)	81/90	<0.0001 (<0.0001 $^{ctrl+glc.}$)	
	13.4±0.4	16	-20% (-11% $^{ctrl+glc.}$)	85/120	<0.0001 (0.0047 $^{ctrl+glc.}$)	
WT/*tir-1* RNAi	19.6±0.4	22	-8%	77/90	0.0029	
	18.4±0.3	20	-10%	101/120	<0.0001	
WT/*tir-1* RNAi + glc.	13.4±0.3	17	-31% (-11% $^{ctrl+glc.}$)	79/90	<0.0001 (<0.0001 $^{ctrl+glc.}$)	
	12.0±0.3	14	-35% (-21% $^{ctrl+glc.}$)	101/120	<0.0001 (<0.0001 $^{ctrl+glc.}$)	
WT/*adr-2* RNAi	22.6±0.6	26	+6%	59/90	0.1177	
	22.5±0.5	26	+11%	97/120	0.0150	
WT/*adr-2* RNAi + glc.	16.1±0.4	19	-29% (+7% $^{ctrl+glc.}$)	81/90	<0.0001 (0.0275 $^{ctrl+glc.}$)	
	17.5±0.5	22	-22% (+16% $^{ctrl+glc.}$)	96/120	<0.0001 (0.0042 $^{ctrl+glc.}$)	
WT/*cgh-1* RNAi	10.1±0.5	13	-52%	21/90	<0.0001	
	9.5±0.3	12	-53%	28/120	<0.0001	
WT/*cgh-1* RNAi + glc.	12.8±0.4	15	+27% (-15% $^{ctrl+glc.}$)	70/90	0.0002 (0.0001 $^{ctrl+glc.}$)	
	6.8±0.5	10	-29% (-55% $^{ctrl+glc.}$)	8/120	<0.0001 (<0.0001 $^{ctrl+glc.}$)	
WT/*abcf-2* RNAi	22.2±0.6	26	+4%	75/90	0.1697	
	21.0±0.5	24	+3%	93/120	0.6335	
WT/*abcf-2* RNAi + glc.	14.3±0.3	17	-36% (-5% $^{ctrl+glc.}$)	81/90	<0.0001 (0.0293 $^{ctrl+glc.}$)	
	14.8±0.5	18	-30% (-2% $^{ctrl+glc.}$)	51/90	<0.0001 (0.7749 $^{ctrl+glc.}$)	
WT/*glb-30* RNAi	21.6±0.6	24	+1%	76/90	0.5304	

	20.4±0.5	24	0%	95/120	0.7188	
WT/*glb-30* RNAi + glc.	15.9±0.3	17	-26% (+6% $^{ctrl+glc.}$)	85/90	<0.0001 (0.0734$^{ctrl+glc.}$)	
	15.4±0.5	20	-24% (+2%$^{ctrl+glc.}$)	70/90	<0.0001 (0.8973$^{ctrl+glc.}$)	
WT/*kvs-5* RNAi	20.0±0.6	22	-6%	72/90	0.2292	
	21.9±0.8	26	+3%	43/60	0.7213	
WT/*kvs-5* RNAi + glc.	14.5±0.3	17	-27% (-3% $^{ctrl+glc.}$)	63/90	<0.0001 (0.1703$^{ctrl+glc.}$)	
	16.8±0.5	22	-19% (+11% $^{ctrl+glc.}$)	92/120	<0.0001 (0.0484$^{ctrl+glc.}$)	
WT/*R08C7.1* RNAi	20.3±0.6	24	-5%	77/90	0.4910	
	19.5±0.6	24	-4%	76/120	0.3050	
WT/*R08C7.1* RNAi + glc.	14.8±0.5	17	-27% (-1% $^{ctrl+glc.}$)	83/90	<0.0001 (0.8291$^{ctrl+glc.}$)	
	16.1±0.5	20	-17% (+7%$^{ctrl+glc.}$)	88/120	<0.0001 (0.2739$^{ctrl+glc.}$)	
WT/control RNAi	19.1±0.4	22		87/116		
	20.4±0.5	22		45/90		
WT/control RNAi + glc.	15.4±0.4	18	-19%	81/119	<0.0001	
	17.3±0.4	20	-15%	69/90	<0.0001	
WT/*nhr-49* RNAi$^{\delta}$	13.1±0.2	16	-31%	100/117	<0.0001	
WT/*nhr-49* RNAi + glc.$^{\delta}$	8.4±0.2	12	-36% (-46% $^{ctrl+glc.}$)	65/102	<0.0001 (<0.0001$^{ctrl+glc.}$)	
WT/*F22D6.2* RNAi	23.9±0.6	31	+25%	88/117	<0.0001	
	22.4±0.6	25	+10%	59/90	0.0064	
WT/*F22D6.2* RNAi + glc.	18.5±0.4	22	-22% (+20%$^{ctrl + glc.}$)	92/117	<0.0001 (<0.0001$^{ctrl+glc.}$)	

	19.6±0.5	22	-12% (+13%$^{ctrl+glc.}$)	74/90	0.0003 (0.0003$^{ctrl+glc.}$)	
WT/*T26A8.4* RNAi	12.8±0.6	16	-33%	13/50	<0.0001	
	11.4±0.4	14	-44%	17/90	<0.0001	
WT/*T26A8.4* RNAi + glc.	8.1±0.3	12	-37% (-48% $^{ctrl+glc.}$)	34/100	<0.0001 (<0.0001$^{ctrl+glc.}$)	
	10.2±0.2	14	-11 % (-41% $^{ctrl+glc.}$)	24/60	0.0182 (<0.0001$^{ctrl+glc.}$)	
WT/*nhr-11* RNAi	18.7±0.3	20	-2%	86/115	0.2513	
	18.6±0.4	22	-9%	58/90	0.0027	
WT/*nhr-11* RNAi + glc.	16.3±0.4	18	-13% (+6%$^{ctrl+glc.}$)	77/115	<0.0001 (0.0716$^{ctrl+glc.}$)	
	12.9±0.6	16	-31% (-26% $^{ctrl+glc.}$)	26/90	<0.0001 (<0.0001$^{ctrl+glc.}$)	
WT/*sma-9* RNAi	20.1±0.4	24	+5%	87/118	0.0592	
	20.2±0.4	22	-1%	59/90	0.8725	
WT/*sma-9* RNAi + glc.	17.0±0.4	20	-16 (+10%$^{ctrl+glc.}$)	77/118	<0.0001 (0.0019$^{ctrl+glc.}$)	
	17.9±0.7	20	-12% (+3%$^{ctrl+glc.}$)	38/60	0.0065 (0.3176$^{ctrl+glc.}$)	
WT/*icd-2* RNAi	17.5±0.3	20	-8%	100/113	0.0002	
	12.9±0.2	16	-37%	80/90	<0.0001	
WT/*icd-2* RNAi + glc.	12.1±0.3	14	-31% (-21% $^{ctrl+glc.}$)	98/119	<0.0001 (<0.0001$^{ctrl+glc.}$)	
	10.9±0.4	14	-15% (-37% $^{ctrl+glc.}$)	46/90	<0.0001 (<0.0001$^{ctrl+glc.}$)	
WT/*ogt-1* RNAi	17.8±0.3	20	-7%	76/117	<0.0001	
	16.8±0.5	18	-18%	36/90	<0.0001	
WT/*ogt-1* RNAi + glc.	14.7±0.3	16	-18% (-5% $^{ctrl+glc.}$)	82/119	<0.0001 (0.0724$^{ctrl+glc.}$)	

	14.1±0.6	18	-16% (-19% ctrl+glc.)	42/90	0.0031 (<0.0001 ctrl+glc.)	
WT/control RNAi	20.3±0.6	25		62/90		
	21.3±0.5	27		93/120		
WT/control RNAi + glc.	15.0±0.6	17	-26%	69/90	<0.0001	
	14.5±0.4	17	-32%	98/120	<0.0001	
WT/*msp-51* RNAi	20.7±0.6	25	+2%	70/90	0.8819	
	19.4±0.4	22	-9%	99/120	0.0025	
WT/*msp-51* RNAi + glc.	15.3±0.5	19	-26% (+2% ctrl+glc.)	74/90	<0.0001 (0.9828 ctrl+glc.)	
	14.3±0.4	17	-26% (-1% ctrl+glc.)	95/120	<0.0001 (0.7434 ctrl+glc.)	
WT/*ZK829.7* RNAi	19.4±0.7	23	-5%	68/90	0.4962	
	20.4±0.5	24	-4%	100/120	0.2682	
WT/*ZK829.7* RNAi + glc.	15.5±0.4	17	-20% (+3% ctrl+glc.)	78/90	<0.0001 (0.8138 ctrl+glc.)	
	16.7±0.5	21	-18% (+15% ctrl+glc.)	109/120	<0.0001 (<0.0001 ctrl+glc.)	
WT/*F59E11.2* RNAi	19.5±0.6	23	-4%	51/90	0.3021	
	18.6±0.4	22	-13%	96/120	<0.0001	
WT/*F59E11.2* RNAi + glc.	15.8±0.4	19	-19% (+6% ctrl+glc.)	80/90	<0.0001 (0.6541 ctrl+glc.)	
	14.5±0.4	17	-22% (0% ctrl+glc.)	99/120	<0.0001 (0.7948 ctrl+glc.)	
WT/*F25G6.9* RNAi	19.5±0.5	23	-4%	69/90	0.1253	
	20.5±0.5	24	-4%	95/120	0.1721	
WT/*F25G6.9* RNAi + glc.	14.4±0.5	17	-26% (-4% ctrl+glc.)	75/90	<0.0001 (0.2929 ctrl+glc.)	
	15.8±0.4	19	-23%	103/120	<0.0001	

			(+9%$^{ctrl+glc.}$)		(0.0152$^{ctrl+glc.}$)	
WT/*Y50E8A.12* RNAi	18.7±0.5	21	-8%	63/90	0.0122	
	19.4±0.5	22	-9%	73/90	0.0078	
WT/*Y50E8A.12* RNAi + glc.	14.9±0.4	17	-20% (0% $^{ctrl+glc.}$)	78/90	<0.0001 (0.3873$^{ctrl+glc.}$)	
	15.5±0.4	19	-20% (+7%$^{ctrl+glc.}$)	103/120	<0.0001 (0.0586$^{ctrl+glc.}$)	
WT/*srh-276* RNAi	20.3±0.5	23	0%	70/90	0.5818	
	21.4±0.4	24	0%	101/120	0.5246	
WT/*srh-276* RNAi + glc.	15.8±0.4	19	-22% (+6%$^{ctrl+glc.}$)	77/90	<0.0001 (0.7076$^{ctrl+glc.}$)	
	13.8±0.4	17	-35% (-5% $^{ctrl+glc.}$)	92/120	<0.0001 (0.3402$^{ctrl+glc.}$)	

Lifespan data within the solid lines are individual experimental sets and same shades indicate same experimental sets performed at the same times. All *p* values were calculated within the individual sets by using the log-rank (Mantel-Cox) method (Yang et al., 2011).

Percent (%) changes and *p* values for glucose-rich diet (glc.)-fed worms were calculated against control diet-fed worms within dashed lines in the same experimental sets.

Percent (%) changes and *p* values for RNAi-treated worms grown on a control diet were calculated against WT/control RNAi worms in the same experimental sets.

$^{ctrl+glc.}$: percent (%) changes and *p* values calculated against WT/control RNAi + glc. worms in the same experimental sets.

* indicates an adult-only RNAi treatment.

γ indicates additional repeats of the experiments that are also shown in Supplemental Table S4 and S5.

δ indicates additional repeats of the experiments that are also shown in Supplemental Table S4.

Table S4. Lifespan data regarding inhibition of *mdt-15* or *sbp-1*, related to Figure 2 (and Supplemental Figure S3)

Strain/treatment	Mean lifespan ±s.e.m. (days)	75th percentile	% change	Number of animals that died/total	*p* value vs. control	Figure in text
WT/control RNAi	20.1±0.4	24		121/150		Fig. 2A and 2B
	19.4±0.4	23		131/150		
	22.0±0.4	26		145/180		
	20.4±0.5	25		105/180		
	20.9±0.5	24		105/125		
WT/control RNAi + glc.	15.2±0.2	20	-24%	122/150	<0.0001	Fig. 2A and 2B
	14.5±0.3	17	-25%	140/150	<0.0001	
	11.3±0.4	14	-49%	137/180	<0.0001	
	18.0±0.4	22	-29%	157/180	0.0001	
	13.4±0.4	16	-36%	76/150	<0.0001	
WT/*mdt-15* RNAi*γ	19.2±0.3	22	-5%	120/150	0.0009	Fig. 2A
*	17.3±0.2	19	-11%	121/150	<0.0001	
WT/*mdt-15* RNAi + glc.*γ	5.9±0.1	11	-69%	140/150	<0.0001	Fig. 2A
*	6.9±0.1	12	-60%	112/150	<0.0001	
WT/*sbp-1* RNAi	18.3±0.2	21	-9%	134/150	<0.0001	Fig. 2B
	16.5±0.2	18	-15%	136/150	<0.0001	

	15.1±0.2	18	-32%	135/180	<0.0001	
	14.5±0.2	17	-12%	136/180	<0.0001	
	18.0±0.4	22	-14%	118/150	<0.0001	
WT/*sbp-1* RNAi + glc.	5.5±0.1	10	-70%	129/150	<0.0001	Fig. 2B
	6.8±0.2	12	-59%	132/150	<0.0001	
	4.7±0.1	7	-69%	151/180	<0.0001	
	4.8±0.1	9	-73%	174/180	<0.0001	
	5.6±0.2	8	-69%	104/150	<0.0001	
WT/control RNAi	24.6±0.6	27		79/90		Fig. 2D
	22.7±0.3	26		98/120		
	25.4±0.4	30		81/119		
WT/control RNAi + glc.	17±0.2	19	-31%	57/120	<0.0001	Fig. 2C
	16.4±0.3	19	-28%	101/120	<0.0001	
	13.8±0.4	18	-46%	83/120	<0.0001	
WT/*mdt-15* RNAi (1/2)*	18.7±0.4	21	-24%	86/120	<0.0001	Fig. 2D
*	18.4±0.3	22	-19%	95/120	<0.0001	
*	20.2±0.5	24	-20%	82/120	<0.0001	
WT/*mdt-15* RNAi (1/2) + glc. *	4.8±0.1	8	-74%	105/120	<0.0001	Fig. 2C
*	5.2±0.1	6	-71%	118/119	<0.0001	
*	5.7±0.1	6	-72%	63/116	<0.0001	
WT/*sbp-1* RNAi (1/2)	19.4±0.4	23	-21%	91/120	<0.0001	Fig. 2D
	18.4±0.3	22	-19%	90/120	<0.0001	
				88/120	<0.0001	
WT/*sbp-1* RNAi (1/2) + glc.	8.2±0.2	11	-58%	106/120	<0.0001	Fig. 2C
	7.6±0.2	11	-59%	116/120	<0.0001	
	7.5±0.2	10	-63%	101/120	<0.0001	
WT/*mdt-15*//*sbp-1* RNAi*	18±0.3	21	-27% (-4%$^{mdt-15}$)	109/120	<0.0001 (0.1839^{mdt-15})	Fig. 2D
*	17.7±0.3	22	-22% (-3%$^{mdt-15}$)	94/120	<0.0001 (0.0920^{mdt-15})	
*	20±0.5	24	-22% (-1%$^{mdt-15}$)	72/90	<0.0001 (0.6464^{mdt-15})	

WT/*mdt-15*/*sbp-1* + glc. *	5±0.1	8	-72% (+4%$^{mdt-15+glc.}$)	110/120	<0.0001 (0.2316$^{mdt-15+glc.}$)	Fig. 2C
*	5.2±0.1	6	-71% (-1%$^{mdt-15+glc.}$)	118/120	<0.0001 (0.7296$^{mdt-15+glc.}$)	
*	5.6±0.1	8	-72% (-2%$^{mdt-15+glc.}$)	112/120	<0.0001 (0.1786$^{mdt-15+glc.}$)	
WT/control	16.3±0.3	18		125/150		Fig. S3D
	21.8±0.5	25		107/150		
	20.8±0.4	24		108/120		
@$	23.4±0.5	26		90/150		
#$	21.2±0.4	25		92/120		
WT/glc.	13.9±0.4	17	-15%	128/150	0.0002	Fig. S3D
	17.8±0.4	20	-18%	106/120	<0.0001	
	17.8±0.3	20	-14%	114/150	<0.0001	
@$	14.9±0.3	18	-37%	57/150	<0.0001	
#$	13.7±0.4	18	-35%	116/150	<0.0001	
mdt-15(tm2182)/control	15.2±0.4	17	-7%	132/150	0.0825	Fig. S3D
	16.5±0.3	19	-33%	140/150	<0.0001	
	15.2±0.3	18	-27%	132/150	<0.0001	
$	17.1±0.4	20	-27%	101/150	<0.0001	
$	16.6±0.4	21	-22%	88/150	<0.0001	
mdt-15(tm2182)/glc.	8.4±0.2	12	-45%	65/150	<0.0001	Fig. S3D
	11.1±0.2	14	-24%	135/150	<0.0001	
	11.4±0.2	15	-25%	135/150	<0.0001	
$	9.6±0.2	12	-44%	95/150	<0.0001	
$	8.3±0.1	13	-50%	133/150	<0.0001	
WT/control at 25°C	9.1±0.1	11		139/150		Fig. S3G
	11.7±0.2	14		133/150		
	15.0±0.3	17		96/120		
	15.4±0.4	18		99/120		
WT/glc. at 25°C	8.6±0.1	10	-6%	140/150	0.0070	Fig. S3G
	11.8±0.2	16	+1%	142/150	0.5567	
	15.9±0.2	19	+7%	64/120	0.1179	
	16.4±0.2	21	+7%	105/120	0.3766	

sbp-1(ep79)/control at 25°C	8.6±0.3	11	-5%	90/150	0.4727	Fig. S3G
	11.7±0.3	14	0%	70/150	0.8015	
	11.8±0.3	15	-21%	92/120	<0.0001	
	12.2±0.3	14	-21%	86/90	<0.0001	
sbp-1(ep79)/glc. at 25°C	5.0±0.2	6	-42%	124/150	<0.0001	Fig. S3G
	4.9±0.2	7	-52%	144/150	<0.0001	
	10.0±0.4	13	-16%	44/66	0.0006	
	8.0±0.4	12	-34%	50/57	<0.0001	
WT/control RNAi without FUdR	17.1±0.6	20		46/90		Fig. S3E and S3H
	15.1±0.4	17		59/90		
WT/control RNAi + glc. without FUdR	14.9±0.3	18	-12%	66/120	0.0008	Fig. S3E and S3H
	12.7±0.3	15	-16%	72/90	<0.0001	
WT/*mdt-15* RNAi without FUdR**	15.0±0.3	18	-12%	98/120	0.0003	Fig. S3E
*	14.4±0.2	17	-5%	101/120	0.0116	
WT/*mdt-15* RNAi + glc. without FUdR**	6.8±0.1	11	-55%	105/120	<0.0001	Fig. S3E
*	6.6±0.1	13	-54%	100/120	<0.0001	
WT/*sbp-1* RNAi without FUdR	14.1±0.4	18	-17%	70/90	<0.0001	Fig. S3H
	13.1±0.3	15	-13%	93/120	<0.0001	
WT/*sbp-1* RNAi + glc. without FUdR	5.2±0.1	9	-63%	64/120	<0.0001	Fig. S3H
	4.0±0.1	7	-69%	85/120	<0.0001	
WT/control dead bacteria	24.1±0.4	27		99/120		
	22.2±0.3	25		98/120		Fig. S3F
WT/glc. dead bacteria	15.1±0.5	20	-38%	45/120	<0.0001	
	13.3±0.5	17	-40%	64/90	<0.0001	Fig. S3F

mdt-15(tm2182)/control dead bacteria	17.9±0.5	23	-26%	115/120	<0.0001	
	19.0±0.4	23	-14%	74/120	<0.0001	Fig. S3F
mdt-15(tm2182)/glc. dead bacteria	7.7±0.1	11	-57%	57/120	<0.0001	
	6.4±0.1	8	-67%	97/120	<0.0001	Fig. S3F
WT/control dead bacteria at 25°C	15.0±0.3	17		98/120		
	15.5±0.3	18		102/120		Fig. S3I
WT/glc. dead bacteria at 25°C	12.0±0.2	15	-20%	38/120	<0.0001	
	12.4±0.2	16	-20%	74/120	0.0106	Fig. S3I
sbp-1(ep79)/control dead bacteria at 25°C	10.7±0.3	13	-28%	56/67	0.0043	
	11.8±0.4	14	-24%	56/69	<0.0001	Fig. S3I
sbp-1(ep79)/glc. dead bacteria at 25°C	5.2±0.3	9	-51%	26/44	<0.0001	
	4.9±0.3	9	-59%	34/39	<0.0001	Fig. S3I
WT/control RNAi	21.8±0.5	26		96/120		
	20.2±0.5	23		90/120		Fig. S3J and S3K
WT/control RNAi + glc.	15.9±0.3	18	-27%	57/120	0.0008	
	15.7±0.4	19	-22%	103/120	<0.0001	Fig. S3J and S3K
WT/*nhr-49* RNAi*$^{\delta}$	14.4±0.2	18	-34%	103/120	<0.0001	
*	14.2±0.2	17	-30%	100/120	<0.0001	Fig. S3J
WT/*nhr-49* RNAi + glc.*$^{\delta}$	10.6±0.2	14	-27%	63/120	<0.0001	
*	9.6±0.2	13	-22%	110/120	<0.0001	Fig. S3J
WT/*skn-1* RNAi	19.8±0.3	22	-9%	106/120	<0.0001	
	18.5±0.3	21	-8%	110/120	<0.0001	Fig. S3K
WT/*skn-1* RNAi + glc.	14.0±0.2	16	-29%	81/120	<0.0001	
	13.2±0.2	17	-29%	108/120	<0.0001	Fig. S3K

Lifespan data within the solid lines are individual experimental sets and same shades indicate same experimental sets performed at the same times. All *p* values were calculated within the individual sets by using the log-rank (Mantel-Cox) method (Yang et al., 2011).

Percent (%) changes and *p* values for glucose-rich diet (glc.)-fed worms were calculated against control diet-fed worms within dashed lines in the same experimental set.

Percent (%) changes and *p* values for mutant and RNAi-treated worms grown on control diets were calculated against WT and control RNAi-treated worms in the same experimental set, respectively.

$^{\gamma}$ indicates additional repeats of the experiments that are also shown in Supplemental Table S3 and S5.

$^{\delta}$ indicates an additional repeat of the experiment that is also shown in Supplemental Table S3.

* indicates an adult-only RNAi treatment. For the *mdt-15*/*sbp-1* double RNAi, worms were cultured on *sbp-1* RNAi bacteria from hatching and then transferred to *mdt-15*/*sbp-1* RNAi bacteria at day 1 adulthood.

(1/2) indicates RNAi bacteria mixed with control RNAi bacteria (dilution to 50%)

$^{@}$ and $^{\#}$ indicate same controls used for *gpi-1* RNAi experiments, which are also shown in Supplemental Table S9.

$^{\$}$ indicates control RNAi-treated conditions instead of OP50.

Table S5. Statistics for locomotion and feeding rate assays, related to Figure 2 (and Supplemental Figure S4)

Body bends in liquid media							
Experimental set 1		Mean body bends in liquid media (/min) ± S.E.M.					Figure
		Day 0	Day 1	Day 3	Day 5	Day 7	
Condition	*Control(RNAi)*	118.1±1.9	86.7±2.1	79.2±2.6	58.9±3	47.2±2.1	Fig. 2E,F
	Control(RNAi) +glc.	117.3±2.5	79.2±2.6	59.2±2.6	45.7±2	31.7±1.8	Fig. 2E,F
	mdt-15(RNAi)	122.7±3.1	99.6±3.1	86.7±2.3	48.8±2.8	35.2±3.2	Fig. 2E
	mdt-15(RNAi)+glc.	115.6±2.4	53.1±2.9	60±2.4	10.8±4.2	0±0.0	Fig. 2E
	sbp-1(RNAi)	119.7±3.8	67.3±6.8	62.8±2.4	45.1±2.6	26.5±2.3	Fig. 2F
	sbp-1(RNAi)+glc.	108±4.3	49.6±5.3	30.7±3.1	1.3±1.1	1.9±1.9	Fig. 2F
Statistics	*Control(RNAi)* vs *Control(RNAi)* +glc.	p=0.7997	p=0.0354	p<0.0001	p=0.0011	p<0.0001	
	Control(RNAi) vs *mdt-15(RNAi)*	p=0.2261	p=0.0019	p=0.0421	p=0.0210	p=0.0043	
	Control(RNAi) vs *sbp-1(RNAi)*	p=0.7074	p=0.0109	p=0.0001	p=0.0017	p<0.0001	
	Control(RNAi) +glc. vs *mdt-15(RNAi)*+glc.	p=0.6201	p<0.0001	p=0.8231	p<0.0001	p<0.0001	
	Control(RNAi) +glc. vs *sbp-1(RNAi)*+glc.	p=0.0707	p<0.0001	p<0.0001	p<0.0001	p<0.0001	
	Control(RNAi) vs *Control(RNAi)*+glc.				p<0.0001		
	Control(RNAi) vs *mdt-15(RNAi)*				p=0.7420		

Two-way ANOVA	*Control(RNAi)* vs *sbp-1(RNAi)*				p<0.0001		
	Control(RNAi)+glc. vs *mdt-15(RNAi)*+glc.				p<0.0001		
	Control(RNAi)+glc. vs *sbp-1(RNAi)*+glc.				p<0.0001		
Experimental set 2		Mean body bends in liquid media (/min) ± S.E.M.					Figure
		Day 0	Day 1	Day 3	Day 5	Day 7	
Condition	*Control(RNAi)*	132.3±2.8	88.8±3.9	78.7±4.5	68.4±4.3	47.9±4.7	Fig S4A and S4B
	Control(RNAi) +glc.	118±2.4	85.1±4.6	30.5±2.2	28.8±2.3	24.1±2.9	Fig S4A and S4B
	mdt-15(RNAi)	133.6±3.2	96.8±2.7	65.9±3.9	57.6±2.9	47.3±4.1	Fig S4A
	mdt-15(RNAi)+glc.	124.4±2.5	62.4±3.8	17.6±10.1	0±0.0	N.D.	Fig S4A
	sbp-1(RNAi)	151.3±3.5	116.4±3.2	81.9±4.6	55.2±6.3	58.8±7.9	Fig S4B
	sbp-1(RNAi)+glc.	152.9±5.1	95.6±7.2	28.9±5.8	6.3±3.5	N.D.	Fig S4B
Statistics	*Control(RNAi)* vs *Control(RNAi)* +glc.	p=0.0005	p=0.5390	p<0.0001	p<0.0001	p=0.0002	
	Control(RNAi) vs *mdt-15(RNAi)*	p=0.7575	p=0.0995	p=0.0399	p=0.0468	p=0.9324	
	Control(RNAi) vs *sbp-1(RNAi)*	p=0.0002	p<0.0001	p=0.6223	p=0.0961	p=0.2437	
	Control(RNAi) +glc. vs *mdt-15(RNAi)*+glc.	p=0.0710	p=0.0007	p=0.2211	p<0.0001	N.D.	
	Control(RNAi) +glc. vs *sbp-1(RNAi)*+glc.	p<0.0001	p=0.2294	p=0.7966	p<0.0001	N.D.	

Two-way ANOVA	*Control(RNAi)* vs *Control(RNAi)*+glc.	p<0.0001	
	Control(RNAi) vs *mdt-15(RNAi)*	p=0.2153	
	Control(RNAi) vs *sbp-1(RNAi)*	p=0.0021	
	Control(RNAi)+glc. vs *mdt-15(RNAi)*+glc.	p<0.0001	
	Control(RNAi)+glc. vs *sbp-1(RNAi)*+glc.	p=0.0947	

Body bends on solid media

Experimental set 1		Mean body bends on solid media (/min) ± S.E.M.					Figure
		Day 0	Day 1	Day 3	Day 5	Day 7	
Condition	*Control(RNAi)*	23.9±0.8	21.2±0.8	22±0.6	14.9±0.6	14.5±0.8	Fig. S4C and S4D
	Control(RNAi) +glc.	24.4±1.0	16.3±0.9	16.7±0.6	14±0.4	11.5±0.6	Fig. S4C and S4D
	mdt-15(RNAi)	23.9±1.2	21.4±0.9	20.5±0.8	11.7±1.5	10.9±1.1	Fig. S4C
	mdt-15(RNAi)+glc.	24.4±0.7	15.2±0.7	15.5±0.8	1.9±0.8	0±0.0	Fig. S4C
	sbp-1(RNAi)	16.9±0.8	11.1±0.8	8.4±1.0	7.5±1.0	2.1±0.9	Fig. S4D
	sbp-1(RNAi)+glc.	18.1±1.0	9.9±0.6	0.7±0.4	0±0.0	0±0.0	Fig. S4D
Statistics	*Control(RNAi)* vs *Control(RNAi)* +glc.	p=0.6824	p=0.0002	p<0.0001	p=0.2252	p=0.0039	
	Control(RNAi) vs *mdt-15(RNAi)*	p=1.0000	p=0.8633	p=0.1552	p=0.0596	p=0.0114	
	Control(RNAi) vs *sbp-1(RNAi)*	p<0.0001	p<0.0001	p<0.0001	p<0.0001	p<0.0001	
	Control(RNAi) +glc. vs *mdt-15(RNAi)*+glc.	p=1.0000	p=0.3398	p=0.2303	p<0.0001	p<0.0001	

	Control(RNAi) +glc. vs *sbp-1(RNAi)*+glc.	p<0.001	p<0.0001	p<0.0001	p<0.0001	p<0.0001	
Two-way ANOVA (from day 0 to day 5)	*Control(RNAi)* vs *Control(RNAi)*+glc.				p<0.0001		
	Control(RNAi) vs *mdt-15(RNAi)*				p=0.0079		
	Control(RNAi) vs *sbp-1(RNAi)*				p<0.0001		
	Control(RNAi)+glc. vs *mdt-15(RNAi)*+glc.				p<0.0001		
	Control(RNAi)+glc. vs *sbp-1(RNAi)*+glc.				p<0.0001		
Experimental set 2		Mean body bends on solid media (/min) ± S.E.M.					Figure
		Day 0	Day 1	Day 3	Day 5	Day 7	
Condition	*Control(RNAi)*	36±0.9	34.3±1.1	24.3±0.9	17.2±1.0	16.8±1.8	Fig. S4E and S4F
	Control(RNAi) +glc.	36.8±1.4	25.3±1.0	11.6±0.7	9.2±0.8	10.3±0.5	Fig. S4E and S4F
	mdt-15(RNAi)	37.2±0.9	29.6±1.0	22.5±1.1	22.3±1.4	16.4±1.5	Fig. S4E
	mdt-15(RNAi)+glc.	37.3±1.4	16.7±1.1	8.9±1.8	0±0.0	N.D.	Fig. S4E
	sbp-1(RNAi)	23.1±0.9	27.1±1.2	15.9±1.1	14.5±0.8	10.4±1.0	Fig. S4F
	sbp-1(RNAi)+glc.	32±1.5	19.2±1.3	6.8±0.9	2.8±1.0	N.D.	Fig. S4F
Statistics	*Control(RNAi)* vs *Control(RNAi)* +glc.	p=0.6347	p<0.0001	p<0.0001	p<0.0001	p=0.0016	
	Control(RNAi) vs *mdt-15(RNAi)*	p=0.3554	p=0.0043	p=0.2425	p=0.0061	p=0.8647	
	Control(RNAi) vs *sbp-1(RNAi)*	p<0.0001	p=0.0001	p<0.0001	p=0.0568	p=0.0042	

	Control(RNAi) +glc. vs *mdt-15(RNAi)*+glc.	p=0.7871	p<0.0001	p=0.1786	p<0.0001	N.D.	
	Control(RNAi) +glc. vs *sbp-1(RNAi)*+glc.	p=0.0288	p=0.0012	p=0.0002	p<0.0001	N.D.	

Two-way ANOVA (from day 0 to day 5)	*Control(RNAi)* vs *Control(RNAi)*+glc.	p<0.0001	
	Control(RNAi) vs *mdt-15(RNAi)*	p=0.8881	
	Control(RNAi) vs *sbp-1(RNAi)*	p<0.0001	
	Control(RNAi)+glc. vs *mdt-15(RNAi)*+glc.	p<0.0001	
	Control(RNAi)+glc. vs *sbp-1(RNAi)*+glc.	p<0.0001	

Feeding rates

Experimental set 1		Mean feeding rates (/min) ± S.E.M.					Figure
		Day 0	Day 1	Day 3	Day 5	Day 7	
Condition	*Control(RNAi)*	235.5±3.4	223.2±3.6	220.3±4.8	204±6.6	168.3±7.0	Fig. S4G and S4H
	Control(RNAi) +glc.	234.4±2.5	217.1±3.2	175.7±6.5	162.9±4.5	154.1±8.0	Fig. S4G and S4H
	mdt-15(RNAi)	226.7±3.7	228±3.9	209.6±2.8	2.1±1.0	4.9±1.8	Fig. S4G
	mdt-15(RNAi)+glc.	235.5±2.2	198.9±4.4	70.4±8.6	0±0.0	0±0.0	Fig. S4G
	sbp-1(RNAi)	209.6±3.8	163.5±6.0	118.7±7.8	0±0.0	0±0.0	Fig. S4H
	sbp-1(RNAi)+glc.	206.9±4.7	144±7.9	13.1±2.4	0±0.0	0±0.0	Fig. S4H
Statistics	*Control(RNAi)* vs *Control(RNAi)* +glc.	p=0.8013	p=0.2096	p<0.0001	p<0.0001	p=0.1926	

	Control(RNAi) vs *mdt-15(RNAi)*	p=0.0898	p=0.3701	p=0.0655	p<0.0001	p<0.0001	
	Control(RNAi) vs *sbp-1(RNAi)*	p<0.0001	p<0.0001	p<0.0001	p<0.0001	p<0.0001	
	Control(RNAi) +glc. vs *mdt-15(RNAi)*+glc.	p=0.7493	p=0.0023	p<0.0001	p<0.0001	p<0.0001	
	Control(RNAi) +glc. vs *sbp-1(RNAi)*+glc.	p<0.0001	p<0.0001	p<0.0001	p<0.0001	p<0.0001	

Two-way ANOVA	*Control(RNAi)* vs *Control(RNAi)*+glc.	p<0.0001	
	Control(RNAi) vs *mdt-15(RNAi)*	p<0.0001	
	Control(RNAi) vs *sbp-1(RNAi)*	p<0.0001	
	Control(RNAi)+glc. vs *mdt-15(RNAi)*+glc.	p<0.0001	
	Control(RNAi)+glc. vs *sbp-1(RNAi)*+glc.	p<0.0001	

Experimental set 2		Mean feeding rates (/min) ± S.E.M.					Figure
		Day 0	Day 1	Day 3	Day 5	Day 7	
Condition	*Control(RNAi)*	247.5±2.2	225.6±4.3	198.9±7.7	201.1±8.8	188.5±6.3	Fig. S4I and S4J
	Control(RNAi) +glc.	243.5±2.4	189.1±8.2	161.6±13.0	154.7±11.7	151.7±14.3	Fig. S4I and S4J
	mdt-15(RNAi)	244±2.9	221.9±3.5	178.4±11.2	168±11.4	61.1±19.4	Fig. S4I
	mdt-15(RNAi)+glc.	243.5±2.3	194.9±6.9	28.8±5.1	0±0.0	N.D.	Fig. S4I
	sbp-1(RNAi)	224.5±3.0	182.9±9.1	135.7±6.7	129.1±11.0	71.7±13.0	Fig. S4J
	sbp-1(RNAi)+glc.	226.4±3.1	152.5±11.4	46.7±7.7	10.7±5.3	N.D.	Fig. S4J

Statistics	*Control(RNAi)* vs *Control(RNAi)* +glc.	p=0.2332	p=0.0005	p=0.0196	p=0.0036	p=0.0260	
	Control(RNAi) vs *mdt-15(RNAi)*	p=0.3569	p=0.5083	p=0.1422	p=0.0298	p<0.0001	
	Control(RNAi) vs *sbp-1(RNAi)*	p<0.0001	p=0.0002	p<0.0001	p<0.0001	p<0.0001	
	Control(RNAi) +glc. vs *mdt-15(RNAi)*+glc.	p=1.0000	p=0.5882	p<0.0001	p<0.0001	N.D.	
	Control(RNAi) +glc. vs *sbp-1(RNAi)*+glc.	p=0.0002	p=0.0145	p<0.0001	p<0.0001	N.D.	

Two-way ANOVA (from day 0 to day 5)	*Control(RNAi)* vs *Control(RNAi)*+glc.	p<0.0001	
	Control(RNAi) vs *mdt-15(RNAi)*	p<0.0001	
	Control(RNAi) vs *sbp-1(RNAi)*	p<0.0001	
	Control(RNAi)+glc. vs *mdt-15(RNAi)*+glc.	p<0.0001	
	Control(RNAi)+glc. vs *sbp-1(RNAi)*+glc.	p<0.0001	

Significance at specific time points was calculated using two-tailed Student's *t*-test, and differences among treatments were calculated by using two-way ANOVA test. Please note that the two-way ANOVA tests were performed by using data from day 0 to day 5 in all experimental set 2, because all of the glucose-treated *mdt-15(RNAi)* or *sbp-1(RNAi)* worms were dead at day 7.

Worms were treated with *mdt-15* RNAi only during adulthood, and treated with *sbp-1* RNAi for whole life.

N.D. indicates "Not Determined".

Table S6. Lifespan data regarding tissue-specific knockdown of *mdt-15* or *sbp-1*, related to Figure 2 (and Supplemental Figure S5)

Strain/treatment	Mean lifespan ±s.e.m. (days)	75th percentile	% change	Number of animals that died/total	*p* value vs. control	Figure in text
rde-1(ne219); intestine/control RNAi	18.2±0.4	16		100/150		Fig. 2G and 2H
	18.7±0.4	15		72/150		
	19.2±0.3	22		110/150		
	19.6±0.5	22		79/150		
rde-1(ne219); intestine/control RNAi + glc.	13.2±0.3	11	-27%	120/150	<0.0001	Fig. 2G and 2H
	12.7±0.3	9	-32%	130/150	<0.0001	
	14.0±0.3	18	-27%	93/150	<0.0001	
	13.7±0.3	15	-30%	94/150	<0.0001	
rde-1(ne219); intestine/*mdt-15* RNAi*	16.0±0.3	14	-12%	98/150	<0.0001	Fig. 2G
*	15.4±0.3	13	-18%	87/150	<0.0001	
*	17.8±0.3	20	-7%	124/150	0.0011	
*	16.1±0.4	18	-18%	76/150	<0.0001	
rde-1(ne219); intestine/*mdt-15* RNAi + glc.*	8.9±0.2	9	-44%	124/150	<0.0001	Fig. 2G
*	9.9±0.2	9	-36%	136/150	<0.0001	
*	8.1±0.2	10	-54%	134/150	<0.0001	
*	9.3±0.2	13	-42%	121/150	<0.0001	
rde-1(ne219); intestine/*sbp-1* RNAi	16.5±0.3	14	-9%	141/150	0.0004	Fig. 2H
	14.5±0.3	13	-22%	119/125	<0.0001	
	19.5±0.3	22	+2%	133/150	0.6711	
	14.6±0.4	18	-26%	134/150	<0.0001	

rde-1(ne219); intestine/sbp-1 RNAi + glc.	4.9±0.1	3	-70%	150/150	<0.0001	Fig. 2H
	6.1±0.2	4	-58%	129/150	<0.0001	
	11.8±0.2	15	-39%	131/150	<0.0001	
	12.1±0.2	15	-17%	107/150	<0.0001	
rde-1(ne219); hypodermis/control RNAi	26.3±0.5	31		128/150		Fig. S5C and S5H
	20.7±0.5	24		79/120		
	22.2±0.4	26		138/150		
	19.8±0.4	24		111/150		
rde-1(ne219); hypodermis/control RNAi + glc.	16.9±0.3	21	-36%	101/150	<0.0001	Fig. S5C and S5H
	17.1±0.3	22	-17%	131/150	<0.0001	
	15.2±0.3	19	-31%	125/150	<0.0001	
	14.5±0.3	18	-27%	113/150	<0.0001	
rde-1(ne219); hypodermis/mdt-15 RNAi*	23.0±0.3	25	-13%	118/150	<0.0001	Fig. S5C
*	19.6±0.3	24	-5%	111/150	0.0016	
*	19.4±0.4	23	-12%	118/150	<0.0001	
*	17.0±0.3	21	-14%	107/150	<0.0001	
rde-1(ne219); hypodermis/mdt-15 RNAi + glc.*	5.3±0.1	9	-77%	117/120	<0.0001	Fig. S5C
*	5.8±0.1	10	-71%	110/150	<0.0001	
*	6.0±0.1	10	-69%	150/150	<0.0001	
*	7.1±0.2	10	-58%	119/150	<0.0001	
rde-1(ne219); hypodermis/sbp-1 RNAi	25.0±0.5	29	-5%	117150	0.0162	Fig. S5H
	19.5±0.4	24	-6%	110/150	0.0083	
	21.0±0.4	23	-5%	127/150	0.1267	
	19.4±0.4	21	-2%	111/150	0.3785	
rde-1(ne219); hypodermis/sbp-1 RNAi + glc.	16.0±0.3	18	-36%	105/150	<0.0001	Fig. S5H
	15.9±0.3	22	-18%	107/120	<0.0001	
	14.7±0.2	19	-30%	141/150	<0.0001	

	13.8±0.3	16	-29%	128/150	<0.0001	
rde-1(ne219); body wall muscle/control RNAi	18.1±0.5	21		57/86		
	16.5±0.4	20		48/150		Fig. S5D and S5I
rde-1(ne219); body wall muscle/control RNAi + glc.	13.4±0.4	17	-26%	43/150	<0.0001	
	12.0±0.3	16	-27%	85/150	<0.0001	Fig. S5D and S5I
rde-1(ne219); body wall muscle/mdt-15 RNAi*	17.0±0.4	19	-6%	101/146	0.1458	
*	17.3±0.3	20	+5%	52/139	0.1297	Fig. S5D
rde-1(ne219); body wall muscle/mdt-15 RNAi + glc.*	13.2±0.4	17	-23%	47/150	<0.0001	
*	11.6±0.3	16	-33%	96/138	<0.0001	Fig. S5D
rde-1(ne219); body wall muscle/sbp-1 RNAi	16.5±0.3	19	-8%	90/113	0.0107	
	16.9±0.4	20	+2%	55/150	0.5760	Fig. S5I
rde-1(ne219); body wall muscle/sbp-1 RNAi + glc.	13.3±0.3	17	-20%	41/126	<0.0001	
	11.4±0.4	16	-33%	87/127	<0.0001	Fig. S5I
rde-1(ne219)/control RNAi	22.0±0.3	19		140/150		Fig. S5E and S5J
	20.2±0.3	21		143/150		
	18.8±0.2	18		136/150		
	18.5±0.3	22		136/150		
rde-1(ne219)/control RNAi + glc.	15.4±0.2	13	-30%	132/150	<0.0001	Fig. S5E and S5J
	15.2±0.2	17	-25%	133/150	<0.0001	
	15.2±0.4	13	-19%	61/150	<0.0001	
	13.8±0.3	15	-25%	136/150	<0.0001	
rde-1(ne219)/mdt-15 RNAi*	22.6±0.4	19	+3%	122/150	0.1556	Fig. S5E

*	18.8±0.3	21	-7%	131/150	0.0001	
*	18.2±0.2	18	-3%	139/150	0.1132	
*	17.5±0.3	20	-5%	136/150	0.0323	
rde-1(ne219)/*mdt-15* RNAi + glc.*	14.9±0.2	13	-34%	129/150	<0.0001	Fig. S5E
*	14.9±0.2	17	-21%	134/150	<0.0001	
*	14.4±0.3	13	-21%	65/150	<0.0001	
*	13.1±0.2	15	-25%	136/150	<0.0001	
rde-1(ne219)/*sbp-1* RNAi	22.6±0.3	19	+3%	134/150	0.2070	Fig. S5J
	20.4±0.3	21	+1%	140/150	0.5835	
	19.0±0.2	18	+1%	138/150	0.4364	
	19.1±0.3	22	+4%	136/150	0.0814	
rde-1(ne219)/*sbp-1* RNAi + glc.	15.2±0.2	13	-33%	108/150	<0.0001	Fig. S5J
	15.3±0.2	17	-25%	133/150	<0.0001	
	14.5±0.3	13	-23%	67/150	<0.0001	
	13.9±0.3	18	-27%	136/150	<0.0001	
sid-1(pk3321)/control RNAi	19.5±0.4	22		134/150		Fig. S5F and S5K
	19.0±0.4	22		110/150		
sid-1(pk3321)/control RNAi + glc.	16.6±0.2	20	-15%	117/120	<0.0001	Fig. S5F and S5K
	16.3±0.3	18	-14%	116/150	<0.0001	
sid-1(pk3321)/*mdt-15* RNAi*	17.0±0.3	20	-13%	111/150	<0.0001	Fig. S5F
*	17.7±0.4	22	-7%	99/150	0.0196	
sid-1(pk3321)/*mdt-15* RNAi + glc.*	12.5±0.2	16	-26%	134/150	<0.0001	Fig. S5F
*	16.0±0.3	18	-10%	116/150	0.0008	
sid-1(pk3321)/*sbp-1* RNAi	18.9±0.3	22	-3%	134/150	0.0310	Fig. S5K
	16.4±0.4	18	-14%	112/150	<0.0001	
sid-1(pk3321)/*sbp-1* RNAi + glc.	11.3±0.2	16	-40%	133/150	<0.0001	Fig. S5K
	8.3±0.2	14	-49%	125/150	<0.0001	
sid-1(pk3321); neuron/control RNAi	20.1±0.4	23		138/150		Fig. S5G and S5L

	18.3±0.4	21		104/150		
sid-1(pk3321); neuron/control RNAi + glc.	16.6±0.3	19	-18%	133/150	<0.0001	Fig. S5G and S5L
	16.1±0.3	18	-12%	128/150	<0.0001	
sid-1(pk3321); neuron/*mdt-15* RNAi*	16.4±0.4	19	-19%	75/90	<0.0001	Fig. S5G
*	15.2±0.4	18	-17%	64/90	<0.0001	
sid-1(pk3321); neuron/*mdt-15* RNAi + glc.*	4.6±0.1	10	-72%	145/150	<0.0001	Fig. S5G
*	6.2±0.1	10	-59%	145/150	<0.0001	
sid-1(pk3321); neuron/*sbp-1* RNAi	19.6±0.3	23	-2%	127/150	0.0714	Fig. S5L
	15.2±0.3	18	-17%	112/150	<0.0001	
sid-1(pk3321); neuron/*sbp-1* RNAi + glc.	10.9±0.2	14	-44%	144/150	<0.0001	Fig. S5L
	7.7±0.1	10	-50%	149/150	<0.0001	

Lifespan data within the solid lines are individual experimental sets and same shades indicate same experimental sets performed at the same times. All *p* values were calculated within the individual sets by using the log-rank (Mantel-Cox) method (Yang et al., 2011).

Percent (%) changes and *p* values for glucose-rich diet (glc.)-fed worms were calculated against control diet-fed worms within dashed lines in the same experimental set.

Percent (%) changes and *p* values for mutant and RNAi-treated worms grown on control diets were calculated against WT and control RNAi-treated worms in the same experimental set, respectively.

* indicates an adult-only RNAi treatment.

Following strains were used for tissue-specific RNAi experiments: RNAi defective: WM27 *rde-1(ne219) V*, systemic RNAi defective: NL3321 *sid-1(pk3321) V*, *Intestine*: VP303 *rde-1(ne219) V; kbIs7[nhx-2p::rde-1; rol-6(su1006)]*, *hypodermis*: JM43 *rde-1(ne219) V; Is[wrt-2p::rde-1; myo-2p::RFP]; Is[sur-5p::NLS::GFP]*, *body wall muscle*: NR350 *kzIs20[hlh-1p::rde-1; sur-5p::NLS::GFP]*, and *neuron*: TU3401 *sid-1(pk3321) V; uIs69 [unc-119p::sid-1; myo-2p::mCherry]*

Table S7. Lifespan data regarding up-regulation of *mdt-15* or *sbp-1*, related to Figure 3 and 5 (and Supplemental Figure S6, S7 and S10)

Strain/treatment	Mean lifespan ±s.e.m. (days)	75th percentile	% change	Number of animals that died/total	*p* value vs. control	Figure in text
paqr-2(tm3410)/control	12.6±0.3	12		78/84		Fig. 3D and S7A
	10.9±0.2	14		99/120		
	12.8±0.2	15		117/120		
paqr-2(tm3410)/ 0.2% glc.[#]	8.5±0.2	12	-33%	44/66	<0.0001	Fig. S7A
[#]	8.1±0.1	12	-26%	102/120	<0.0001	
[#]	8.6±0.1	11	-33%	110/120	<0.0001	
paqr-2(tm3410)/ 2% glc.[#]	8.5±0.3	12	-32%	29/60	<0.0001	Fig. 3D
[#]	7.7±0.2	10	-30%	99/120	<0.0001	
[#]	7.7±0.1	11	-40%	94/120	<0.0001	
mdt-15(et14) paqr-2(tm3410)/control	17.8±0.4	22	+41%	84/120	<0.0001	Fig. 3D and S7A
	15.8±0.4	18	+45%	100/120	<0.0001	
	17.0±0.4	13	+32%	92/120	<0.0001	

mdt-15(et14) paqr-2(tm3410)/ 0.2% glc.[#]	18.7±0.4	22	+5%	62/93	0.4189	Fig. S7A
[#]	17.3±0.3	20	+9%	49/90	0.1107	
[#]	17.3±0.4	15	+2%	77/120	0.9224	
mdt-15(et14) paqr-2(tm3410)/ 2% glc.[#]	16.6±0.4	19	-7%	53/94	0.0054	Fig. 3D
[#]	17.1±0.3	20	+8%	52/120	0.3570	
[#]	16.6±0.3	15	-2%	63/120	0.0713	
WT (roller)/control	18.4±0.5	22		108/120		Fig. 3E and S7B
	17.9±0.4	21		99/120		
WT (roller)/0.2% glc.	13.1±0.3	16	-30%	88/120	<0.0001	Fig. S7B
	16.7±0.4	21	-7%	105/120	0.0067	
WT (roller)/2% glc.	14.5±0.4	18	-23%	60/120	<0.0001	Fig. 3E
	16.2±0.4	21	-9%	105/120	0.0008	
sbp-1 OE/control	18.9±0.6	26	+5%	103/120	0.0752	Fig. 3E and S7B
	17.9±0.4	21	0%	96/120	0.9189	
sbp-1 OE/0.2% glc.	18.2±0.4	20	-8%	100/120	0.0911	Fig. S7B
	18.6±0.4	23	+4%	92/120	0.3624	
sbp-1 OE/2% glc.	17.5±0.4	22	-11%	81/120	0.0402	Fig. 3E
	17.3±0.4	21	-3%	90/120	0.1798	
WT/control	19.8±0.5	22		91/120		Fig. 3F and S7C
	19.3±0.4	23		89/120		
	20.7±0.5	23		92/120		
WT/0.2% glc.	11.8±0.2	16	-40%	98/120	<0.0001	Fig. S7C
	16.6±0.5	21	-14%	48/120	<0.0001	
	18.3±0.6	21	-11%	40/120	0.0064	
WT/2% glc.	11.1±0.2	16	-44%	39/120	<0.0001	Fig. 3F
	16.4±0.4	19	-15%	63/120	<0.0001	
	15.5±0.4	19	-25%	69/120	<0.0001	
sams-1(ok3033)/control	19.7±0.5	22	0%	102/120	0.8870	Fig. 3F and S7C
	17.6±0.5	21	-9%	95/120	0.0616	
	17.2±0.5	21	-17%	85/120	0.0001	

sams-1(ok3033)/0.2% glc.	19.6±0.7	24	0%	87/120	0.5055	Fig. S7C
	20.2±0.5	23	+15%	83/120	0.0026	
	20.2±0.4	23	+17%	83/120	0.0006	
sams-1(ok3033)/2% glc.	20.2±0.5	24	+3%	70/120	0.5083	Fig. 3F
	19.4±0.3	21	+10%	93/120	0.0552	
	19.3±0.3	23	+12%	89/120	0.0391	
WT/control RNAi	19.1±0.4	23		134/150		Fig. S7E
	17.3±0.4	19		122/150		Fig. S7D
WT/control RNAi + glc.	16.0±0.3	19	-16%	75/150	<0.0001	Fig. 3H
	15.1±0.3	19	-13%	139/150	<0.0001	Fig. 3G
WT/*mdt-15* RNAi*$^{\gamma}$	16.5±0.2	19	-14%	141/150	<0.0001	
*	16.7±0.3	21	-3%	122/150	0.1300	Fig. S7D
WT/*mdt-15* RNAi + glc.*$^{\gamma}$	5.6±0.1	6	-66%	125/150	<0.0001	
*	5.2±0.1	9	-69%	136/150	<0.0001	Fig. 3G
WT/*sbp-1* RNAi	16.9±0.3	19	-12%	102/120	<0.0001	Fig. S7E
	15.7±0.3	19	-9%	110/150	0.0004	
WT/*sbp-1* RNAi + glc.	7.5±0.2	9	-56%	60/150	<0.0001	Fig. 3H
	4.5±0.1	7	-71%	125/150	<0.0001	
sams-1(ok3033)/control RNAi	19.5±0.5	23	+2%	128/150	0.1991	Fig. S7E
	18.2±0.5	21	+5%	126/150	0.0665	Fig. S7D
sams-1(ok3033)/control RNAi + glc.	19.2±0.3	21	0% (+20%$^{ctrl+glc.}$)	116/150	0.2522 (<0.0001$^{ctrl+glc.}$)	Fig. 3H
	19.5±0.4	21	+7% (+30%$^{ctrl+glc.}$)	139/150	0.1418 (<0.0001$^{ctrl+glc.}$)	Fig. 3G
sams-1(ok3033)/*mdt-15* RNAi*	15.0±0.4	19	-21%	128/150	<0.0001	
*	15.7±0.4	19	-10%	112/150	0.0001	Fig. S7D
sams-1(ok3033)/*mdt-15*	7.3±0.2	11	-52%	117/150	<0.0001 (<0.0001^{m}	

RNAi + glc.*			(+31%$^{mdt-15+glc.}$)		$^{dt-15+glc.}$)	
*	6.1±0.1	9	-61% (+17%$^{mdt-15+glc.}$)	118/150	<0.0001 (<0.0001^{m} $^{dt-15+glc.}$)	Fig. 3G
sams-1(ok3033)/sbp-1 RNAi	17.4±0.3	19	-9%	124/150	0.0002	Fig. S7E
	15.9±0.3	19	-8%	108/150	0.0001	
sams-1(ok3033)/sbp-1 RNAi + glc.	7.6±0.2	9	-56% (+2%$^{sbp-1+glc.}$)	76/150	<0.0001 (0.5287$^{sbp-1+glc.}$)	Fig. 3H
	5.9±0.2	9	-63% (+30%$^{sbp-1+glc.}$)	110/120	<0.0001 (<0.0001^{sb} $^{p-1+glc.}$)	
WT/control	20.6±0.6	25		105/120		Fig. S6G
	19±0.5	23		83/120		
	18.8±0.5	22		99/120		
WT/glucose	13.9±0.4	17	-33%	56/120	<0.0001	Fig. S6G
	15±0.4	18	-21%	102/120	<0.0001	
	11.8±0.3	14	-37%	71/119	<0.0001	
WT/fructose	14.2±0.5	17	-31%	50/120	<0.0001	Fig. S6G
	14.9±0.4	18	-22%	95/120	<0.0001	
	13.8±0.4	16	-26%	66/120	<0.0001	
WT/control RNAi	18.1±0.4	21		91/120		
	16.8±0.3	18		105/120		Fig. S10B
WT/control RNAi + glc.	13.4±0.5	15	-26%	52/120	<0.0001	
	14.6±0.3	18	-13%	105/120	<0.0001	Fig. S10B
ges-1p::fat-2,5,6,7/control RNAi	19.7±0.5	24	+9%	82/120	0.0005	
	18.1±0.5	22	+8%	65/120	0.0280	Fig. S10B
ges-1p::fat-2,5,6,7/control RNAi + glc.	13.9±0.4	17	-30% (+3%$^{ctrl+glc.}$)	62/120	<0.0001 (0.5934 $^{ctrl+glc.}$)	
	13.5±0.4	17	-26% (-8%$^{ctrl+glc.}$)	65/120	<0.0001 (0.0410$^{ctrl+glc.}$)	Fig. S10B
WT/*sbp-1* RNAi	17.3±0.4	21	-4%	103/120	0.1240	

	15.6±0.3	18	-7%	80/90	0.0097	Fig. 5M
WT/*sbp-1* RNAi + glc.	7.6±0.2	11	-56%	78/120	<0.0001	
	5.9±0.2	9	-62%	108/120	<0.0001	Fig. 5M
ges-1p::fat-2,5,6,7/*sbp-1* RNAi	17.5±0.4	20	-11% (+1%$^{sbp-1}$)	97/120	0.0003 (0.6199^{sbp-1})	
	16.4±0.3	19	-10% (+5% $^{sbp-1}$)	90/120	0.0007 (0.0314^{sbp-1})	Fig. 5M
ges-1p::fat-2,5,6,7/*sbp-1* RNAi + glc.	11.1±0.4	13	-37% (+46%$^{sbp-1+glc.}$)	80/120	<0.0001 (<0.0001$^{sbp-1+glc.}$)	
	11.3±0.3	14	-31% (+90%$^{sbp-1+glc.}$)	83/120	<0.0001 (<0.0001$^{sbp-1+glc.}$)	Fig. 5M
WT/*mdt-15* RNAi*	17.3±0.3	19	-4%	98/120	0.0743	
*	16.1±0.2	18	-4%	101/120	<0.0001	Fig. S10A
WT/*mdt-15* RNAi + glc.*	5.2±0.1	7	-70%	111/120	<0.0001	
*	4.9±0.1	9	-70%	107/120	<0.0001	Fig. S10A
ges-1p::fat-2,5,6,7/*mdt-15* RNAi*	16.8±0.4	20	-15% (-3%$^{mdt-15}$)	74/90	<0.0001 (0.3608^{mdt-15})	
*	17.1±0.4	19	-5% (+6%$^{mdt-15}$)	74/120	0.0571 (0.0004^{mdt-15})	Fig. S10A
ges-1p::fat-2,5,6,7/*mdt-15* RNAi + glc. *	5.8±0.1	9	-65% (+11%$^{mdt-15+glc.}$)	76/120	<0.0001 (<0.0001$^{mdt-15+glc.}$)	
*	6.2±0.1	10	-64% (+28%$^{mdt-15+glc.}$)	70/120	<0.0001 (<0.0001$^{mdt-15+glc.}$)	Fig. S10A
WT/control RNAi	25.0±0.5	28		104/150		Fig. S10C
	24.3±0.4	28		104/150		
WT/control RNAi + glc.	15.1±0.4	19	-40%	57/200	<0.0001	Fig. S10C
	15.36±0.3	20	-37%	116/200	<0.0001	
fat-5(tm420)/*fat-*	18.4±0.3	22	-27%	120/150	<0.0001	Fig. S10C

6/7 RNAi*						
*	15.6±0.3	20	-36%	127/150	<0.0001	
fat-5(tm420)/fat-6/7 RNAi + glc.*	11.5±0.1	14	-37% (-23%$^{ctrl+ glc.}$)	155/200	<0.0001 (<0.0001$^{ctrl+ glc.}$)	Fig. S10C
*	11.1±0.2	17	-30% (-28%$^{ctrl+ glc.}$)	164/200	<0.0001 (<0.0001$^{ctrl+ glc.}$)	
WT/control RNAi	22.4±0.5	27		94/120		Fig. S10D
	21.3±0.5	27		131/150		
WT/control RNAi + glc.	15.1±0.5	18	-33%	64/150	<0.0001	Fig. S10D
	14.4±0.4	19	-32.13%	60/120	<0.0001	
fat-2(wa17)/fat-5 RNAi	22.8±0.4	25	+2%	136/150	0.8605	Fig. S10D
	18.2±0.4	23	-14.53%	130/150	<0.0001	
fat-2(wa17)/fat-5 RNAi + glc.	16.2±0.2	20	-29% (+8%$^{ctrl+ glc.}$)	145/150	<0.0001 (0.0613$^{ctrl+ glc.}$)	Fig. S10D
	13.0±0.3	17	-28.34% (-9.77% $^{ctrl+ glc.}$)	125/150	<0.0001 (0.0356$^{ctrl+ glc.}$)	

Lifespan data within the solid lines are individual experimental sets and same shades indicate same experimental sets performed at the same times. All *p* values were calculated within the individual sets by using the log-rank (Mantel-Cox) method (Yang et al., 2011).

Percent (%) changes and *p* values for glucose-rich diet (glc.)-fed worms were calculated by comparing data obtained with control diet-fed worms within dashed lines in the same experimental sets.

Percent (%) changes and *p* values for mutant and transgenic worms grown on control diet-fed conditions were calculated against WT, and those for RNAi-treated worms were calculated

against control RNAi-treated worms in the same experimental sets.

* indicates an adult-only RNAi treatment.

# indicates an adult-only glucose treatment.

γ indicates additional repeats of the experiments that are also shown in Supplemental Table S3 and S4.

ctrl+glc.: percent (%) changes and *p* values calculated against WT/control RNAi + glc. worms in the same experimental sets

mdt-15+glc.: percent (%) changes and *p* values calculated against WT/*mdt-15* RNAi + glc. worms in the same experimental sets.

sbp-1+glc.: percent (%) changes and *p* values calculated against WT/*sbp-1* RNAi + glc. worms in the same experimental sets.

Roller indicates transgenic worms carrying roller injection marker (CF1290), which are used as controls for *sbp-1 OE* transgenic animals.

Table S8. Summary of RNA sequencing data, related to Figure 4 (and Supplemental Figure S8)

Supplied as a separated Excel file

Data in "Induced by glucose" sheet are genes that were induced by a glucose-rich diet (2%) in an SBP-1/MDT-15 dependent manner.

Data in "Repressed by glucose" are genes that were repressed by a glucose-rich diet (2%) in an SBP-1/MDT-15 dependent manner.

Genes were sorted by using the orders of average fold change values for "*sbp-1(RNAi)*+glc." and "*mdt-15(RNAi)*+glc." conditions.

Ctrl.(RNAi): control RNAi-treated N2 animals

Ctrl.(RNAi)+glc.: control RNAi-treated N2 animals on a glucose-rich diet

sbp-1(RNAi): *sbp-1* RNAi-treated N2 animals on a control diet

sbp-1(RNAi)+glc.: *sbp-1* RNAi-treated N2 animals on a glucose-rich diet

mdt-15(RNAi)+glc.: *mdt-15* RNAi-treated N2 animals on a control diet

mdt-15(RNAi)+glc.: *mdt-15* RNAi-treated N2 animals on a glucose-rich diet

Ctrl.(RNAi)+glc. vs. *Ctrl.(RNAi)*: gene expression fold changes between *Ctrl.(RNAi)* +glc. and *Ctrl.(RNAi)*

sbp-1(RNAi)+glc. vs. *Ctrl.(RNAi)*+glc.: gene expression fold changes between *sbp-1(RNAi)*+glc. and *Ctrl.(RNAi)*+glc.

mdt-15(RNAi)+glc. vs. *Ctrl.(RNAi)*+glc.: gene expression fold changes between *mdt-15(RNAi)*+glc. and *Ctrl.(RNAi)*+glc.

Average fold change of "*sbp-1(RNAi)*+glc." and "*mdt-15(RNAi)*+glc.": average values of fold changes calculated from "*sbp-1(RNAi)*+glc. vs. *Ctrl.(RNAi)*+glc." and "*mdt-15(RNAi)*+glc. vs. *Ctrl.(RNAi)*+glc."

# indicates genes that are also repressed in *sbp-1(RNAi)* and *mdt-15(RNAi)* animals on a control diet.

* indicates genes that are also induced in *sbp-1(RNAi)* and *mdt-15(RNAi)* animals on a control diet.

Table S9. Lifespan data regarding accumulation of intermediate metabolites and fatty acids, related to Figure 7 (and Supplemental Figure S13-S15)

Strain/treatment	Mean lifespan ±s.e.m. (days)	75th percentile	% change	Number of animals that died/total	*p* value vs. control	Figure in text
WT/control RNAi	18.5±0.6	24		54/120		Fig. S13B
	17.5±0.4	20		82/120		
α	20.4±0.5	25		112/120		Fig. 7B
	22.4±0.6	28		107/120		
	25.4±0.5	30		104/120		
β	20.2±0.4	23		113/120		
γ	19.4±0.4	23		112/120		Fig. S13F and S13G
δ	19.1±0.4	21		109/120		
WT/control RNAi + glc.	15.3±0.4	18	-17%	66/120	<0.0001	Fig. S13B
	14.6±0.2	18	-16%	97/120	<0.0001	
α	15.9±0.5	20	-22%	79/115	<0.0001	Fig. 7B
	15.4±0.4	18	-31%	72/90	<0.0001	
	16.9±0.3	21	-33%	96/120	<0.0001	
β	17.9±0.3	21	-11%	102/120	<0.0001	
γ	13.1±0.3	17	-32%	31/120	<0.0001	Fig. S13F and S13G
δ	10.3±0.2	13	-46%	59/120	<0.0001	

WT/control RNAi + UFAs	18.6±0.5	24	0%	98/120	0.7653	Fig. S13B
	18.6±0.4	23	+6%	85/120	0.0566	
α	15.7±0.4	19	-23%	107/110	<0.0001	
	26±0.6	30	+16%	78/90	0.0018	
	26.4±0.5	30	4%	106/120	0.3272	
WT/control RNAi + glc. + UFAs	12.5±0.5	16	-18%	105/120	<0.0001	Fig. S13B
	12.4±0.3	16	-15%	84/120	<0.0001	
α	7.9±0.2	11	-50%	68/120	<0.0001	
	14.9±0.2	18	-3%	85/120	0.1126	
	14.7±0.2	18	-13%	108/120	<0.0001	
WT/*sbp-1* RNAi	14.3±0.4	18	-23%	86/150	<0.0001	Fig. 7A
	14.2±0.4	16	-19%	90/120	<0.0001	
α	18.2±0.3	21	-11%	101/120	<0.0001	
	20.1±0.3	22	-10%	113/120	<0.0001	
	19.7±0.3	23	-23%	107/120	<0.0001	
WT/*sbp-1* RNAi + glc.	7.5±0.2	11	-47%	86/150	<0.0001	Fig. 7A
	5.5±0.1	9	-61%	109/120	<0.0001	
α	10.5±0.3	14	-42%	87/120	<0.0001	
	11.8±0.4	14	-41%	88/120	<0.0001	
	11.7±0.3	14	-41%	103/120	<0.0001	
WT/*sbp-1* RNAi + UFAs	16.2±0.4	18	+13%	86/150	0.0004	Fig. 7A
	14.3±0.4	16	+1%	64/90	0.8293	
α	18.8±0.4	21	+4%	111/120	0.0479	
	18.5±0.4	22	-8%	111/120	0.0019	
	19.6±0.3	23	0%	92/120	0.8360	
WT/*sbp-1* RNAi + glc. + UFAs	8.4±0.2	13	+12%	86/150	0.0030	Fig. 7A
	9.2±0.3	14	+67%	100/120	<0.0001	
α	11.1±0.3	13	+7%	46/80	0.4461	
	16.6±0.3	18	+41%	83/120	<0.0001	
	16.6±0.3	21	+42%	103/120	<0.0001	
WT/*mdt-15* RNAi*	15.5±0.3	20	-17%	70/90	<0.0001	
*	15.5±0.2	18	-12%	83/120	<0.0001	Fig. S13A
* α	14.7±0.3	19	-28%	109/120	<0.0001	
	17.2±0.4	20	-23%	83/120	<0.0001	

	16.4±0.3	18	-36%	91/120		
WT/*mdt-15* RNAi + glc.*	5.6±0.3	9	-64%	64/120	<0.0001	
*	4.8±0.1	9	-69%	91/120	<0.0001	Fig. S13A
*α	6.3±0.1	9	-57%	94/120	<0.0001	
	6.1±0.1	10	-64%	111/120	<0.0001	
	6.1±0.1	9	-63%	111/120	<0.0001	
WT/*mdt-15* RNAi + UFAs*	17.4±0.2	20	+12%	86/150	<0.0001	
*	15.7±0.2	18	+1%	87/120	0.7106	Fig. S13A
*α	13.4±0.5	17	-9%	74/120	0.2774	
	17±0.4	20	-1%	93/120	0.4633	
	15.3±0.3	18	-6%	104/120	0.0215	
WT/*mdt-15* RNAi + glc. + UFAs*	5.4±0.3	9	-4%	86/150	0.8029	
*	4.7±0.1	9	-2%	94/120	0.5111	Fig. S13A
*α	4.6±0.1	7	-27%	115/120	<0.0001	
	7.9±0.1	12	+30%	104/120	<0.0001	
	8.3±0.2	12	36%	82/120	<0.0001	
WT/control RNAi + SFAs α	20.3±0.4	23	-1%	108/120	0.5262	Fig. 7B
β	19.5±0.6	23	-3%	116/120	0.2315	
γ	20.5±0.4	23	+6%	113/120	0.0157	
δ	19.1±0.4	23	0%	97/120	0.8801	
WT/control RNAi + glc. + SFAs α	3.9±0.1	6	-76%	106/120	<0.0001	Fig. 7B
β	4.0±0.1	7	-78%	85/90	<0.0001	
γ	4.6±0.1	7	-77%	103/120	<0.0001	
δ	5.7±0.1	6	-70%	98/117	<0.0001	
WT/control RNAi + 14:0 γ	19.7±0.6	23	+2%	73/120	0.2303	Fig. S13F
δ	19.6±0.5	23	+3%	104/120	0.1835	
WT/control RNAi + glc. + 14:0 γ	3.2±0.1	6	-84%	101/120	<0.0001	Fig. S13F
δ	4.3±0.1	6	-78%	96/120	<0.0001	
WT/control RNAi + 16:0 γ	20.7±0.5	25	+7%	111/120	0.0028	Fig. S13G
δ	19.5±0.4	23	+2%	114/120	0.3787	
WT/control RNAi + glc. + 16:0 γ	9.4±0.2	13	-54%	74/120	<0.0001	Fig. S13G

δ	7.6±0.1	11	-61%	112/120	<0.0001	
WT/control	16.9±0.4	20		115/150		
	20.6±0.5	23		63/120		Fig. S13E
WT/glc.	14.0±0.4	17	-17%	74/155	<0.0001	
	13.4±0.5	16	-35%	69/180	<0.0001	Fig. S13E
WT/C18:1n-9	18.2±0.4	22	+8%	90/150	0.0416	
	19.8±0.3	23	-4%	90/120	0.0847	Fig. S13E
WT/glc. + C18:1n-9	12.7±0.3	15	-9%	116/150	0.0070	
	13.4±0.3	16	0%	123/180	0.7849	Fig. S13E
mdt-15(tm2182)/control	13.9±0.4	15	-18%	121/150	<0.0001	
	13.8±0.2	16	-33%	151/180	<0.0001	Fig. S13D
mdt-15(tm2182)/glc.	6.7±0.1	10	-52%	81/150	<0.0001	
	8.1±0.2	11	-42%	80/180	<0.0001	Fig. S13D
mdt-15(tm2182)/C18:1n-9	20.0±0.6	25	+44%	130/150	<0.0001	
	19.3±0.6	24	+39%	102/150	<0.0001	Fig. S13D
mdt-15(tm2182)/glc. + C18:1n-9	5.2±0.1	8	-22%	112/150	<0.0001	
	5.7±0.1	9	-30%	148/180	<0.0001	Fig. S13D
WT/control RNAi	21.3±0.5	27		93/120		
	22.9± 0.5	28		137/180		Fig. 7C and 7D
	18.2± 0.5	21		117/149		
WT/control RNAi + glc.	14.5±0.4	17	-32%	98/120		
	14.8± 0.4	18	-35%	144/180	<0.0001	Fig. 7C and 7D
	14.4± 0.3	17	-21%	131/149	<0.0001	
WT/*pod-2* RNAi	21.2± 0.4	25	-8%	156/180	0.0005	Fig. 7C
	19.5±0.5	23	+7%	104/149	0.0601	
WT/*pod-2* RNAi + glc.	8.8±0.1	13	-59%	123/180	<0.0001 (<0.0001^{ctrl+}	Fig. 7C

			(-41% ctrl+glc.)		glc.)	
	10.8±0.2	14	-45% (-25% ctrl+glc.)	103/149	<0.0001 (<0.0001 ctrl+ glc.)	
WT/*fasn-1* RNAi	16.5± 0.3	18	-22%	109/120	<0.0001	
	19.4± 0.3	22	-16%	139/180	<0.0001	Fig. 7D
WT/*fasn-1* RNAi + glc.	7.2± 0.2	10	-56% (-51% ctrl+glc.)	56/120	<0.0001 (<0.0001 ctrl+ glc.)	
	7.2± 0.1	10	-63% (-50% ctrl+glc.)	108/180	<0.0001 (<0.0001 ctrl+ glc.)	Fig. 7D
WT/control RNAi	21.1±0.5	26		91/120		
	21.2±0.5	26		105/120		Fig. S14D, S14F, S14H, and S14J
WT/control RNAi + glc.	15.2±0.3	18	-28%	75/120	<0.0001	
	15.5±0.3	18	-27%	104/120	<0.0001	Fig. S14C, S14E, S14G, and S14I
WT/*mdt-15* RNAi (1/2)*	18.4±0.3	22	-13%	88/120	<0.0001	
*	17±0.3	21	-20%	111/120	<0.0001	Fig. S14H and S14J
WT/*mdt-15* RNAi (1/2) + glc.*	5.7±0.1	10	-69%	116/120	<0.0001	
*	5.4±0.1	8	-68%	120/120	<0.0001	Fig. S14G and S14I
WT/*pod-2* RNAi (1/2)*	20.6±0.3	24	-3%	108/120	0.9249	
*	21.3±0.5	23	0%	76/90	0.9540	Fig. S14D and S14H
WT/*pod-2* RNAi (1/2) + glc.*	11.2±0.2	14	-45%	95/120	<0.0001	

*	11.2±0.2	15	-47%	105/120	<0.0001	Fig. S14C and S14G
WT/*fasn-1* RNAi (1/2)*	21.5±0.4	24	+2%	94/120	0.7030	
*	20±0.4	23	-6%	112/120	0.0014	Fig. S14F and S14J
WT/*fasn-1* RNAi (1/2) + glc.*	10.8±0.3	14	-50%	86/120	<0.0001	
*	10.6±0.2	15	-47%	112/120	<0.0001	Fig. S14E and S14I
WT/*mdt-15*/*pod-2* RNAi*	18.7±0.3	20	-12% (+1% $^{mdt-15}$)	91/120	<0.0001 (0.8382^{mdt-15})	
*	16.9±0.3	21	-20% (-1% $^{mdt-15}$)	109/120	<0.0001 (0.7028^{mdt-15})	Fig. S14H
WT/*mdt-15*/*pod-2* RNAi + glc.*	6.2±0.1	10	-67% (+8%$^{mdt-15+glc.}$)	118/120	<0.0001 (0.0004$^{mdt-15+glc.}$)	
*	5.9±0.1	8	-65% (+9%$^{mdt-15+glc.}$)	110/120	<0.0001 (0.0003$^{mdt-15+glc.}$)	Fig. S14G
WT/*mdt-15*/*fasn-1* RNAi*	16.7±0.3	18	-21% (-9% $^{mdt-15}$)	97/120	<0.0001 (0.0003^{mdt-15})	
*	16.1±0.3	21	-24% (-5% $^{mdt-15}$)	103/120	<0.0001 (0.0530^{mdt-15})	Fig. S14J
WT/*mdt-15*/*fasn-1* RNAi + glc.*	5.9±0.1	10	-65% (+4%$^{mdt-15+glc.}$)	119/120	<0.0001 (0.0376$^{mdt-15+glc.}$)	
*	5.7±0.1	8	-65% (+5%$^{mdt-15+glc.}$)	118/120	<0.0001 (0.0470$^{mdt-15+glc.}$)	Fig. S14I
WT/*sbp-1* RNAi (1/2)	17.5±0.3	20	-17%	98/120	<0.0001	
	17±0.3	21	-20%	99/120	<0.0001	Fig. S14D and S14F
WT/*sbp-1* RNAi (1/2) + glc.	8.8±0.2	12	-50%	102/120	<0.0001	

	8.2±0.2	12	-52%	114/120	<0.0001	Fig. S14C and S14E
WT/*sbp-1*/*pod-2* RNAi*	15.3±0.3	18	-28% (13% $^{sbp-1}$)	102/120	<0.0001 (<0.0001^{sbp-1})	
*	15.7±0.3	21	-26% (-8% $^{sbp-1}$)	100/120	<0.0001 (0.0040^{sbp-1})	Fig. S14D
WT/*sbp-1*/*pod-2* RNAi + glc.*	9.5±0.2	12	-38% (+8%$^{sbp-1+glc.}$)	102/120	<0.0001 (0.0136$^{sbp-1+glc.}$)	
*	7.7±0.16	10	-51% (-6% $^{sbp-1+glc.}$)	115/120	<0.0001 (0.0461$^{sbp-1+glc.}$)	Fig. S14C
WT/*sbp-1*/*fasn-1* RNAi*	17.1±0.4	20	-19% (+3% $^{sbp-1}$)	107/120	<0.0001 (0.5160^{sbp-1})	
*	16±0.3	21	-25% (6% $^{sbp-1}$)	94/120	<0.0001 (0.0430^{sbp-1})	Fig. S14F
WT/*sbp-1*/*fasn-1* RNAi + glc.*	8.8±0.2	12	-48% (+1%$^{sbp-1+glc.}$)	100/120	<0.0001 (0.9845$^{sbp-1+glc.}$)	
*	8±0.2	10	-50% (-2% $^{sbp-1+glc.}$)	109/120	<0.0001 (0.3321$^{sbp-1+glc.}$)	Fig. S14E
WT/control RNAi	23.5±0.6	29		88/120		
	21.9±0.5	25		88/120		Fig. 7G
WT/control RNAi + glc.	14.4±0.4	17	-38%	79/120	<0.0001	
	15.7±0.4	18	-28%	34/120	<0.0001	Fig. 7G
WT/*F14B4.2* RNAi and *Y77E11A.1* RNAi	20.4±0.5	24	-13%	92/120	<0.0001	
	20.0±0.5	23	-9%	99/120	0.0043	
WT/*F14B4.2* RNAi and *Y77E11A.1* RNAi	12.9±0.4	15	-37% (-11% $^{ctrl+glc.}$)	81/120	<0.0001 (0.0041$^{ctrl+glc.}$)	
	15.1±0.5	18	-24% (-4% $^{ctrl+glc.}$)	32/120	<0.0001 (0.1530$^{ctrl+glc.}$)	

aldo-1(tm5782)/*aldo-2* RNAi	19.8±0.5	24	-16%	100/120	<0.0001	
	20.2±0.5	25	-8%	100/120	0.0336	Fig. 7G
aldo-1(tm5782)/*aldo-2* RNAi + glc.	18.1±0.3	21	-8% (+25%$^{ctrl+glc.}$)	98/120	0.0002 (<0.0001$^{ctrl+glc.}$)	
	19.7±0.4	23	-3% (+25%$^{ctrl+glc.}$)	79/120	0.0304 (<0.0001$^{ctrl+glc.}$)	Fig. 7G
WT/*pdhb-1* RNAi and *C30H8.7* RNAi	19.3±0.5	24	-18%	106/120	<0.0001	
	20.0±0.4	23	-9%	107/120	0.0015	
WT/*pdhb-1* RNAi and *C30H8.7* RNAi + glc.	15.4±0.4	19	-20% (+7%$^{ctrl+glc.}$)	98/120	<0.0001 (0.0798$^{ctrl+glc.}$)	
	16.4±0.5	20	-18% (+4%$^{ctrl+glc.}$)	47/120	<0.0001 (0.4253$^{ctrl+glc.}$)	
WT/control RNAi	27.8±0.6	32		103/120		
	28.7±0.5	34		64/120		
WT/control RNAi + glc.	16.6±0.3	20	-40%	65/120	<0.0001	
	14.6±0.3	18	-49%	89/120	<0.0001	
WT/*gpd-1* and *gpd-2* RNAi	28.7±0.6	32	+3%	90/120	0.4350	
	27.4±0.7	34	-4%	53/90	0.6490	
WT/*gpd-1* and *gpd-2* RNAi + glc.	16±0.3	20	-44%(-4%$^{ctrl+glc.}$)	76/120	<0.0001 (0.0646 $^{ctrl+glc.}$)	
	15.9±0.3	18	-42%(+9 % $^{ctrl+glc.}$)	82/120	<0.0001 (0.0042$^{ctrl+glc.}$)	
WT/control RNAi$^{@}$	23.4±0.5	26		90/150		Fig. 7F
$^{\#}$	21.2±0.4	25		92/120		
WT/control RNAi + glc.$^{@}$	14.9±0.3	18	-37%	57/150	<0.0001	Fig. 7F
$^{\#}$	13.7±0.4	18	-35%	116/150	<0.0001	

WT/*gpi-1* RNAi	23.1±0.5	28	-1%	80/150	0.9831	Fig. 7F
	21.9±0.3	25	+4%	124/150	0.3165	
WT/*gpi-1* RNAi + glc.	17.8±0.3	20	-23% (+20%$^{ctrl+glc.}$)	78/150	<0.0001 (<0.0001$^{ctrl+glc.}$)	Fig. 7F
	16.2±0.2	21	-26% (+18%$^{ctrl+glc.}$)	122/150	<0.0001 (<0.0001$^{ctrl+glc.}$)	
WT/control RNAi	16.3±0.3	18		93/120		
	21.7±0.5	25		84/120		
WT/control RNAi + glc.	13.5±0.3	16	-17%	78/120	<0.0001	
	15.4±0.4	19	-29%	53/120	<0.0001	
WT/*pgk-1* RNAi	16.9±0.4	20	+4%	70/120	0.1809	
	24.0±0.6	29	+11%	83/120	0.0002	
WT/*pgk-1* RNAi + glc.	14.1±0.3	18	-17% (+4%$^{ctrl+glc.}$)	80/120	<0.0001 (0.2069$^{ctrl+glc.}$)	
	16.0±0.4	19	-33% (+4%$^{ctrl+glc.}$)	55/120	<0.0001 (0.3223$^{ctrl+glc.}$)	
WT/*enol-1* RNAi	16.1±0.3	18	-2%	95/120	0.6684	
	23.5±0.5	27	+8%	89/120	0.0078	
WT/*enol-1* RNAi + glc.	15.1±0.3	18	-6% (+12%$^{ctrl+glc.}$)	57/120	0.0181 (0.001$^{ctrl+glc.}$)	
	17.4±0.4	21	-26% (+13%$^{ctrl+glc.}$)	55/120	<0.0001 (0.0035$^{ctrl+glc.}$)	
WT/*ipgm-1* RNAi	16.0±0.4	18	-2%	88/120	0.7294	
	24.4±0.7	29	+13%	81/120	<0.0001	
WT/*ipgm-1* RNAi + glc.	13.5±0.3	16	-16% (0% $^{ctrl+glc.}$)	83/120	<0.0001 (0.9212$^{ctrl+glc.}$)	
	16.6±0.4	21	-32% (+7%$^{ctrl+glc.}$)	46/120	<0.0001 (0.0923$^{ctrl+glc.}$)	
WT/control RNAi	20.5±0.5	25		91/120		
	19.3±0.4	24		91/120		

WT/control RNAi + glc.	16.5±0.3	19	-19%	45/120	<0.0001	
	15.0±0.4	18	-22%	102/120	<0.0001	
WT/*tpi-1* RNAi	20.3±0.5	25	-1%	89/120	0.9718	
	18.3±0.5	21	-5%	86/120	0.3753	
WT/*tpi-1* RNAi + glc.	16.9±0.4	21	-17% (+2%$^{ctrl+glc.}$)	40/120	0.0003 (0.4525$^{ctrl+glc.}$)	
	14.1±0.4	18	-23% (-6% $^{ctrl+glc.}$)	95/120	<0.0001 (0.0812$^{ctrl+glc.}$)	
pyk-1(ok1754)/*pyk-2* RNAi	26.0±0.4	29	+27%	105/120	<0.0001	
	23.4±0.4	26	+21%	107/120	<0.0001	
pyk-1(ok1754)/*pyk-2* RNAi + glc.	18.7±0.3	21	-28% (+13%$^{ctrl+glc.}$)	80/120	<0.0001 (<0.0001$^{ctrl+glc.}$)	
	16.7±0.3	21	-29% (+11%$^{ctrl+glc.}$)	108/120	<0.0001 (0.0003$^{ctrl+glc.}$)	
WT/NaCl 111mM	16.1±0.8	20		58/61		Fig. S15A and S15D
ε	27.5±0.9	33		46/70		Fig. S15F and S15I
WT/G6P	18±0.8	22	+12%	35/63	0.0995	Fig. S15A
ε	19.4±0.7	22	-30%	35/61	<0.0001	Fig. S15F
WT/2PG	17.0±0.6	20	+6%	23/28	0.4783	Fig. S15D
ε	25.2±0.9	31	-8%	47/55	0.0095	Fig. S15I
WT/NaCl 222mM	16.1±0.5	19		65/79		Fig. S15B
WT/F6P	18.5±0.8	22	+15%	34/37	0.0099	Fig. S15B
WT/NaCl 333mM	12.2±0.5	14		36/40		Fig. S15C
ε	18.6±1.0	22		21/21		Fig. S15G

WT/FBP	14.5±1.0	20	+19%	43/56	0.0824	Fig. S15C
ε	18.0±0.8	22	-3%	41/48	0.8006	Fig. S15G
WT/LiCl 111mM	15.6±0.8	19		25/43		Fig. 7H
ε	16.7±0.5	15		22/55		Fig. S15H
WT/DHAP	7.7±0.5	11	-51%	63/63	<0.0001	Fig. 7H
ε	15.0±0.8	19	-24%	47/47	<0.0001	Fig. S15H
WT/KCl 111mM	21.3±1.1	29		50/53		Fig. S15E
ε	29.0±0.9	35		53/64		Fig. S15J
WT/PEP	19.8±1.2	30	-7%	63/69	0.7506	Fig. S15E
ε	22.3±0.6	25	-23%	58/65	<0.0001	Fig. S15J

Lifespan data within the solid lines are individual experimental sets and same shades and $^{\alpha, \beta, \gamma,}$ and $^{\delta}$ indicate same experimental sets performed at the same times. All *p* values were calculated within the individual sets by using the log-rank (Mantel-Cox) method (Yang et al., 2011).

Percent (%) changes and *p* values for data with glucose-enriched diet (glc.)-fed worms were calculated against data with control diet-fed worms within dashed lines in the same experimental sets.

Percent (%) changes and *p* values for mutant and transgenic worms grown on a control diet were calculated against WT, and those for RNAi-treated worms were calculated against control RNAi-treated worms in the same experimental sets.

Percent (%) changes and *p* values for unsaturated fatty acids (UFAs)- or saturated fatty acids (SFAs)-treated worms were calculated against worms in the same conditions in the same experimental sets, without respective fatty acid treatments.

$^{ctrl+glc.}$: percent (%) changes and *p* values calculated against WT/control RNAi + glc. worms in

the same experimental sets.

$^{sbp\text{-}1+glc.}$: percent (%) changes and *p* values calculated against WT/*sbp-1* RNAi + glc. or WT/*sbp-1* RNAi (1/2) + glc. worms in the same experimental sets.

$^{mdt\text{-}15+glc.}$: percent (%) changes and *p* values calculated against WT/*mdt-15* RNAi + glc. or WT/*mdt-15* RNAi + glc. worms in the same experimental sets.

(1/2) indicates RNAi bacteria mixed with control RNAi bacteria (dilution to 50%)

$^{sbp\text{-}1}$: percent (%) changes and *p* values calculated against WT/*sbp-1* RNAi or WT/*sbp-1* RNAi (1/2) worms in the same experimental sets.

$^{mdt\text{-}15}$: percent (%) changes and *p* values calculated against WT/*mdt-15* RNAi or WT/*mdt-15* RNAi (1/2) worms in the same experimental sets.

$^{@}$ and $^{\#}$ indicate the same controls that are also shown in Supplemental Table S4.

* indicates an adult-only RNAi treatment. For double RNAi assays, worms were cultured on control RNAi bacteria and transferred to *mdt-15*/*pod-2* RNAi or *mdt-15*/*fasn-1* RNAi bacteria at day 1 adulthood. Worms grown on *sbp-1* RNAi bacteria were treated with *sbp-1*/*pod-2* RNAi or *sbp-1*/*fasn-1* RNAi from day 1 adulthood.

$^{\varepsilon}$ indicates an experiment performed on dead bacteria (OP50).

Following treatments were used for genetically inhibiting each step of the glycolysis pathway shown in Figure 7E. Hexokiase: *F14B4.2* RNAi and *Y77E11A.1* RNAi; GPI: *gpi-1* RNAi; aldolases: *aldo-1(tm5782)* and *aldo-2* RNAi; TPI: *tpi-1* RNAi; GAPDH: *gpd-1*/*2* RNAi; PGK: *pgk-1* RNAi; PGAM: *ipgm-1* RNAi; enolase: *enol-1* RNAi; PK: *pyk-1(ok1754)* and *pyk-2* RNAi;

PDH: *pdhb-1* RNAi and *C30H8.7* RNAi. Average percent changes of mean lifespan from the two repeats are shown in Fig. 7E.

C. elegans genome encodes four *gpd* genes, *gpd-1*, *-2*, *-3*, and *-4*, which encode GAPDH proteins. We treated worms with *gpd-1* and *gpd-2* double RNAi (Fig. 7E), which may have down-regulated *gpd-1, gpd-2, gpd-3* and *gpd-4*, because the sequences of *gpd-1* and *gpd-4* genes are very similar, and *gpd-2* and *gpd-3* are almost identical.

Following metabolites were used for the lifespan assays: glucose-6-phosphate sodium salt (G6P), fructose-6-phosphate disodium salt (F6P), fructose-1,6-bisphosphate trisodium salt (FBP), 2-phosphoglycerate sodium salt (2PG), phosphoenolpyruvate potassium salt (PEP), dihydroxyacetone phosphate lithium salt (DHAP). NaCl (111, 222, or 333 mM), KCl (111 mM), or LiCl (111 mM) was used as a control depending on the salts accociated with the obtained metabolites. Average percent changes in mean lifespan from the two repeats are shown in Fig. 7E except F6P, which was tested once.

Supplemental Materials and Methods

Strains. All strains were maintained on nematode growth medium (NGM) agar plates seeded with *E. coli* (OP50) at 20°C unless otherwise mentioned. Following strains were used in this study. N2 wild-type, IJ106 *dpy-5(e907) I; yhIs11[far-3p::GFP; dpy-5(+)]* outcrossed 4 times with Lee lab N2 after UV integration of BC14852, BC12350 *dpy-5(e907) I; sIs12119 [C53A3.2p::GFP; dpy-5(+)]*, BC15650 *dpy-5(e907) I; sEx15650[F44E7.2p::GFP; dpy-5(+)]*, IJ45 *yhEx13[Y40B10A.6p::GFP; rol-6(su1006)]*, IJ235 *mdt-15(tm2182) III* obtained by outcrossing XA7702 (a gift from Taubert lab) 4 times with Lee lab N2, IJ441 *sbp-1(ep79) III*, obtained by outcrossing CE541 7 times with Lee lab N2, BC11928 *dpy-5(e907) I; sIs10491[mdt-15p::GFP; dpy-5(+)]*, CE1338 *epIs14[sbp-1p::GFP; rol-6(su1006)]*, WM27 *rde-1(ne219) V*, VP303 *rde-1(ne219) V; kbIs7[nhx-2p::rde-1; rol-6(su1006)]*, JM43 *rde-1(ne219) V; Is[wrt-2p::rde-1; myo-2p::RFP]* (a gift from Ruvkun lab), NR350 *rde-1(ne219) V; kzIs20[hlh-1p::rde-1; sur-5p::NLS::GFP],* NL3321 *sid-1(pk3321) V*, TU3401 *sid-1(pk3321) V; uIs69 [unc-119p::sid-1; myo-2p::mCherry]*, CF1290 N2 carrying pRF4 (*rol-6(su1006)*) alone (a gift from Kenyon lab), IJ1208 *yhEx279[sbp-1p::GFP::sbp-1,odr-1p::RFP]*, IJ582 *epEx141[sbp-1p::GFP::sbp-1; rol-6(su1006)]* obtained by outcrossing CE548 4 times with Lee lab N2, IJ421 *yhEx82[mdt-15p::mdt-15::GFP; rol-6(su1006)]*, IJ666 *paqr-2(tm3410) III*, obtained by outcrossing QC121 (a gift from Pilon lab) 4 times with Lee lab N2, IJ638 *mdt-15(et14) III paqr-2(tm3410) III* obtained by outcrossing QC127 (a gift from Pilon lab) 4 times with Lee lab N2, IJ442 *sams-1(ok3033) X* obtained by outcrossing RB2240 7 times with Lee lab N2, BC15777 *dpy-5(e907) I; sEx15777[fat-7p::GFP; dpy-5(+)]*, IJ746 *dpy-5(e907) I; paqr-2(tm3410) III; sEx15777[fat-7p::GFP; dpy-5(+)]* obtained by crossing BC15777 and IJ666, IJ665 *dpy-5(e907)*

I; mdt-15(et14) paqr-2(tm3410) III; sEx15777[fat-7p::GFP; dpy-5(+)] obtained by crossing BC15777 and IJ638, IJ588 *yhEx144[fat-5p::fat-5::GFP; odr-1p::RFP]*, IJ532 *yhEx122[fat-6p::fat-6::GFP; odr-1p::RFP]*, IJ893 *yhIs50[sbp-1::GFP::sbp-1; rol-6(su1006)]* outcrossed 6 times with Lee lab N2 after UV integration of IJ582, CL2070 *dvIs70[hsp-16.2p::GFP; rol-6(su1006)]*, IJ1243 *dvIs70[hsp-16.2p::GFP; rol-6(su1006)]* obtained by outcrossing CL2070 4 times with Lee lab N2, FX05782 *aldo-2(tm5782) III*, VC1265 *pyk-1(ok1754) I*, IJ694 *yhEx170[ges-1p::fat-2::GFP; ges-1p::fat-5::GFP; ges-1p::fat-6::GFP; ges-1p::fat-7::GFP]*. Please note that we were unable to generate *mdt-15(tm2182) sbp-1(ep79)* double mutants, perhaps due to sterility or lethality caused by the double mutations.

Genome-wide RNAi screen. Genome-wide RNAi screen was performed as described previously with modifications (Lamitina et al., 2006). A commercially available RNAi feeding library (Geneservice Ltd, Cambridge, UK) was used for a genome-wide RNAi screen. *E. coli* expressing double-stranded RNA (dsRNA) replicated from the RNAi library were cultured in 96-well plates with LB media containing 50 μg/ml ampicillin (USB, Santa Clara, CA, USA) overnight at 37°C. Cultured RNAi bacteria were seeded onto 24-well solid media plates containing 2% glucose (JUNSEI, Tokyo, Japan), 50 μg/ml ampicillin and 1 mM isopropyl β-D-1-thiogalactopyranoside (IPTG, GOLDBIO, St. Louis, MO, USA), and incubated overnight at 37℃ to induce dsRNA. *far-3p::GFP* transgenic worms cultured on OP50-seeded high growth (HG) media were synchronized by hypochlorite bleaching and incubated in M9 buffer overnight at 20℃. Twenty to thirty L1 larvae in the M9 buffer were transferred into each well of specific RNAi bacteria-seeded 24-well plates by pipetting. After 3 days, three researchers independently scored the fluorescence changes in adult worms from -3 to +3 (arbitrary units) by comparing

with fluorescence intensity of control RNAi (L4440)-treated worms. Total sum scores above +5 and below -4 obtained by the three researchers were defined as enhancers and suppressors, respectively. The initial positive hits were re-examined at least 4 times and RNAi clones that increased or decreased the fluorescence intensity at least twice were used for further analysis.

Lifespan assays. Lifespan assays were performed as described previously with some modifications (Lee et al., 2010). Synchronized worms were transferred onto plates containing 5-10 μM 5-fluoro-2'-deoxyuridine (FUdR, Sigma, St Louis, MO, USA) at young adult stage (day 1) to prevent their progeny from hatching. Deaths of worms were determined by no response upon gently touching with a platinum wire. Animals that crawled off the plates, ruptured, bagged, or burrowed were censored but included in the statistical analysis. The concentration of glucose used in lifespan assays was 2% unless otherwise mentioned. For lifespan assays using dead bacteria, OP50 bacteria that were cultured overnight in liquid LB media were concentrated 20 times by centrifugation and seeded onto NGM plates containing 10 μg/ml kanamycin (Sigma, St Louis, MO, USA). Worms were transferred to fresh plates every other day until they stopped producing progeny for lifespan assays without FUdR treatment. For RNAi treatment that caused slow growth or developmental arrest, worms were cultured on control RNAi (L4440) bacteria-seeded plates during development and treated with specific RNAi bacteria from day 1 adult stage. For example, worms were treated with *mdt-15* RNAi, *ACC* RNAi, or *FAS* RNAi only during adulthood; worms were treated with *sbp-1* RNAi for whole life as *sbp-1* RNAi did not display developmental arrest phenotypes (Yang et al., 2006). Other adult-only RNAi or glucose treatment experiments are indicated in Supplemental Tables. For double RNAi experiments, RNAi bacteria were cultured in liquid LB containing 50 μg/ml ampicillin (USB, Santa Clara,

CA, USA) at 37°C and mixed when OD590 was 0.9 as described previously (Rea et al., 2007). Worms were cultured on *sbp-1* RNAi (50% *sbp-1* RNAi bacteria mixed with 50% control RNAi bacteria) bacteria from hatching and then transferred to *sbp-1*/*mdt-15* RNAi, *sbp-1*/*ACC* RNAi, or *sbp-1*/*FAS* RNAi bacteria-seeded plates at day 1 adult for double RNAi treatments. For other assays such as staining, RNA extraction, and GC/MS, worms were treated with *mdt-15* RNAi for whole life, because the glucose-treated *mdt-15(RNAi)* worms displayed only a mild developmental defect on large size plates, which contained thin bacterial lawn. *mdt-15(tm2182)* and *paqr-2(tm3410)* mutants that displayed developmental defects upon glucose feeding were transferred from control diet plates to glucose-enriched diet plates at young adult stage (day 1). In the same set of the lifespan experiments of *mdt-15(tm2182)* or *paqr-2(tm3410)*, wild-type or *mdt-15(et14) paqr-2(tm3410)* worms were also treated with glucose only during adulthood for consistent experimental conditions, although the wild-type or *mdt-15(et14) paqr-1(tm3410)* mutants did not display severe developmental defects on a glucose-rich diet. Lifespan assays with glycolysis intermediate metabolites were performed as follows. Intermediate metabolites including glucose-6-phosphate sodium salt (G6P, Sigma, St Louis, MO, USA), fructose-6-phosphate disodium salt (F6P, Sigma, St Louis, MO, USA), fructose-1,6-bisphosphate trisodium salt (FBP, Sigma, St Louis, MO, USA), dihydroxyacetone phosphate lithium salt (DHAP, Sigma, St Louis, MO, USA), 2-phosphoglycerate sodium salt (2PG, Sigma, St Louis, MO, USA), and phosphoenolpyruvate potassium salt (PEP, Sigma, St Louis, MO, USA) were used. All these tested chemicals were dissolved in ddH_2O to 1.11 M. NaCl (DAEJUNG, Siheung, South Korea), KCl (DAEJUNG, Siheung, South Korea), or LiCl (Sigma, St Louis, MO, USA) was used as a salt control. pH of G6P and PEP was adjusted to 6 with NaOH (Sigma, St Louis, MO, USA). To prepare media containing 111 mM of each compound, which is comparable to 2% glucose, 0.5

ml of the each stock solution was added to 4.5 ml of NGM in 35 mm plates and mixed sufficiently before the media were solidified. Synchronized worms were cultured on OP50-seeded plates until L4 stage and then treated with 100 μM 5-fluoro-2'-deoxyuridine (FUdR, Sigma, St Louis, MO, USA) to prevent progeny production. Statistical analysis of lifespan results was performed by using OASIS (online application of survival analysis, http://sbi.postech.ac.kr/oasis) and *p* values were calculated by using log-rank (Mantel-Cox method) test (Yang et al., 2011).

Assays for *far-3p::GFP* expression changes upon various stressor treatments. For potential osmotic stresses, *far-3p::GFP* transgenic animals were cultured on the NGM media containing 100 mM NaCl, or 200 mM NaCl from eggs to day 1 adults. *far-3p::GFP* transgenic animals were treated with 25 mM paraquat (methyl viologen, Sigma, St Louis, MO, USA) for 12 hours at young adult stage (day 1) for applying an oxidative stress. For an ER stress, young adult (day 1) *far-3p::GFP* worms were transferred onto plates containing 5 μg/ml tunicamycin (Sigma, St Louis, MO, USA) and incubated for 12 hours. *far-3p::GFP* transgenic worms were incubated at 35°C for 1 hour at young adult stage (day 1) and recovered at 20°C for 12 hours for heat shock treatment. Images of the worms were captured by using AxioCam HRc (Zeiss Corporation, Jena, Germany) camera attached to a Zeiss Axioscope A.1 microscope (Zeiss Corporation, Jena, Germany). ImageJ was used to quantify the fluorescence intensity (Schneider et al., 2012).

Generation of transgenic animals. To generate *sbp-1p::GFP::sbp-1* DNA construct, a DNA fragmant that contained 1.5 kb upstream of startcodon of *sbp-1* from *C. elegans* genomic DNA, GFP from pPD95.75 (Fire lab *C. elegans* vector kit), and *sbp-1* ORF from cDNA were PCR-amplified. The DNA fragments were inserted into the GFP-deleted pPD95.75, which contains

unc-54 3'UTR by using EZ-fusion cloning kit (Enzynomics, Daejeon, South Korea). For generation of *fat-5p::fat-5::GFP* DNA construct, a DNA fragment that contained approximately 2 kb upstream of start codon and the coding region was PCR-amplified from *C. elegans* genomic DNA. The PCR product was inserted into pPD95.75, which contains *GFP* and *unc-54* 3'UTR. *mdt-15p::mdt-15::GFP*, *fat-6p::fat-6::GFP*, *ges-1p::fat-2::GFP*, *ges-1p::fat-6::GFP*, and *ges-1p::fat-7::GFP* DNA constructs were generated by using Gateway cloning system (Invitrogen, Carlsbad, CA, USA). Briefly, a promoter region and ORF of each gene were PCR amplified from *C. elegans* genomic DNA and cDNA, respectively, and cloned into Gateway donor vectors using BP clonase. The DNA constructs containing the promoters and the ORFs were fused into Gateway destination vectors containing *GFP* and *unc-54* 3'UTR using LR clonase. *ges-1p::fat-5::GFP* construct was prepared by using a PCR fusion method (Hobert, 2002) with a PCR-amplified *ges-1* promoter and *fat-5* cDNA, and then inserted into pPD95.75 vector. For a single gene overexpression, the DNA construct was injected into the gonads of young adult worms (day 1) that contained several eggs at concentration of 25 ng/μl with 75 ng/μl of injection marker *odr-1p::RFP*. To generate transgenic animals that overexpressed intestinal *fat-2*, *fat-5*, *fat-6*, and *fat-7*, 25 ng/μl of each DNA construct (*ges-1p::fat-2::GFP*, *ges-1p::fat-5::GFP*, *ges-1p::fat-6::GFP*, and *ges-1p::fat-7::GFP*) was mixed and injected into young adult worms (day 1).

Nile red staining. Nile red staining was performed as previously described (Pino et al., 2013). Worms were treated with indicated RNAi from eggs to adulthood with or without 2% glucose addition. The worms were then harvested at young adulthood (day 1) with M9 buffer and fixed with 40% isopropanol at room temperature for 3 minutes in dark conditions. A working solution [3 μg/ml Nile red (Sigma, St Louis, MO, USA) in 40% isopropanol] was added to the fixed

worms and incubated at room temperature for 2 hours in dark conditions. Stained worms were washed with PBS (137 mM NaCl, 2.7 mM KCl, 10 mM Na_2HPO_4, and 2 mM KH_2PO4) with 0.01% Triton X-100 (DAEJUNG, Siheung, South Korea) and incubated at room temperature for 30 minutes in dark conditions. Images of the worms were captured by using AxioCam HRc (Zeiss Corporation, Jena, Germany) camera attached to a Zeiss Axioscope A.1 microscope (Zeiss Corporation, Jena, Germany) using GFP filter. ImageJ was used for quantification (Schneider et al., 2012).

Coherent anti-Stokes Raman scattering (CARS) imaging and quantification. CARS microscopy was set up as described previously with modifications (Cheng and Xie, 2004). The CARS contrast with regard to 2850 cm^{-1} vibrational mode was built by combining 802 nm pump and 1040 nm Stokes pulse trains (approximately 120 fs, 80 MHz) emitted from a dual mode Ti:Sapphire laser (Insight deepsee dual; Spectra-physics). A chemically sensitive spectral resolution (approximately 1 nm) was achieved by allowing these beams to pass through one narrow spectral bandpass filter (010FC14-25, 802 nm; Andover Corporation, Salem, NH, USA) and the other narrow spectral bandpass filter (01FC16-25, 1040 nm; Andover Corporation, Salem, NH, USA), respectively. CARS imaging was performed as described previously with modifications (Yen et al., 2010). Worms were fed with specific RNAi bacteria from hatched L1 stage to adulthood with or without additional 2% glucose. The worms at young adult (day 1) stage were anesthetized by using 500 mM sodium azide (DAEJUNG, Siheung, South Korea) on 2% agarose pads for imaging. Sixty to eighty images were flattened by Z-projection using ImageJ and inverted. In each image, the part that displayed an intensity higher than the threshold for CARS signals was measured and divided by the total part of a worm in the image. The signal

thresholds for CARS were set for each experimental set, because of the variability among experimental sets. Relative values compared to control RNAi-treated worms in the same experimental sets were calculated and used for statistics.

Locomotion assays. Locomotion was measured as described previously with modifications (Bansal et al., 2015). Please see Supplemental Materials and Methods for details. Briefly, synchronized wild-type worms were transferred onto each RNAi bacteria-seeded plates containing 10 μM 5-fluoro-2'-deoxyuridine (FUdR, Sigma, St Louis, MO, USA), 50 μg/ml ampicillin (USB, Santa Clara, CA, USA), and 1 mM isopropyl β-D-1-thiogalactopyranoside (IPTG, GOLDBIO, St. Louis, MO, USA) at young adult stage (day 1). To set the experimental conditions consistent with lifespan assays, worms were treated with *mdt-15* RNAi from day 1 adult stage, or with *sbp-1* RNAi from eggs to adulthood. Worms in glucose-rich diet conditions were fed with 2% glucose, starting from hatching. To measure body bending in liquid, worms at specific ages were transferred into each well of 24-well plates containing 1 ml of M9 buffer. After 30 seconds for equilibration, movements of the worms were recorded by using DIMIS-M (Siwon Optical Technology, Anyang, South Korea) camera and the body bends of individual worms were counted for 30 seconds and calculated for the number of bending per minute. Body bending on solid media was measured as described previously with modifications (Welz et al., 2011). RNAi-treated worms at specific ages were transferred to plates without bacteria and adjusted for 1 min. Subsequently, body bends were counted for 30 seconds and calculated for the number of bending per minute. A single body bend is defined as one sinusoidal movement of a worm. In these locomotion assays, all the glucose-treated *sbp-1(RNAi)* and *mdt-15(RNAi)* worms were dead by day 10 adulthood, and only live worms were used for the assays.

Feeding rate assays. Feeding rate measurements were performed as described previously with some modifications (Bansal et al., 2015). Synchronized young adult (day 1) wild-type worms were transferred onto each RNAi plate containing 10 μM 5-fluoro-2'-deoxyuridine (FUdR, Sigma, St Louis, MO, USA), 50 μg/ml ampicillin (USB, Santa Clara, CA, USA), and 1 mM isopropyl β-D-1-thiogalactopyranoside (IPTG, GOLDBIO, St. Louis, MO, USA). Consistent with lifespan assays, worms were treated with *mdt-15* RNAi from young adult stage (day 1), or treated with *sbp-1* RNAi from hatching. For glucose feeding experiments, worms were treated with 2% glucose starting from hatching. Pharyngeal pumping (feeding) rates were counted for 15 seconds by observing the pharynx of a worm at a specific age under a dissecting microscope, and converted to the number of pumping per minute. All of the *mdt-15(RNAi)* and *sbp-1(RNAi)* worms that were treated with a glucose-rich diet were dead by day 10 adulthood, and dead worms were excluded from the assays.

Primers used for quantitative RT-PCR assays.

ama-1-F: TGGAACTCTGGAGTCACACC

ama-1-R: CATCCTCCTTCATTGAACGG

far-3-F: GGACGTGGTCTTTATGCTCGTTCTG

mdt-15-F: CAGAGACTTGAGCCTGAGTTGGCG

mdt-15-R: GTCCTTCGACATACACTTTGCGAAC

sbp-1-F: GGATGATATTGCGCCATTTC

sbp-1-R: GGATCCGGTTGTTGTGATGG

far-3-R: GTATGCAGCAACTTGGGTTTCAATG

fat-1-F: TTCACCATGCTTTCACCAACCAC

fat-1-R: GTGTACACTGGGAACCATTTAAGCC

fat-2-F: AGTTTCTGGAGTTGCATGCGCTATC

fat-2-R: CAGCTTCGTAGACCTCAATATCCTC

fat-3-F: GGCAACAATTCGGATGGTTAACAC

fat-3-R: GATGAGTGTTATGCTTGTCCTTCC

fat-4-F: GGTCTTAACTATCAGATTGAGCACC

fat-4-R: CGGAATTGCTCAATTTCAAGCC

fat-5-F: GTTCCAGAGGAAGAACTACCTCCCC

fat-5-R: GGGTGAAGCAGTAACGGAAGAGGGC

fat-6-F: GCGCTGCTCACTATTTCGGATGG

fat-6-R: GTGGGAATGTGTGATGGAAGTTGTG

fat-7-F: GCTGACGAGAAGCCAGTTCTTC

fat-7-R: GAGACCTCGTCAATCATTTCACCAC

pod-2-F: CAGTCAATGTCAGAATCCCTCCGAATG

pod-2-R: CAGACGGCATCGACCTCGTAC

fasn-1-F: GGTTGATGCGGGCATAAATCCCAC

fasn-1-R: CCCGTCAACGTGTAGCCCG

Preparation of plates for fatty acid feeding assays. Fatty acid feeding assays were performed as described previously with modifications (Yang et al., 2006). Briefly, 600 μM of oleic acid (C18:1n-9, Sigma, St Louis, MO, USA), vaccenic acid (C18:1n-7, Sigma, St Louis, MO, USA), and linoleic acid (C18:2n-6, Sigma, St Louis, MO, USA) dissolved in ethanol were mixed with NGM containing 0.1% NP-40 (abcam plc, Cambridge, UK) for unsaturated fatty acid mixture feeding, and 600 μM of myristic acid (C14:0, Sigma, St Louis, MO, USA) and palmitic acid (C16:0, Sigma, St Louis, MO, USA) dissolved in ethanol were mixed with NGM containing

0.1% NP-40 for saturated fatty acid mixture feeding before pouring the media into plates. For individual saturated fatty acid feeding, 600 μM of myristic acid (C14:0) or palmitic acid (C16:0) dissolved in ethanol was mixed with NGM containing 0.1% NP-40. Saturated fatty acids were not completely dissolved in the 0.1% NP-40 treated media. However, there was no difference in the precipitation of saturated fatty acids between control plates and glucose-added plates, suggesting that the specific effects of saturated fatty acids on the lifespan of glucose-fed worms are not due to the lipid precipitation. For oleic acid (C18:1n-9) feeding assay, 600 μM of oleic acid (C18:1n-9) was mixed with NGM without NP-40 before pouring the media into plates.

Supplemental References

Brokate-Llanos AM, Garzon A, Munoz MJ. 2014. *Escherichia coli* carbon source metabolism affects longevity of its predator *Caenorhabditis elegans*. *Mech Ageing Dev* **141-142**: 22-25.

Brooks KK, Liang B, Watts JL. 2009. The influence of bacterial diet on fat storage in *C. elegans*. *PLoS One* **4**: e7545.

Cheng J-X, Xie XS. 2004. Coherent anti-Stokes Raman scattering microscopy: instrumentation, theory, and applications. *The Journal of Physical Chemistry B* **108**: 827-840.

Guillet-Deniau I, Pichard AL, Kone A, Esnous C, Nieruchalski M, Girard J, Prip-Buus C. 2004. Glucose induces de novo lipogenesis in rat muscle satellite cells through a sterol-regulatory-element-binding-protein-1c-dependent pathway. *Journal of cell science* **117**:1937-1944.

Hobert O. 2002. PCR fusion-based approach to create reporter gene constructs for expression analysis in transgenic *C. elegans*. *Biotechniques* **32**: 728-730.

O'Rourke EJ, Kuballa P, Xavier R, Ruvkun G. 2013. omega-6 Polyunsaturated fatty acids extend life span through the activation of autophagy. *Genes Dev* **27**: 429-440.

Pino EC, Webster CM, Carr CE, Soukas AA. 2013. Biochemical and high throughput microscopic assessment of fat mass in *Caenorhabditis elegans*. *J Vis Exp*.

Rea SL, Ventura N, Johnson TE. 2007. Relationship between mitochondrial electron transport chain dysfunction, development, and life extension in *Caenorhabditis elegans*. *PLoS Biol* **5**: e259.

Welz C, Kruger N, Schniederjans M, Miltsch SM, Krucken J, Guest M, Holden-Dye L, Harder

A, von Samson-Himmelstjerna G. 2011. SLO-1-channels of parasitic nematodes reconstitute locomotor behaviour and emodepside sensitivity in *Caenorhabditis elegans slo-1* loss of function mutants. *PLoS Pathog* **7**: e1001330.

Ye J, DeBose-Boyd RA. 2011. Regulation of cholesterol and fatty acid synthesis. *Cold Spring Harb Perspect Biol* **3**.

Yen K, Le TT, Bansal A, Narasimhan SD, Cheng JX, Tissenbaum HA. 2010. A comparative study of fat storage quantitation in nematode *Caenorhabditis elegans* using label and label-free methods. *PLoS One* **5**.